UNIVERSITÄT BERN

AEC

ALBERT EINSTEIN CENTER FOR FUNDAMENTAL PHYSICS

INSTITUTE FOR THEORETICAL PHYSICS

On the Effect of Global Cosmological Expansion on Local Dynamics

Masterarbeit der Philosophisch-naturwissenschaftlichen Fakultät der Universität Bern

vorgelegt von

Adrian Oeftiger

im Frühjahr 2013

Leiter der Arbeit

Prof. Dr. Matthias Blau

Abstract

Our Universe is subject to a global intrinsic expansion that becomes apparent e.g. when observing the redshift of distant galaxies or the cosmic microwave background radiation. The Friedmann-Lemaître-Robertson-Walker metric approximately models this behaviour on large scales where galaxies are averaged out, i.e. the scale of galaxy superclusters and larger. However, zooming into the more complex local structure in galaxies, solar systems and even atoms, gravitational attraction and other fundamental forces dominate the situation. Throughout the course of this master thesis, the effect of global cosmological expansion on local dynamics will be examined in different frameworks: first, a Newtonian approach will provide for a basic discussion of the phenomenon. Subsequently, the full general relativistic framework will be employed starting with the analysis of the Einstein-Straus vacuole. Finally, the thesis is rounded off by a study of the local dynamics in the $k = 0$ McVittie space-time, which depicts a mass-particle embedded in an expanding spatially flat cosmos. In each of these situations, the respective predictions for the evolution of local binary systems are elaborated. The corresponding scales, from which on systems follow the Hubble flow, consistently indicate an apparent recession of intergalactic objects from proper distances of about 10 million light years on. In contrast, systems of the size of (electromagnetically bound) hydrogen atoms or on the scale of (gravitationally bound) solar systems remain unaffected by cosmic expansion.

Contents

List of Figures

List of Tables

to my family

Acknowledgements

It was during a wonderful introductory course to General Relativity that I got interested in the local effects of cosmic expansion and extensively discussed this matter with the lecturer, Matthias Blau. I am cordially thankful for his suggestion to write a master thesis on this very topic, his offer for supervision and the valuable guidance he provided throughout the progress of the thesis. We had many splendid and enlightening discussions and I feel that I have learnt a lot about general relativity beyond the scope of my master courses.

I was supported by many people during my studies, countless inspiring conversations arose with fellow students, physicists and friends. In this regard, I am especially indebted to my office mate Peter Stoffer, whose time I made demands on quite frequently, I fear, and who never spared his enthusiasm to discuss whatever I asked him. I also wish to thank the various friends who took the time to read my work and suggest refinements, among whom are Jason Aebischer, Gian Calgeer and Manuel Meyer.

At long last, I want to express all my profound respect to my parents, Eva Maria and Uwe Oeftiger: raising that tot, always being available to answer a child's riddling questions and not least wholeheartedly supporting my studies in physics – I owe you my deepest gratitude!

Adrian Oeftiger

1 Motivation

1.1 Some History

Modern cosmology commenced in 1916 when Albert Einstein published his general theory of relativity [Stachel *et al.* , 1987–2012]. General relativity embodies the present description of gravitation and all of its tested predictions have been verified so far, e.g. the apsidal precession of planetary orbits (most prominently Mercury), gravitational lensing, indirect observations of gravitational waves in pulsar systems, the Shapiro time delay effect, gravitational time dilation... And yet, one of the most staggering achievements during the early 20th century has been the discovery and explanation of the redshift of objects in deep space. The first person to derive this effect from Einstein's field equations of general relativity was Georges Lemaître in his paper [Lemaître, 1927]. At the same time as Alexander Friedmann, he proposed that the Universe expands on average – however, as opposed to Friedmann, Lemaître referred to the observed redshift of "extragalactic nebulae" and explained it with the aid of his model. The experimental discovery of the redshift is attributed to Vesto Slipher, who had measured the linear relation between the distance of objects and their apparent recessional velocity a decade before. Lemaître presented an estimated value

for the rate of the expansion, which was to be independently improved by U.S. American astronomer Edwin Hubble only two years after Lemaître's publication in 1929. The linear relation, initially established by Slipher and first derived by Lemaître, nowadays bears Hubble's name, who made the discovery widely known. Hubble interpreted the redshift of the galaxies as a Doppler shift, his law states that the recessional velocity v increases with proper distance D by the Hubble constant H_0,

$$v = H_0 \cdot D \quad . \tag{1.1}$$

Friedmann's and Lemaître's model exhibits a scale factor $a(t)$ in the spatial part of the metric. To explain its meaning, choose two fixed points to delimit a volume which contains a constant mass portion of the diluting cosmic matter fluid filling the space-time. This would be the case for galaxies at a sufficient high distance from each other. Since the scale factor depends on the cosmological time, the physical (proper) distance between these two "comoving" points may change with elapsing t. For the purpose of visualising this concept, one often refers to the picture of a balloon with many spots all over it representing galaxies. Blowing the balloon leads to an *intrinsic* expansion of the two-dimensional space on the balloon's surface which translates to a growing scale factor $a(t)$. One can see the spots recede from each other and, no matter which spot is fixed, all of the others will appear to move away from it. This feature of a homogeneous space-time, in this case the expanding two-dimensional surface of the balloon, is called isotropy. We assume that our Universe also exhibits isotropy and homogeneity at large scales – hence, we observers on Earth do not occupy a privileged location within the Universe as a whole. Instead, any observer in another galaxy would measure redshifts in the spectra of sufficiently distant galaxies in the same way as we do. If the Universe was collapsing, one would analogously observe a systematic blueshift of distant galaxies.

The shift in the spectra is due to the finite time distance between the emission and the detection of the photons. Within this time interval, the proper distance between observer and emitter has increased by a certain amount. At the time of detection, as viewed from the emitter, the observer appears to have picked up a certain velocity compared to the time of emission. Due

to this apparent velocity, the observer detects the photon with a certain redshift. These apparent recession velocities of the galaxies are attributed to the intrinsic expansion of space and the corresponding redshift are directly related to the expansion rate itself (within the Friedmann-Lemaître model). This is where one retrieves Hubble's relation (to first-order approximation),

$$v \approx \frac{\dot{a}(t)}{a(t)}\, D \doteq H(t)\, D \quad . \tag{1.2}$$

A quick derivation of this can be found in almost any text book on general relativity, a good example is given in [Wald, 1984]. Note that the Hubble constant $H(t) = (\dot{a}/a)(t)$ may change over time, the label *constant* refers to the spatial universality (to avoid confusion, we rather call it Hubble parameter). Since the derivative of the Hubble parameter is extremely small, the linearity of (1.2) as well as the current value $H_0 \doteq H(t_0)$ are applicable over a long time episode of our Universe. This translates to the validity of Hubble's original law (3.1) to objects measured at large distances, resp. high redshifts. Figures 1.1 and 1.2 show the final results of the Hubble constant determination as a key project of the famous Hubble Space Telescope (HST) launched in 1990 by the NASA and ESA [Freedman *et al.* , 2001]. The shown Hubble diagrams plot the apparent velocities over distances, where 1 pc (Parsec) amounts to ≈ 3.26 ly (light years). [Riess *et al.* , 2011] published a numerical value for the Hubble constant amounting to

$$H_0 = h \text{ km s}^{-1} \text{ Mpc}^{-1} \quad \text{with} \quad h = 73.8 \pm 2.4 \tag{1.3}$$

including systematic errors, which is based upon the results of the HST key project.

At the beginning of the 20th century, it was commonly believed that the Universe is static. There had been no evidence for any dynamical behaviour of space itself, which explains why Hubble interpreted his results as a Doppler shift of receding galaxies. Initially, Einstein did not have enough confidence in his field equations to support the idea of global expansion resp. contraction, which the particular solutions found by Friedmann (and Lemaître) suggested. He therefore introduced a positive cosmological constant Λ to his field equations, which acts like "anti-gravity" in order to counter-balance the attractive effect of ordinary matter. However, on sight of Hubble's results,

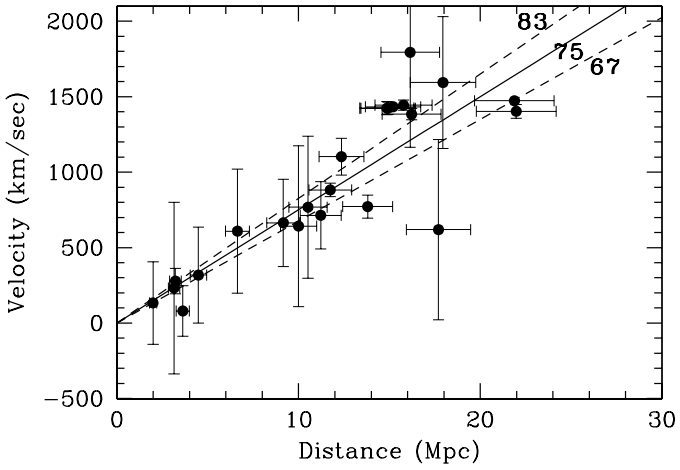

Figure 1.1: Hubble diagram of velocity vs. distance for galaxies in the low redshift regime. A formal fit to these data yields a slope of $h = 75$ which is shown flanked by 10% lines. This is in good agreement with the value obtained by methods that extend to much greater distances. [Freedman *et al.* , 2001]

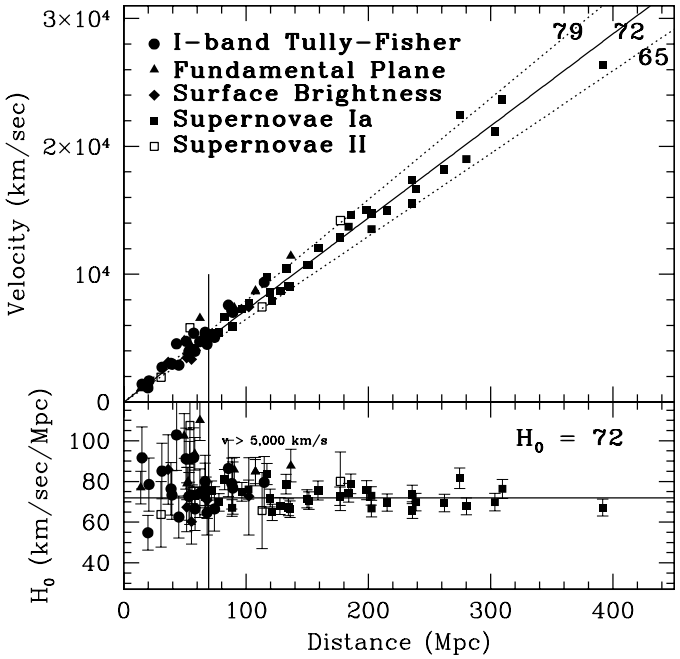

Figure 1.2: Top: Hubble diagram of velocity vs. distance for some higher redshifts (up to $z = 0.1$) including supernovae of the closer type Ia up to distances of 400 Mpc. Note that the recession velocities go up to 10% of the speed of light. A slope of $h = 72$ is shown flanked by 10% lines. Bottom: apparent variation of h as a function of distance. [Freedman *et al.* , 2001]

Einstein veered his opinion and (according to George Gamow's autobiography [Gamow, 1970]) would later call his cosmological model (often referred to as the static Einstein universe) and especially the introduction of Λ his "biggest blunder".

Some decades later in 1965, the detection of the cosmic microwave background (CMB) radiation by Arno Penzias and Robert W. Wilson confirmed the indication that the Universe indeed exhibits global expansion and is everything but static. Together with the redshift of galaxies, the CMB radiation constitutes the most important empirical evidence for Lemaître's Big Bang model, which states that the expansion of the Universe necessarily gives rise to a singularity in the past. We will elaborate on this in the next chapter.

After Einstein had given up the cosmological constant, it was commonly believed that the Universe is merely filled with radiation and cosmic matter (such as stars, hydrogen clouds, ...). Their gravitational attraction acts like a deceleration to the expansion of the universe and one introduced the time-dependent deceleration parameter

$$q \doteq -\frac{a\ddot{a}}{\dot{a}^2} = -\frac{\ddot{a}}{a} H^{-2} \tag{1.4}$$

(with the previously introduced scale parameter $a(t)$ of the Friedmann-Lemaître model).

However, in 1998, two research teams obtained astounding results: the High-Z Supernova Search Team around Brian P. Schmidt and Adam G. Riess and the Supernova Cosmology Project around Saul Perlmutter established the fact that the expansion of our Universe essentially *accelerates*, i.e. for us, q assumes a negative value in contrast to what had been widely believed before the two revolutionary papers [Riess *et al.* , 1998; Perlmutter *et al.* , 1999]. The three named persons were awarded the Nobel Prize in 2011 for their ground-breaking work. To the present day, statistics from the experiments are still low – it is thus not surprising that current results for q vary wildly depending on which method resp. detailed model is used and which data sets are taken into account (see e.g. [Xu *et al.* , 2007] or [Kumar, 2012]). For our purpose of evaluating orders of magnitude, we use a rough estimate

of $q_0 \approx -0.5$ (the subscript 0 denotes 'today'). In comparison, a universe dominated solely by dark energy would exhibit $q = -1$ corresponding to a positive cosmological constant $\Lambda > 0$.

1.2 State-of-the-Art Cosmology and Expansion

The presently widely acknowledged cosmological model is the ΛCDM model ("Λ" for cosmological constant and "CDM" for Cold Dark Matter, where cold refers to it being non-relativistic). It is based upon general relativity and implements the Cosmological Principle, i.e. the matter distribution in the Universe being spatially homogeneous and isotropic on large scales. This essentially boils down to the above-mentioned Friedmann-Lemaître model. A decade after Friedmann's and Lemaître's model in 1935, Howard P. Robertson and Arthur G. Walker independently proved in a geometric approach (without a priori assuming Einstein's field equations to be satisfied) that the corresponding metric is the only metric (up to coordinate transformations) describing a space-time that features spatial homogeneity and isotropy [Robertson, 1935; Walker, 1935]. To do justice to all four contributing scientists, we refer to the metric by the *Friedmann-Lemaître-Robertson-Walker* (henceforth abbreviated FLRW) metric.

While relying on the dynamics (i.e. the equations Alexander Friedmann derived in 1922) entailed by the FLRW metric, the ΛCDM model reintroduces the concept of a cosmological constant that Einstein had abandoned so many years before. Λ accounts for the accelerated expansion of the Universe indicated by the measured negative values of q. A positive Λ implies a negative pressure since the equation of state reads $p = -\rho$ for a (positive) matter density ρ. The physical manifestation of this "dark energy" is still obscure – whether it simply is a cosmological constant in the above sense or whether it is something more complicated and dynamic (as for instance quintessence scalar fields) is one of the big questions of present cosmological research. The cosmological constant variant permeates space very much like a vacuum energy while its nature prevents it from taking part in the cosmic expansion. Such being the case, it determines the long-term behaviour of the global dynamics of the FLRW space-time, since at late times the con-

stant Λ dominates over the diluting cosmic matter fluid. In a Λ-dominated space-time, the scale factor reads $a(t) \propto \exp(Ht)$ with an expansion rate of $H = \dot{a}/a = \sqrt{\Lambda/3} = \text{const}$. Right now (in terms of a cosmic time epoch), we are in a period of transition from matter to dark energy domination. A short summary is contained in the neat depiction by the NASA WMAP team in figure 1.3.

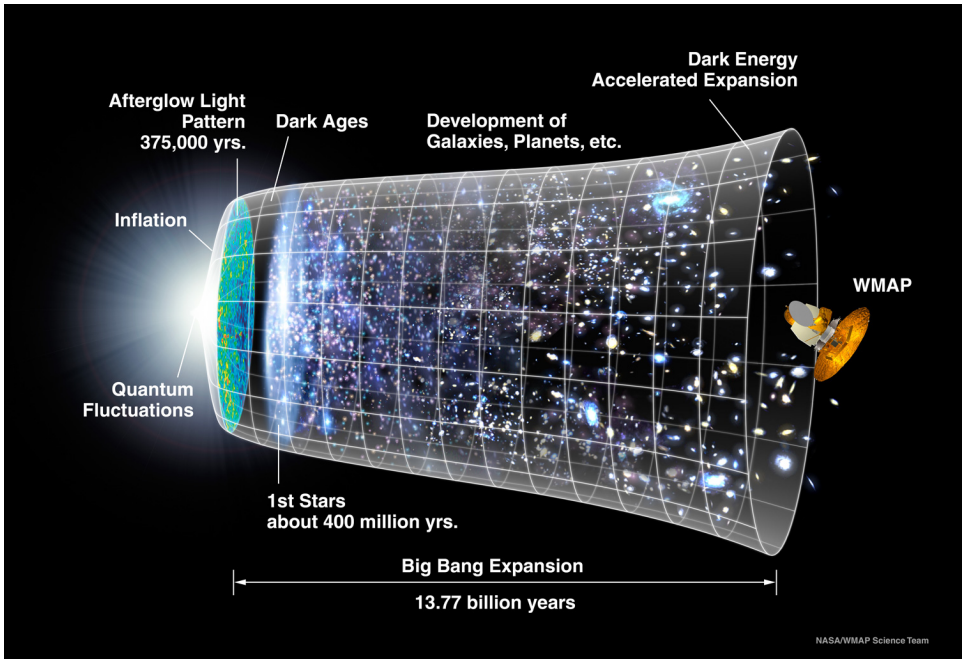

Figure 1.3: The famous timeline of the Universe by the NASA WMAP team (see references).

The ΛCDM model also suggests an explanation for the isotropy of the CMB radiation by including a period of cosmic inflation very early after the Big Bang singularity. The idea of inflation had originally been proposed by Alan H. Guth in 1980. Its main purpose is to reason the isotropy, homogeneity and flatness of the visible Universe by tracing it back to a tiny and causally connected region being in some sort of equilibrium before the inflationary epoch begins. Moreover, inflation suggests a mechanism for the formation of the sponge-like large scale composition of our Universe, which consists of galaxy filaments (also called great walls) delimiting huge voids between them. These structures are reduced to quantum effects of the epoch before inflation, which are imagined to function as seeds for matter accumulation

and are then magnified to cosmic sizes by inflation. Within the filaments, there are galaxy superclusters consisting of clusters, which themselves comprise single galaxies. Our own galaxy, the Milky Way, belongs to the Local Group within the Virgo Supercluster – the order of structures encountered when zooming out from the Earth are displayed in figure 1.4.

The Universe's web-like structure is predicted to eternally move apart in the outlined accelerated fashion, which consequently makes our Universe become a darker and colder place the longer it lives. The Friedmann-Lemaître model satisfying the Cosmological Principle is applicable on scales from roughly 100 Mly on. As can be seen in the low redshift Hubble diagram in figure 1.1, the recession phenomenon sets in at the order of 10 Mly already, which corresponds to structural level above the Local Group. However, on lower scales we expect the attractive gravitation of ordinary matter to counteract the expansion of the Universe. There are some immediately arising questions:

1. **Can we understand and reproduce the scale at which the global expansion begins to prevail over the gravitational attraction by means of theoretical models?**
2. **To what extent are local dynamics (such as planetary orbits or even the stability of a hydrogen atom) affected by global expansion?**

Let us go back to the balloon model for illustration purposes and extend it by gluing coins onto the surface of the balloon (this idea goes back to [Misner *et al.* , 1973]). They correspond to the local neighbourhood around a galaxy or a star. At the time when the balloon is blown and the surface stretches, the glued regions below the coins will in general not follow the expansion. This picture is often referred to when students ask whether the local structure within a galaxy takes part in the expansion of the Universe. The publication [Francis *et al.* , 2007] is a well-formulated, precise and easy-to-read reference defining the framework w.r.t. this problem. The authors clarify frequent misconceptions that arise with the notion of "expanding space", especially with the above picture of coins glued onto a balloon. As such, they refer to the specific situation of a bedroom and to the question whether it expands in the sense of the global dynamics of the Universe.

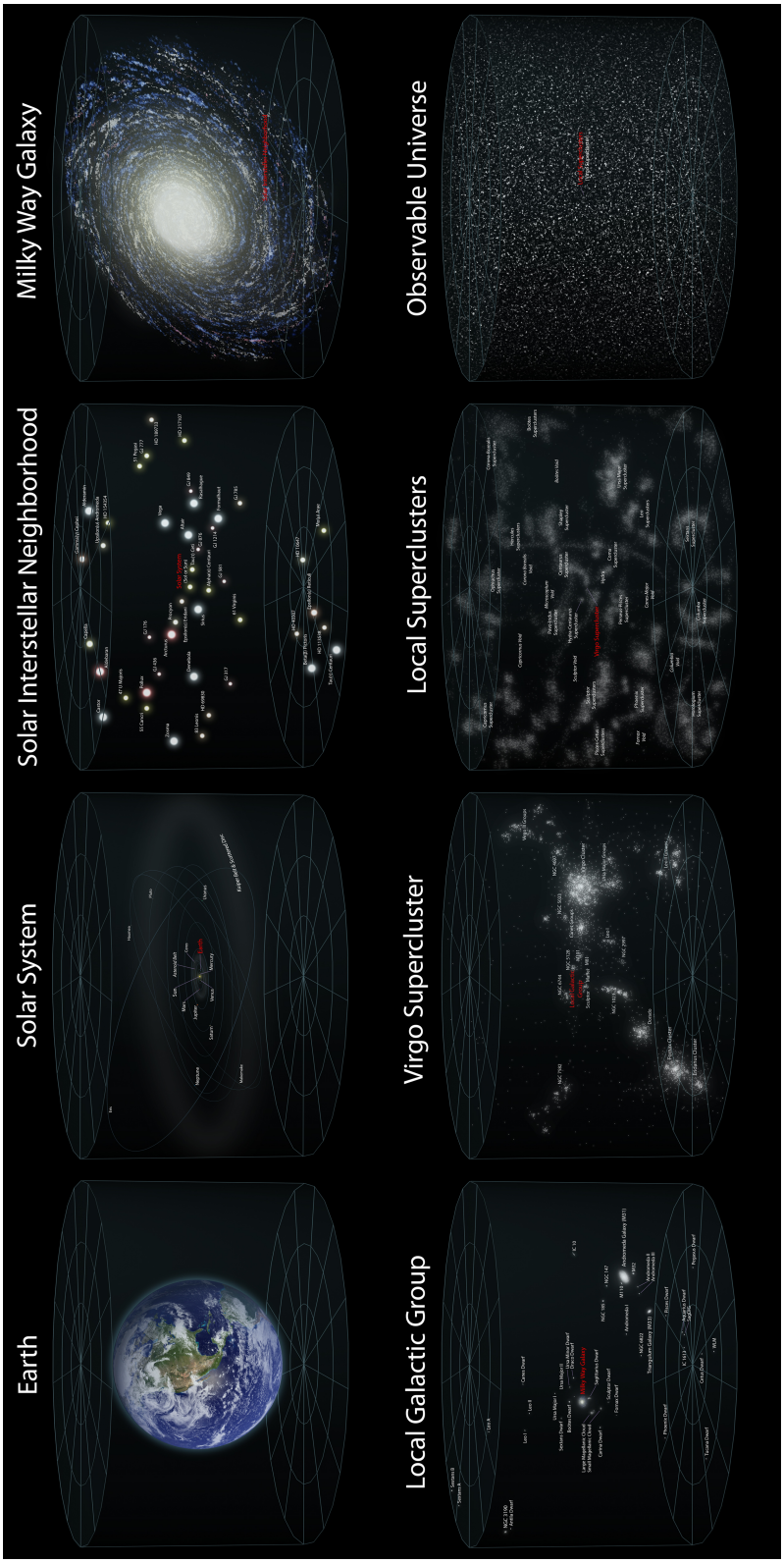

Figure 1.4: Overview of the observable Universe. (source: Wikimedia Commons, see references)

"We should not expect the global behaviour of a perfectly homogeneous and isotropic model [the FLRW space-time] to be applicable [to the bedroom] when these conditions are not even approximately met. The expansion of space fails to have a 'meaningful local counterpart' not because there is some sleight of hand involved in considering the two regimes but because the physical conditions that manifest the effects described as the expansion of space are not met in the average suburban bedroom."

Evidently, the notion of "expanding space" and visualisations thereof (such as the balloon picture) can in general lead to false predictions when interpreted too literally: as an example, one might expect particles moving at relative velocities with respect to the diluting cosmic matter to experience some sort of expansion-induced friction. This is in direct contradiction to what the exact geodesic equations (trajectories of freely moving particles) in the FLRW space-time reveal. Here, Einstein's Equivalence Principle provides a quick and intuitive reason to see that the expectation is wrong. In a sufficiently small region, the effects of acceleration and gravitation cannot be distinguished, i.e. within this region general relativity reduces to special relativity. Hence, global general relativistic effects cannot have an impact on the local dynamics of test particles, the expectation of frictional forces must be wrong. To put it in a nutshell, while using the notion of expanding space to describe the growing physical proper distance between comoving points (like two galaxies) may help understanding many cosmological phenomena (the galaxies' redshifts), it may just as well misguide intuition about local dynamics [Barnes *et al.* , 2006]. The fail-safe option is to work within the general relativistic framework and to draw conclusions by mathematical deduction only, instead of imagining a depiction and leap to further conclusions from the reduced picture.

If we want to not only study test particles but also to allow for a back-effect of the particle on the surrounding space, things quickly become awfully complicated within the full general relativistic framework. For systems that are themselves reasonably well described by Newtonian physics, one might nonetheless address the above posed central questions to some part in a pseudo-Newtonian model (as well-understood general relativistic solutions are indeed scarce) – however, one really has to take special care to not

exceed the applicability and include wrongful expectations into the projected approximation model. Here, the expansion may be included in a dynamical way: not by realising the notion of expanding "space" itself but rather by a change of the inertial structure, cf. [Carrera & Giulini, 2009a] for this idea. By this means we avoid false conclusions such as frictional forces and the like. The Next-to-Newtonian picture may then give first estimates about the order of magnitude of the effect of global expansion on local dynamics.

We will subsequently proceed to the full general relativistic framework, not only to back up the Newtonian discussion but in fact to analyse some of the few existent solutions of Einstein's field equations describing the embedding of a massive object (such as for instance a star or a galaxy) within an expanding cosmos. We know that plain vacuum, i.e. a Minkowski space-time, is curved by the presence of a massive object. Its gravitational effect on the surrounding space is uniquely described by the Schwarzschild metric. In its standard form, it applies to the (empty) region outside of the Schwarzschild radius R_S which depends on the mass M of the central object,

$$R_S \doteq \frac{2GM}{c^2} \quad . \tag{1.5}$$

G denotes the gravitational constant and c the speed of light. The Schwarzschild radius for most astrophysical objects is smaller than the actual dimension of the massive body, compressing it below the Schwarzschild radius would result in the phenomenon of a so-called "black hole". To give some examples, the Earth's Schwarzschild radius is of the order of 8.8 mm (compared to its average radius of slightly less than 6 400 km), for the Sun it lies at 2.95 km (compared to its average radius of almost 700 000 km) and the conjectured supermassive black hole at the centre of the Milky Way with a calculated mass of $M \approx 4.3 \times 10^6\, M_\odot = 8.6 \times 10^{36}$ kg (cf. [Gillessen *et al.* , 2009], $M_\odot$ is the Sun's mass) would have a Schwarzschild radius of about 127 000 000 km or 0.085 AU (1 AU is in about the distance Earth-Sun).

On the other side, a space-time filled with uniformly distributed diluting cosmic matter is described by the FLRW metric. These space-times exhibit a Big Bang singularity at a finite time in the past. Our past light cone today thus reveals only a part of the whole Universe called the *observable* Universe (depending on the context, the specification "observable" is some-

times omitted), since objects only had this finite time amounting to the age of the Universe to send their light to us. Assuming the Universe to be more or less isotropic, its observable part forms a sphere around us with its boundary corresponding to an emission time right after the Big Bang. In practice, the farthest and earliest event we can actually see (that is detect via photons) is the CMB radiation resulting from the recombination epoch, where (due to the cooling of the Universe) the charged electrons and protons started to form electrically neutral hydrogen atoms. This part of the Universe is called the *visible* Universe, whereas the observable Universe also includes the region "behind" the visible boundary constituted by the recombination event, which amounts to some 100 000 years after the Big Bang. However, this extended region is only accessible via the presumed neutrino background or events having emitted gravitational waves.

Objects that we see today have been at a much shorter spatial distance to us at the time of emission than they are "right now" (in a cosmological sense of time). Consequently, very distant objects like some quasars, for instance, may by now be located outside of the so-called "Hubble horizon". They have moved past a point corresponding to a recession velocity of the speed of light (which defines the Hubble radius), i.e. they are not causally connected to us anymore and there is no way to see them in the future, given that the Universe continues to expand with the currently observed acceleration. The current (in a cosmological sense) Hubble radius

$$R_H \doteq \frac{c}{H_0} \tag{1.6}$$

amounts to 1.32×10^{26} m which is equivalent to 1.4×10^{10} ly. For a non-accelerated expansion, which translates to a constant Hubble parameter, the Hubble radius constitutes an event horizon. Objects within the (constant) Hubble sphere will always be in causal connection to the observer, whereas objects on the outside have never been causally connected and likewise will never be. However, as already mentioned, our own Universe features an accelerated expansion and certain objects in the vicinity of the Hubble radius will at some point cross the Hubble radius and become causally disconnected to us. The opposite would be the case for a decelerated expansion caused for example by a pure matter content in the Universe (as it was commonly

believed before the 1990s), objects from the outside would cross the Hubble radius and hence suddenly be visible (in principle).

So we have both the Schwarzschild metric describing the exterior field of a massive body and the FLRW metric describing the large scale behaviour and the expansion of the Universe. In a linear theory, the proceeding to embed the star into the expanding cosmos would be straight forward, namely a simple superposition of the Schwarzschild and the FLRW metric. Unfortunately, as anticipated before, in general relativity things turn out to be by far more complicated because Einstein's field equations constitute a coupled set of non-linear differential equations. The recipe of simply superimposing existing solutions does in general not yield a new solution.

According to [Carrera & Giulini, 2009a] and [Carrera & Giulini, 2009b], the few known metrics representing isolated bodies in asymptotically FLRW space-times are mainly based upon the Einstein-Straus vacuole concept or attributable to the McVittie class (at least for $k = 0$). These two serve as the general relativistic models that we examine throughout the course of this thesis in view of the central questions.

The Einstein-Straus vacuole resembles the situation with the coins on the rubber balloon. In their work [Einstein & Straus, 1945] (along with the supplement [Einstein & Straus, 1946]), Albert Einstein and Ernst G. Straus pursued the question whether the simple matching of a sphere containing the environment of a star (thus being described by the Schwarzschild metric) to an exterior expanding (FLRW) space-time poses a solution to the Einstein field equations. They showed that this is indeed the case if the radius of the "vacuole" satisfies a certain condition. A decade later, Engelberg Schücking worked up their discussion in more analytical details and provided the full expression of the solution [Schücking, 1954].

Some years prior to Einstein and Straus, George C. McVittie had thought of a metric representing a transition between the Schwarzschild and the FLRW metric [McVittie, 1933]. His work has raised ramified discussions and sets an interesting example for the relative easiness of obtaining a solution to Einstein's field equations and the incredible difficulties emerging during the process of understanding it. The recent works of Brien C. Nolan have cast

some light on the physical interpretation of the McVittie space-time, especially with respect to (a) the question of what the central singularity actually represents and what not [Nolan, 1998] and (b) the matter of certain horizons [Nolan, 1999a; Nolan, 1999b]. At least in the case of vanishing asymptotic curvature $k = 0$ (i.e. a flat FLRW space-time in the limit of spatial infinity), the central object indeed matches McVittie's original interpretation consisting of a mass-particle embedded into an expanding cosmos.

Concerning the second central question, the Einstein-Straus vacuole does not exhibit any effect of global expansion on local dynamics by construction. The radius of the vacuole, however, provides a good estimate as an answer to the first central question. On the other hand, the more complex situation in the McVittie space-time will provide answers to both questions but comes at the price of questionable characteristics. Falling under the latter are the physically unnatural and rather unacceptable property of a pressure that increases towards the origin, diverges at some point and hence prevents the central mass-particle from accreting mass from its surroundings.

2

Fundamentals

Before we dive into the various models to analyse the central questions posed in the previous motivation chapter, we quickly go through our conventions and review important basic relations and space-times to set the framework for this master thesis. For further details, the interested reader is kindly referred to Robert M. Wald's book [Wald, 1984] and to the lecture notes on General Relativity by [Blau, 2012], on both of which this chapter is based.

2.1 Conventions, Notations and Basics

We work in natural units $\hbar = c = k_{\mathrm{B}} = 1$. For the space-time metric, we adopt the spacelike convention, i.e. the metric tensor features the signature $(-,+,+,+)$. For notational brevity, we employ the Einstein notation so that the same index appearing twice in a single term implies summation of that term over all possible values of the index. In general, Greek indices $\mu, \nu, ...$ indicate a range of $0, 1, 2, 3$ including all time and space components, whereas Latin indices $i, j, k, ...$ refer to the spatial components $1, 2, 3$ only.

Let $\{x^\mu\}$ be a local coordinate system for the space-time manifold $\mathcal{M}$ being equipped with a metric tensor $g_{\mu\nu}$ (we mostly suppress arguments of ten-

sors, such as $g_{\mu\nu}(x) \to g_{\mu\nu}$). Consequently, the tangent vectors $\{\partial_\mu\}$ define a local coordinate basis of the tangent space to $\mathcal{M}$. A vector field V (constituting a first-order differential operator on the manifold) can be expressed in (contravariant) components w.r.t. the coordinate basis by

$$V = V^\mu(x)\frac{\partial}{\partial x^\mu} \quad . \tag{2.1}$$

Its dual vector assumes the covariant components $V_\mu = g_{\mu\nu}V^\nu$ and is therefore also called a covector.
The scalar (i.e. coordinate-independent) quantity $ds^2 = g_{\mu\nu}dx^\mu dx^\nu$ is called the (squared) *line element* associated to the metric $g_{\mu\nu}$. Now, according to our sign convention, a vector field V (we frequently omit the word 'field') is defined to be

$$V : \left\{ \begin{array}{ll} \text{timelike} & \|V\| < 0 \\ \text{null resp. lightlike} \quad \stackrel{\cdot}{\Longleftrightarrow} & \|V\| = 0 \\ \text{spacelike} & \|V\| > 0 \end{array} \right\} \text{ everywhere,} \tag{2.2}$$

for its norm $\|V\| \doteq g_{\mu\nu}V^\mu V^\nu$.

The *Christoffel symbols* $\Gamma^\lambda{}_{\mu\nu}$ encode the first derivatives of the metric tensor and are defined by

$$\begin{aligned} \Gamma^\lambda{}_{\mu\nu} &= g^{\lambda\rho}\Gamma_{\rho\mu\nu} \quad , \\ \Gamma_{\lambda\mu\nu} &\doteq \frac{1}{2}\left(\partial_\nu g_{\lambda\mu} + \partial_\mu g_{\lambda\nu} - \partial_\lambda g_{\mu\nu}\right) \quad . \end{aligned} \tag{2.3}$$

The latter, featuring all lower indices, are called "Christoffel symbols of the first kind", whereas the former ones with one contravariant index are consequently referred to as "Christoffel symbols of the second kind". Note that the Christoffel symbols are symmetric under the exchange of the lower two indices, $\Gamma^\lambda{}_{\mu\nu} = \Gamma^\lambda{}_{\nu\mu}$.

We are now enabled to define the *covariant derivative*. The (1,1) tensor

$$\nabla_\mu V^\nu \doteq \partial_\mu V^\nu + \Gamma^\nu{}_{\mu\lambda}V^\lambda \tag{2.4}$$

reduces to the ordinary partial derivative in a locally inertial coordinate system where fictitious gravitational and pseudo-forces (like centrifugal or Coriolis forces) are absent, i.e. where the Christoffel symbols locally vanish.

We subsequently define the covariant directional derivative of a vector field V along another vector field W by

$$\nabla_W V^\mu \doteq W^\nu \nabla_\nu V^\mu \quad . \tag{2.5}$$

Non-vanishing curvature of space-time manifests itself in non-commutativity of the covariant derivatives of a vector field:

$$[\nabla_\mu, \nabla_\nu] V^\lambda \doteq R^\lambda{}_{\sigma\mu\nu} V^\sigma \quad . \tag{2.6}$$

The (1,3) tensor $R^\lambda{}_{\sigma\mu\nu}$ is called the Riemann-Christoffel Curvature Tensor or simply the *Riemann tensor*. The commutator on the left-hand side depends on V in a purely algebraical way since all partial derivatives commute. The Riemann tensor can be explicitly expressed in terms of the Christoffel symbols,

$$R^\lambda{}_{\sigma\mu\nu} = \partial_\mu \Gamma^\lambda{}_{\sigma\nu} - \partial_\nu \Gamma^\lambda{}_{\sigma\mu} + \Gamma^\lambda{}_{\mu\rho} \Gamma^\rho{}_{\nu\sigma} - \Gamma^\lambda{}_{\nu\rho} \Gamma^\rho{}_{\mu\sigma} \quad . \tag{2.7}$$

It is manifestly antisymmetric in the last two indices (due to the antisymmetric commutator in (2.6)). From the covariant constancy of the metric, $[\nabla_\mu, \nabla_\nu] g_{\rho\sigma} = 0$, one can derive that the first pair of lowered indices is also antisymmetric. These are the skew symmetries of the Riemann tensor,

$$R_{\mu\nu\rho\sigma} = -R_{\mu\nu\sigma\rho} = -R_{\nu\mu\rho\sigma} \quad . \tag{2.8}$$

Furthermore, the fact that there is no curvature torsion is expressed in the Bianchi identity, as a direct consequence one obtains

$$R_{\mu[\nu\rho\sigma]} = R_{\mu\nu\rho\sigma} + R_{\mu\sigma\nu\rho} + R_{\mu\rho\sigma\nu} = 0 \quad . \tag{2.9}$$

These three symmetries entail the interchange symmetry

$$R_{\mu\nu\rho\sigma} = R_{\rho\sigma\mu\nu} \quad . \tag{2.10}$$

Per se, a fourth-order tensor exhibits $4^4 = 256$ degrees of freedom. However, the symmetries presented above eliminate many of them and the Riemann tensor is left with 20 independent components.

There are two important tensors derived from the Riemann tensor, namely the *Ricci tensor*

$$R_{\mu\nu} \doteq R^{\lambda}{}_{\mu\lambda\nu} = g^{\lambda\sigma} R_{\sigma\mu\lambda\nu} \quad , \tag{2.11}$$

which is symmetric, and the curvature scalar or *Ricci scalar*

$$\mathcal{R} \doteq R^{\mu}{}_{\mu} = g^{\mu\nu} R_{\mu\nu} \quad . \tag{2.12}$$

Actually, these three quantities (viz. the Riemann tensor, Ricci tensor and Ricci scalar) are the only tensors that can be constructed from the metric and its first and second derivatives, cf. [Blau, 2012]. They play a crucial role in general relativity.

Our sign convention is such that for the standard metric on S^2,

$$ds^2_{S^2} = d\vartheta^2 + \sin^2(\vartheta) d\varphi^2 \quad , \tag{2.13}$$

the Riemann tensor exhibits a positive angular component $R_{\vartheta\varphi\vartheta\varphi} = \sin^2(\vartheta)$ and the Ricci scalar yields the positive value $\mathcal{R} = 2$.

In general relativity, the famous Einstein field equations ascribe the fundamental interaction of gravity to the curving of space-time (accounted for by the Einstein tensor $G_{\mu\nu}$) by its energy content (collected in the energy-momentum tensor $T_{\mu\nu}$). Hence, the gravitational fields are contained in the metric tensor, the Einstein tensor forms a linear combination of the Ricci tensor and the Ricci scalar.

In its general form, Einstein's tensor equation may explicitly include a cosmological constant Λ,

$$\underbrace{R_{\mu\nu} - \frac{1}{2} g_{\mu\nu} \mathcal{R}}_{\equiv G_{\mu\nu}} + \Lambda \, g_{\mu\nu} = 8\pi G \, T_{\mu\nu} \quad . \tag{2.14}$$

As one can see, 10 of the 20 independent components of the Riemann tensor are algebraically fixed via the symmetric Ricci tensor. Thus, there are 10 remaining components describing the curvature of the vacuum, i.e. they satisfy $R_{\mu\nu} = 0$. We will come back to this point later on.

Space-time manifolds may feature continuous space-time symmetries, so-called isometries. As a coordinate-independent characteristic, they manifest

themselves in the invariance of the metric tensor $g_{\mu\nu}$ w.r.t. a certain vector field K. This statement can be precisely expressed in terms of the Lie derivative. Conceptionally, having a tensor field T and a reference vector field V, the Lie derivative $L_V T$ describes the infinitesimal change one would see when flowing T along V, which is equivalent to the infinitesimal change one would see in T if one oneself flowed along the vector field V. A vector field K is said to infinitesimally generate an isometry if the Lie derivative of the metric along the flow of K vanishes,

$$L_K g_{\mu\nu} = g_{\lambda\nu}\nabla_\mu K^\lambda + g_{\mu\lambda}\nabla_\nu K^\lambda = \nabla_\mu K_\nu + \nabla_\nu K_\mu \stackrel{!}{=} 0 \quad . \tag{2.15}$$

Such a vector field K generating a continuous symmetry is named *Killing* after the German mathematician Wilhelm K. J. Killing, who made significant contributions to the classification of Lie algebras. K preserves the underlying metric structure of the manifold which explains the fact that the thereby generated continuous symmetries are called isometries.

A metric is called *stationary* if it admits an (asymptotically) timelike Killing vector. In this case there is a coordinate system in which the metric does not feature any time-dependent coefficients. A special case of stationary metrics are the *static* ones. For these one can always find a coordinate system which exhibits no off-diagonal spatio-temporal cross terms, i.e. static metrics are essentially symmetric under time reversal $t \to -t$ (in addition to the absence of time-dependent coefficients). In this coordinate system, the asymptotically timelike Killing vector is orthogonal to the spacelike hypersurfaces of constant time.

In the introductory motivation, the Cosmological Principle has been mentioned which essentially states that, at largest distances, a cosmological space-time should exhibit spatial isotropy and homogeneity. There are only three spaces satisfying this requirement, namely flat Euclidean space $\mathbb{R}^n$, the positively curved Sphere S^n and the negatively curved hyperbolic space H^n. They correspond to the notion of *maximally symmetric spaces*.

Maximally symmetric spaces are defined to be spaces of dimension n admitting a maximum of $n(n+1)/2$ Killing vectors. These consist of n *translational* Killing vectors ($\to$ *homogeneity*) and $n(n-1)/2$ *rotational* Killing

vectors such as, for instance, the elements of the Lie algebra $SO(n)$ ($\rightarrow$ *isotropy*), i.e. maximally symmetric spaces are homogeneous and isotropic and vice versa. The isometries of the Minkowski metric, for example, are compiled in the Poincaré group whose dimension of $n(n+1)/2$ exactly coincides with the number of Killing vectors – the Minkowski metric therefore is a maximally symmetric space(-time).

The Riemann tensor for such maximally symmetric spaces assumes a remarkably simple form,

$$R_{ijkl} = k\,(g_{ik}g_{jl} - g_{il}g_{jk}) \quad . \tag{2.16}$$

The three values of the constant $k = -1, 0, 1$ refer to the above-mentioned three space variants of H^3, $\mathbb{R}^3$ and S^3, respectively.

The Ricci tensor and scalar correspondingly become

$$R_{ij} = k(n-1)g_{ij} \quad \text{and} \quad \mathcal{R} = kn(n-1) \quad . \tag{2.17}$$

Therefore, a maximally symmetric four-dimensional space-time automatically solves the vacuum Einstein equations for a cosmological constant

$$G_{\mu\nu} = 3kg_{\mu\nu} - 6kg_{\mu\nu} \stackrel{!}{=} -\Lambda g_{\mu\nu} \quad \Longrightarrow \quad \Lambda = 3k \quad . \tag{2.18}$$

The corresponding space-times are de Sitter ($\Lambda > 0$ for $k = +1$) and anti-de Sitter space ($\Lambda < 0$ for $k = -1$) and, as already said, Minkowski space-time (for $k = 0$).

2.2 Geodesics

A smooth curve γ on the space-time manifold $\mathcal{M}$ is called timelike, lightlike or spacelike if the tangent vector field along the whole path is timelike, lightlike or spacelike, respectively.

The motion of observers or massive pointlike test particles follows timelike world lines. W.l.o.g., we assume these curves to be future-directed and parametrised by their arc length (which is their proper time τ), hence entailing that the velocity of the observer following the trajectory is constant. The

world lines of inertial ("force-free") observers, which are subject to gravity alone, constitute the timelike *geodesics* of the space-time. We define the *covariant differentiation* along a path $x^\mu(\lambda)$ by

$$\nabla_\lambda \doteq \dot{x}^\mu \nabla_\mu \equiv \frac{dx^\mu}{d\lambda}(\lambda)\nabla_\mu \quad , \tag{2.19}$$

which introduces the concept of parallel transport along a curve: a tensor T is said to be parallel transported along the curve $x^\mu(\lambda)$ if $\nabla_\lambda T = 0$.

We are thereby enabled to define the covariant acceleration a^μ of a curve as the covariant derivative of the velocity $u^\mu \doteq \dot{x}^\mu$,

$$a^\mu \doteq \nabla_\lambda \dot{x}^\mu = u^\nu \nabla_\nu u^\mu \quad . \tag{2.20}$$

Consequently, we identify the paths exhibiting vanishing acceleration as geodesics. In this sense, geodesics are the "straightest possible lines" one can draw in a curved geometry, cf. [Wald, 1984].

We may now require vanishing covariant acceleration as the general definition of affinely parametrised geodesics (i.e. geodesics that are parametrised such that their tangent vector $dx^\mu(\lambda)/d\lambda$ remains constant). A geodesic $x^\mu(\lambda)$ has to satisfy

$$\ddot{x}^\mu + \Gamma^\mu{}_{\nu\rho}\dot{x}^\nu \dot{x}^\rho \stackrel{!}{=} 0 \quad . \tag{2.21}$$

We choose affinely parametrised paths to always be normalised to

$$g_{\mu\nu}(x)\, \dot{x}^\mu \dot{x}^\nu = \epsilon \tag{2.22}$$

with $\epsilon = -1, 0, 1$ corresponding respectively to the timelike, lightlike or spacelike character of the path at the point x. Geodesics never change their character along their whole trajectory (see further below). A weaker version of (2.21) allowing for variable velocities would merely require the tangent vector to remain parallel when transported along the curve, $\nabla_\lambda u^\mu \propto u^\mu$.

In principle, one can regard (2.21) as a coupled system of four second-order ordinary differential equations for $x^\mu(\lambda)$. However, this might be a little cumbersome to solve. Instead, one can seize on the above-mentioned interpretation of geodesics to correspond to the locally shortest path between two points and understand them in terms of minimising the length of the curve

connecting these two points (for timelike geodesics this would be translated to maximising the proper time). We are thus enabled to let loose the calculus of variations on the expression for the length of the curve. This provides us with a handy method to actually calculate geodesics for a given metric.

The length l of a curve $x^\mu(\lambda)$ is given by

$$l = \int d\lambda \sqrt{g_{\mu\nu}(x(t))\dot{x}^\mu \dot{x}^\nu} \quad . \tag{2.23}$$

In the case of a timelike world line, one would talk about the proper time rather than length, and correspondingly change the sign inside of the square root. For an affinely parametrised path, it is equivalent to consider the Lagrangian

$$\mathcal{L} = \frac{1}{2}\, g_{\mu\nu}\dot{x}^\mu \dot{x}^\nu \tag{2.24}$$

(neglecting the square root) instead and minimise the corresponding action $S[x] = \int d\lambda\, \mathcal{L}$. Now, either by variation of the action or by means of the Euler-Lagrange equations

$$\frac{\partial \mathcal{L}}{\partial x^\mu} - \frac{d}{d\lambda}\frac{\partial \mathcal{L}}{\partial \dot{x}^\mu} = 0 \quad , \tag{2.25}$$

we find that the solutions of (2.21) indeed extremise the action, i.e. that geodesics constitute the locally shortest paths between two points. By inserting a concrete metric into the Lagrangian one can thereby easily determine the explicit expression for the geodesics via the Euler-Lagrange equations. On top of that, the Lagrangian method provides an efficient means to determine the Christoffel symbols of the metric by comparing the explicit geodesic equations to (2.21) and subsequently reading off the $\Gamma^\lambda{}_{\mu\nu}$. As a last remark, we observe that the quantity $\mathcal{L}$ remains constant along geodesics, which somehow expresses its parametrisation independence,

$$\frac{d}{d\lambda}\mathcal{L}\Big|_{\text{geo.}} = 0 \quad . \tag{2.26}$$

This entails the statement made above, namely that geodesics do not change their character which translates to the statement that a massless particle will always remain a massless particle etc.

The curvature of a manifold causes nearby geodesics to accelerate toward or away from each other. This behaviour is described by the *geodesic deviation equation*. We start from a geodesic $x^\mu(\lambda)$ satisfying (2.21) and consider a small deviation δx^μ from it,

$$\ddot{x}^\mu + \delta\ddot{x}^\mu + \underbrace{\Gamma^\mu{}_{\nu\rho}(x+\delta x)}_{=\Gamma^\mu{}_{\nu\rho}(x)+\left(\partial_\sigma\Gamma^\mu{}_{\nu\rho}(x)\right)\delta x^\sigma+\mathcal{O}(\delta x^2)} \left(\dot{x}^\nu + \delta\dot{x}^\nu\right)\left(\dot{x}^\rho + \delta\dot{x}^\rho\right) = 0 \quad . \tag{2.27}$$

Keeping terms up to $\mathcal{O}(\delta x, \delta\dot{x})$ and using the geodesic equation (2.21) to remove the x part, we obtain

$$\delta\ddot{x}^\mu + 2\Gamma^\mu{}_{\nu\rho}(x)\,\dot{x}^\nu\delta\dot{x}^\rho + \left(\partial_\sigma\Gamma^\mu{}_{\nu\rho}(x)\right)\delta x^\sigma\dot{x}^\nu\dot{x}^\rho = 0 \quad . \tag{2.28}$$

What we finally want to determine is the covariant acceleration of the deviation δx. Its velocity gives

$$\nabla_\lambda\delta x^\mu = \delta\dot{x}^\mu + \Gamma^\mu{}_{\nu\rho}\dot{x}^\nu\delta x^\rho \quad , \tag{2.29}$$

so that applying the covariant derivative for a second time yields

$$\begin{aligned}
\nabla_\lambda\left[\delta\dot{x}^\mu + \Gamma^\mu{}_{\nu\rho}\dot{x}^\nu\delta x^\rho\right] &= \delta\ddot{x}^\mu + \dot{x}^\sigma(\partial_\sigma\Gamma^\mu{}_{\nu\rho})\dot{x}^\nu\delta x^\rho + \\
&\quad - \Gamma^\mu{}_{\nu\rho}\Gamma^\nu{}_{\sigma\kappa}\dot{x}^\sigma\dot{x}^\kappa\delta x^\rho + 2\Gamma^\mu{}_{\nu\rho}\dot{x}^\nu\delta\dot{x}^\rho + \\
&\quad + \Gamma^\mu{}_{\nu\sigma}\Gamma^\nu{}_{\rho\kappa}\dot{x}^\sigma\dot{x}^\kappa\delta x^\rho \\
&\overset{(2.29)}{=} (\Gamma^\mu{}_{\nu\sigma}\Gamma^\nu{}_{\rho\kappa} - \Gamma^\mu{}_{\nu\rho}\Gamma^\nu{}_{\sigma\kappa} + \\
&\quad + \partial_\sigma\Gamma^\mu{}_{\kappa\rho} - \partial_\rho\Gamma^\mu{}_{\nu\sigma})\,\dot{x}^\sigma\dot{x}^\kappa\delta x^\rho \quad .
\end{aligned}$$

Comparing this to the Riemann tensor expressed in terms of the Christoffel symbols as in equation (2.7), we immediately identify the expression in brackets as $R^\mu{}_{\kappa\sigma\rho}$ and thus arrive at the geodesic deviation equation,

$$\nabla_\lambda^2\,\delta x^\mu = R^\mu{}_{\kappa\sigma\rho}\,\dot{x}^\kappa\dot{x}^\sigma\delta x^\rho \quad . \tag{2.30}$$

2.3 Schwarzschild Metric

The Schwarzschild metric describes the stationary gravitational field outside of a spherically symmetric star or (Schwarzschild) black hole of mass M with vanishing intrinsic angular momentum, resp. spin, and vanishing electric charge. It has been found by Karl Schwarzschild in 1916 shortly after Einstein had published his theory of general relativity. In its standard form it reads

$$ds^2 = -\left(1 - \frac{2m}{r}\right) dt^2 + \left(1 - \frac{2m}{r}\right)^{-1} dr^2 + r^2 d\Omega^2 \quad , \tag{2.31}$$

where $2m$ is the famous Schwarzschild radius, the parameter m relates to the mass of the central object by $m \doteq GM$, and $d\Omega^2$ denotes the angular part $d\vartheta^2 + \sin^2(\vartheta) d\varphi^2$. Birkhoff's theorem entails that the Schwarzschild solution is the unique spherically symmetric solution for the vacuum Einstein equations $R_{\mu\nu} = 0$.

We will need the Schwarzschild metric in isotropic coordinates later on (in chapter 5). For this, we seek a coordinate transformation $r \to \rho$ such that the metric

$$ds^2 = -\left(1 - \frac{2m}{r}\right) dt^2 + \underbrace{\left(1 - \frac{2m}{r}\right)^{-1} dr^2 + r^2 d\Omega^2}_{\stackrel{!}{=} B(\rho)\,(d\rho^2 + \rho^2 d\Omega^2)} \tag{2.32}$$

assumes an isotropic form (this is possible due to its spherical symmetry). It follows from the angular part that

$$B(\rho) = \frac{r^2}{\rho^2} \quad , \tag{2.33}$$

which entails for the radial part that

$$\left(1 - \frac{2m}{r}\right)^{-1} dr^2 = \frac{r^2}{\rho^2} d\rho^2 \quad \Longrightarrow \quad \frac{dr}{r\sqrt{1 - \frac{2m}{r}}} = \frac{d\rho}{\rho} \quad . \tag{2.34}$$

This equation can be integrated and exponentiated to obtain

$$r - m + r\sqrt{1 - \frac{2m}{r}} = c\rho \tag{2.35}$$

for some integration constant $c > 0$. Note that $\rho = m/c$ corresponds to

$r = 2m$. In order to obtain a diffeomorphic coordinate transformation, we restrict $\rho > m/c$. Squaring and arbitrarily choosing $c = 2$ leads to the sought expression

$$r(\rho) = \rho \left(1 + \frac{m}{2\rho}\right)^2 \quad . \tag{2.36}$$

Inserting this into (2.32) leads to the isotropic Schwarzschild metric

$$ds^2 = -\left(\frac{1 - \frac{m}{2\rho}}{1 + \frac{m}{2\rho}}\right)^2 dt^2 + \left(1 + \frac{m}{2\rho}\right)^4 \left(d\rho^2 + \rho^2 d\Omega^2\right) \tag{2.37}$$

The Schwarzschild metric features four Killing vectors. It is static and consequently admits a timelike Killing vector $\partial/\partial t$. Furthermore, due to the spherical symmetry of the Schwarzschild space-time, there are three spatial Killing vectors generating the rotational Lie algebra $SO(3)$. Therefore, angular momentum is conserved and inertial motion in the Schwarzschild metric is planar. Accordingly, these two degrees of freedom take up two of the spatial Killing vectors conserving the direction of angular momentum. Let us assume for simplicity, w.l.o.g., that the coordinates are chosen in such a way that the motion lies in the equatorial plane $\vartheta = \pi/2$. Then the third Killing vector $\partial/\partial\varphi$ and it corresponds to the conserved magnitude of the angular momentum. In order to derive the timelike geodesics $x^\mu(\tau)$, we consider the Lagrangian

$$2\mathcal{L} = -\left(1 - \frac{2m}{r}\right)\dot{t}^2 + \left(1 - \frac{2m}{r}\right)^{-1}\dot{r}^2 + r^2\dot{\varphi}^2 \tag{2.38}$$

which is already simplified according to equatorial planar motion.

The four Euler-Lagrange equations (2.25) now determine the exact expression for the motion of test particles. Due to the chosen alignment of our coordinate system, the equation for ϑ is trivial. The two Euler-Lagrange equations for t and φ yield the conserved quantities linked to the respective Killing vectors, which arise because the metric components are independent

of both t and φ:

$$\begin{aligned} \frac{\partial \mathcal{L}}{\partial t} - \frac{\partial}{\partial \tau}\frac{\partial \mathcal{L}}{\partial \dot{t}} = 0 \quad \Longrightarrow \quad \frac{\partial}{\partial \tau}\Bigg[\underbrace{\left(1 - \frac{2m}{r}\right)\dot{t}}_{\doteq E}\Bigg] = 0 \quad \text{and} \\ \frac{\partial \mathcal{L}}{\partial \varphi} - \frac{\partial}{\partial \tau}\frac{\partial \mathcal{L}}{\partial \dot{\varphi}} = 0 \quad \Longrightarrow \quad \frac{\partial}{\partial \tau}\underbrace{\left[r^2\dot{\varphi}\right]}_{\doteq L} = 0 \quad , \end{aligned} \tag{2.39}$$

which can in the same way be expressed in terms of the conservation of the respective canonical momenta $p_t = \partial\mathcal{L}/\partial\dot{t} = -E$ and $p_\varphi = \partial\mathcal{L}/\partial\dot{\varphi} = L$ associated with the translational invariances. L is the magnitude of the angular momentum (per unit rest mass) and E, corresponding to the translational invariance of time, may surely be called the total energy (per unit rest mass) of the test particle. Actually, in the limit $r \to \infty$, $E = \dot{t}_\infty$ matches the special relativistic energy $E = \gamma(v_\infty)$ with the particle's coordinate velocity $v = dr/dt$ at infinity. In the Minkowski metric (to which the Schwarzschild metric converges at spatial infinity and which constitutes the underlying space-time of Special Relativity), proper time is related to coordinate time via $d\tau = \sqrt{1 - v^2}\, dt$. Hence the definition of the Lorentz factor $\gamma(v) = dt/d\tau = (1 - v^2)^{-1/2}$. This backs up our identification of E being the energy of the test particle.

What remains is the radial Euler-Lagrange equation. We know from the last section that the norm (2.24) of affinely parametrised geodesics is constant and that the Lagrangian is parametrisation invariant (2.26). These two statements entail

$$\mathcal{L} = \frac{1}{2}\,\epsilon \quad , \tag{2.40}$$

having $\epsilon = -1$ for timelike and $\epsilon = 0$ for null geodesics. The Lagrangian $\mathcal{L}$ may be expressed in terms of the conserved quantities E and L. Consequently, (2.40) leads to an ordinary first-order differential equation replacing the radial Euler-Lagrange equation:

$$\underbrace{\frac{E^2 + \epsilon}{2}}_{\doteq E_{\text{eff}}} = \frac{1}{2}\,\dot{r}^2 + \underbrace{\epsilon\frac{m}{r} + \frac{L^2}{2r^2} - \frac{mL^2}{r^3}}_{\doteq V_{\text{eff}}} \quad . \tag{2.41}$$

This relation has the form of Newtonian energy conservation, a test particle's motion is determined by the *effective potential* V_{eff} and the conservation of

angular momentum $L = r^2\dot{\varphi}$. From this point one can readily derive a radially in- or outbound particle's trajectory, orbits around the central mass (especially circular orbits considering $r = \text{const}$) or the deflection of light by the gravitational potential and the like.

For a radially outbound massive particle (i.e. $L = 0$ and $\epsilon = -1$), coming to rest at infinity ($v_\infty = 0$), we have $E = 1$ and (2.41) simplifies to

$$\dot{r}^2 = \frac{2m}{r} \quad . \tag{2.42}$$

Its integral and thus the behaviour of radially moving observers yields

$$r(\tau) \propto \tau^{2/3} \quad . \tag{2.43}$$

Let us finish with a brief comment on an extension of the Schwarzschild space-time. As anticipated before, a space-time merely filled with a cosmological constant Λ constitutes an (anti-) de Sitter universe. One can immerse the Schwarzschild black hole into this de Sitter space by switching on $\Lambda \neq 0$ in the Schwarzschild space-time, which, under certain constraints ensuring a small Schwarzschild horizon and a huge cosmic horizon, may be considered as a model to be explored with regard to our central questions posed in the introductory chapter. This Schwarzschild-de-Sitter space-time is described by the Kottler metric

$$ds^2 = -\left(1 - \frac{2m}{r} + \frac{\Lambda r^2}{3}\right) dt^2 + \left(1 - \frac{2m}{r} + \frac{\Lambda r^2}{3}\right)^{-1} dr^2 + r^2 d\Omega^2 \quad . \tag{2.44}$$

However, we will find that this is actually a special case of the McVittie space-time, which we analyse throughout chapter 5.

In appendix A.1.1 one may find the values for various geometric properties of the Schwarzschild metric such as the tensors regarding the curvature.

2.4 Friedmann-Lemaître-Robertson-Walker Metric

In the previous motivation chapter, we have outlined some features of the cosmological standard model, the ΛCDM model. It is based upon the model of Friedmann and Lemaître which describes a homogeneous and isotropic universe that expands (resp. contracts) by the cosmic scale factor $a(t)$. The underlying metric of their model was (independently) derived by Robertson and Walker solely from the geometric requirements of homogeneity and isotropy. According to the contributions of all four scientists, the metric is called Friedmann-Lemaître-Robertson-Walker metric, henceforth FLRW metric.

Our (nearly) flat Universe may at largest distances be described by the flat FLRW metric

$$ds^2 = -dt^2 + a(t)^2 d\vec{x}^2 \quad , \tag{2.45}$$

where $d\vec{x}^2$ stands for a spatial metric in Euclidean space $\mathbb{R}^3$ which may exhibit Cartesian coordinates, spherical coordinates etc. In general, there are three such maximally symmetric geometries further including the open hyperbolic space and the closed sphere. As worked out in the first section, these can be unified by introducing the curvature constant k. Then, the general FLRW metric in standard form featuring *comoving coordinates* reads

$$ds^2 = -dt^2 + a(t)^2 \left(\frac{dr^2}{1 - kr^2} + r^2 \, d\Omega^2 \right) \quad . \tag{2.46}$$

Since the FLRW metric poses a solution to the Einstein field equations, the cosmic scale parameter $a(t)$ is determined by the energy content of the space-time, which is a perfect fluid,

$$T_{tt} = \rho(t) \quad , \quad T_{ti} = 0 \quad \text{and} \quad T_{ij} = p(t) g_{ij} \quad , \tag{2.47}$$

where $\rho(t)$ denotes the energy density and $p(t)$ the pressure. This is physically reasonable, as non-interacting homogeneously distributed cosmic matter may be approximated by a perfect fluid, but it also poses the only possibility seen from the curvature side of the Einstein equations (since the energy-momentum tensor needs to display the same symmetries as the Einstein tensor). Denoting by u^μ the timelike velocity field of the perfect

fluid ($u_\mu u^\mu = -1$), whose components in comoving coordinates simply give $(1, 0, 0, 0)$, one can express the covariant energy-momentum tensor as

$$T_{\mu\nu} = (\rho + p)u_\mu u_\nu + p g_{\mu\nu} \quad . \tag{2.48}$$

Usually, one assumes a linear equation of state $p = p(\rho)$ to relate the pressure and the density,

$$p = w\rho \tag{2.49}$$

with a constant w. For non-interacting cosmic matter or "dust", we have vanishing pressure and therefore $w = 0$. For radiation, the trace of the Maxwell energy-momentum tensor vanishes $T^\mu{}_\mu = 0 \stackrel{!}{=} -\rho + 3p$, hence the linear coefficient amounts to $w = 1/3$. As a last example, the equation of state for a pure cosmological constant Λ features $w = -1$, which can be reconstructed by comparing the form of the energy-momentum tensor (2.48) to the Λ term in the Einstein equations (2.14). Understanding Λ as a contribution to the energy-momentum tensor entails the identification $p_\Lambda = -\Lambda/(8\pi G) = -\rho_\Lambda$, i.e. adding a positive cosmological constant results in a negative pressure (cf. the "anti-gravity" statement in the motivation chapter).

The reason for calling the above coordinates "comoving coordinates" lies in their adaptation to time-like geodesics. Since we have a constant time component of the metric, $g_{tt} = -1$, observers at fixed spatial coordinates are geodesic, their proper time coincides with coordinate time, $d\tau^2 = dt^2$. This can be seen from the vanishing Christoffel symbol

$$\Gamma^\mu{}_{tt} = g^{\mu\nu}\frac{1}{2}(2\partial_t g_{\nu t} - \partial_\nu g_{tt}) = 0 \quad . \tag{2.50}$$

which entails that the vector field $\partial/\partial t$ satisfies the geodesic equation (2.21). Evidently, the perfect fluid follows the flow of $\partial/\partial t$, it is at rest in comoving coordinates. Comoving observers at fixed spatial coordinates, going with the flow of the cosmic matter, hence exactly satisfy

$$u^\mu \nabla_\mu u^\nu = \nabla_t u^\mu = \partial_t u^\mu + \Gamma^\mu{}_{t\nu} u^\nu = 0 \quad , \tag{2.51}$$

which confirms the previous statements.

From conservation of energy-momentum (as the FLRW space-time is a solution to the Einstein equations), $\nabla_\mu T^{\mu\nu} = 0$, we again obtain the same result regarding the spatial equations $\nabla_\mu T^{\mu i} = 0$. The time component yields the conservation law

$$\partial_t \rho = -\Gamma^i{}_{it}\rho - \Gamma^t{}_{ij} p g^{ij} \quad \overset{(A.1)}{\Longrightarrow} \quad \dot{\rho} = -3H(\rho + p) \quad , \tag{2.52}$$

with the dot referring to time derivatives as well as introducing the Hubble parameter $H \doteq \dot{a}/a$. Assuming a linear equation of state according to (2.49), (2.52) yields

$$\frac{\dot{\rho}}{\rho} = -3(1+w)\frac{\dot{a}}{a} \quad \overset{\exp\int}{\Longrightarrow} \quad \rho(t)a(t)^{3(1+w)} = \text{const} \quad . \tag{2.53}$$

Therefore, a dust-filled FLRW space-time with $w = 0$ exhibits

$$\rho(t)a(t)^3 = \text{const} \quad , \tag{2.54}$$

whereas a radiation domination with $w = 1/3$ leads to

$$\rho(t)a(t)^4 = \text{const} \quad . \tag{2.55}$$

In the case of a cosmological constant, we have $w = -1$ and hence reconstruct the statement made in the motivation, namely that an energy density ρ_Λ attributed to a cosmological constant does not scale with $a(t)$ and instead remains constant throughout space and time. An FLRW space-time dominated by a cosmological constant is referred to as an (anti-) de Sitter universe.

Let us now employ the Einstein equation in order to derive the equations that determine the dynamics of the FLRW space-time. From appendix A.1.2, we assemble the Einstein tensor

$$\begin{aligned} G_{tt} &= 3\left(\frac{\dot{a}^2}{a^2} + \frac{k}{a^2}\right) \quad , \quad G_{ti} = 0 \quad \text{and} \\ G_{ij} &= -\left(2\frac{\ddot{a}}{a} + \frac{\dot{a}^2}{a^2} + \frac{k}{a^2}\right) g_{ij} \quad . \end{aligned} \tag{2.56}$$

The Einstein field equations (2.14) with the energy-momentum tensor (2.48)

now lead to the two independent equations

$$\frac{\dot{a}^2}{a^2} + \frac{k}{a^2} - \frac{\Lambda}{3} = \frac{8\pi G}{3}\rho \quad \text{and} \tag{2.57a}$$

$$2\frac{\ddot{a}}{a} + \frac{\dot{a}^2}{a^2} + \frac{k}{a^2} - \Lambda = -8\pi G\, p \quad . \tag{2.57b'}$$

Using the first equation to eliminate the Hubble and curvature terms from the second equation, we find

$$-3\frac{\ddot{a}}{a} + \Lambda = 4\pi G(\rho + 3p) \quad . \tag{2.57b}$$

The two equations (2.57a) and (2.57b) are known as the Friedmann equations, they describe the central dynamics of what we referred to as the Friedmann-Lemaître model before. The conservation law (2.52) can be derived from these two equations as well.

An important consequence of the Friedmann equations is the prediction of a "Big Bang" singularity at $a(t = 0) = 0$ in the past considering a reasonably physical matter content (assume $\Lambda = 0$ for the moment) and given a presently ($t = t_0$) expanding universe, $H_0 > 0$. The right-hand side of (2.57b), i.e. the quantity $\rho + 3p$ is positive for cosmic matter ($p = 0$) and radiation ($p = \rho/3$), which entails (even for a negative cosmological constant) that $\ddot{a} < 0$ or, in other words, that the universe decelerates due to the attraction of its gravitating content. The reasoning now goes as follows: the (per definition) positive cosmic scale factor and the positive expansion rate $H_0 > 0$ lead to $\dot{a}(t_0) > 0$, which, together with a negative bending $\ddot{a} < 0$, require $a = 0$ at some finite time $t = 0$ in the past. At this point, the Friedmann equations predict a diverging energy density $\lim_{a\to 0} \rho = \infty$. This singularity has been given the name "Big Bang". An estimate for the maximal age of the universe is given by the Hubble time, $t_0 \leq 1/H_0$, based on the linearised case $\ddot{a} = 0$.

The energy content of the universe is related to its curvature. By means of the first Friedmann equation we can derive a critical energy density. Setting $\Lambda = 0$ and $k = 0$, (2.57a) yields

$$\rho_{\text{crit}} \doteq \frac{3H^2}{8\pi G} \quad . \tag{2.58}$$

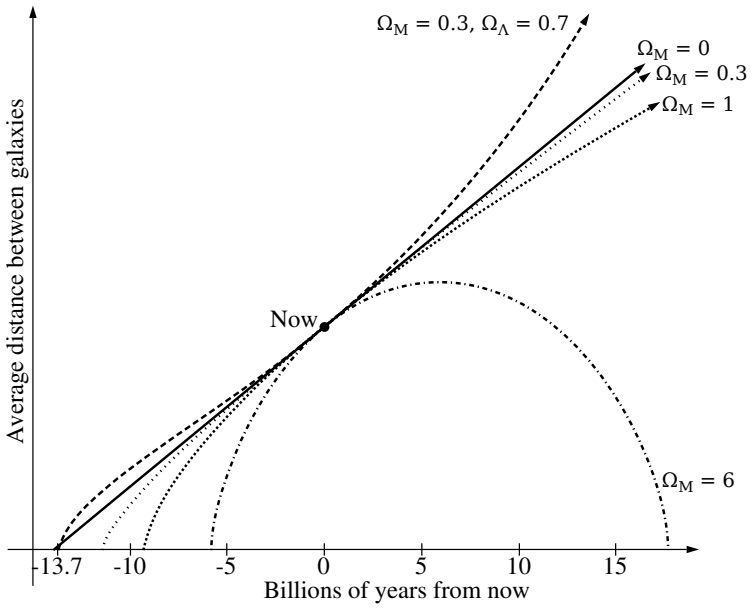

Figure 2.1: Various scenarios for different matter contents of the universe. The curve labeled $\Omega_M = 0$ represents an empty $k = -1$ Milne universe (Minkowski metric in Milne coordinates) with $\ddot{a} = 0$ and $a(t) \propto t$, $\Omega_M = 0.3$ is an open hyperbolic $k = -1$ space-time, $\Omega_M = 1$ represents the flat case $k = 0$, and $\Omega_M = 6$ depicts a closed universe with positive curvature $k = +1$. (source: Wikimedia Commons, see references)

Accordingly, one can define the relative density parameter $\Omega \doteq \rho/\rho_{\text{crit}}$ and immediately sees with regard to (2.57a) that, for vanishing $\Lambda = 0$, $\Omega < 1$ leads to an open hyperbolic universe with negative curvature $k = -1$, $\Omega = 1$ corresponds to the flat case $k = 0$ and $\Omega > 1$ leads to positive curvature $k = +1$ which corresponds to a closed sphere. In the long term, an open hyperbolic universe and a flat universe would expand forever while a closed $k = +1$ universe with $\ddot{a} < 0$ reaches a maximal cosmic radius a_{extr} for $\dot{a} \stackrel{!}{=} 0$, subsequently starts collapsing and finally ends in a "Big Crunch". These different scenarios are outlined in figure 2.1.

A frequently found form of the first Friedmann equation is to rewrite it in terms of the matter contribution $\Omega = \Omega_M$ and analogously define the cosmological constant contribution $\Omega_\Lambda \doteq \Lambda/(3H^2)$ and the curvature contribution

$\Omega_k \doteq -k/(a^2H^2)$ such that

$$\Omega_M + \Omega_\Lambda + \Omega_k = 1 \quad . \tag{2.59}$$

The presently established values amount to $(\Omega_M)_0 \approx 0.3$ (containing only $(\Omega_{M,\text{visible}})_0 \approx 0.04$ of ordinary baryonic and visible matter, the remaining part is due to the obscure matter form of non-relativistic dark matter), $(\Omega_\Lambda)_0 \approx 0.7$ and vanishing curvature $k = 0$.

2.5 Some More Concepts

2.5.1 Some Differential Geometry of Hypersurfaces

In chapter 4 we analyse and manipulate some geometric properties of hypersurfaces, therefore we will briefly introduce them here.

We consider a hypersurface, i.e. a submanifold, embedded in a space-time manifold $\mathcal{M}$ equipped with a metric $g_{\mu\nu}$. Here, we restrict ourselves to a spacelike or timelike hypersurface Σ that is determined by a field of unit normal vectors N which correspondingly exhibit $N^\mu N_\mu = \epsilon = \mp 1$, respectively. The scalar product for vectors on the hypersurface Σ is given by the induced metric $h_{\mu\nu}$ (also called first fundamental form) which characterises the intrinsic curvature on Σ. It is defined by a reduction of $g_{\mu\nu}$ onto Σ by subtracting the contribution normal to the hypersurface,

$$h_{\mu\nu} \doteq g_{\mu\nu} - \epsilon N_\mu N_\nu \quad . \tag{2.60}$$

The induced metric is by construction orthogonal to the normal vector,

$$h_{\mu\nu}N^\nu = g_{\mu\nu}N^\nu - \epsilon N_\mu \underbrace{N_\nu N^\nu}_{=\epsilon} = N_\mu - \epsilon^2 N_\mu = 0 \quad , \tag{2.61}$$

and for any vector V orthogonal to N ($V_\mu N^\mu = 0$, V therefore lies in the tangent space of Σ), the scalar product w.r.t. $h_{\mu\nu}$ corresponds to the full metric $g_{\mu\nu}$, i.e. $h_{\mu\nu}V^\nu = g_{\mu\nu}V^\nu$. The induced metric provides projectors

$$h_\mu{}^\nu = \delta_\mu{}^\nu - \epsilon N_\mu N^\nu \tag{2.62}$$

to project tensor fields (reduced to the hypersurface) onto Σ itself.

The extrinsic curvature of the embedded hypersurface w.r.t. to its surrounding space-time is defined by the covariant derivative of the normal vector field N projected onto Σ,

$$K_{\mu\nu} \doteq h_\mu{}^\rho h_\nu{}^\sigma \nabla_\rho N_\sigma \quad . \tag{2.63}$$

This object is called the *extrinsic curvature tensor*.

2.5.2 Misner-Sharp Energy

We mentioned in the motivation that, by means of the Einstein Equivalence Principle, General Relativity locally always reduces to Special Relativity. Gravitational effects can therefore locally not be distinguished from sole acceleration, one can always find a locally inertial coordinate system, i.e. a coordinate transformation such that the metric $g_{\mu\nu}(x_0)$ at a point x_0 reduces to the Minkowski metric $g_{\mu\nu}(x_0) = \eta_{\mu\nu}(x_0)$ along with vanishing Christoffel symbols $\Gamma^\lambda{}_{\mu\nu}(x_0) = 0$. However, the second derivatives of the metric corresponding to the curvature (and hence constituting the Riemann tensor) cannot simply be removed by coordinate transformations, this is where gravity itself is encoded. This is somewhat intuitive, since the energy content of the space-time determines the curvature (and vice versa, curvature determines the evolution of the energy content) via the Einstein field equations.

This discussion illustrates that in general relativity there exists no simple notion of mass (or energy). Gravitational "field energy", as one knows it, for example, from the source of the Newtonian gravitational potential being a body of mass M, is unfortunately not part of the energy-momentum tensor $T_{\mu\nu}$. Any concept of local energy (as a tensorial quantity in the sense of the metric and its first derivatives) is doomed to fail since it not only necessarily varies under coordinate transformations (which is what one could expect from a physical meaningful energy as in Special Relativity) but can then consequently even be removed for an inertial coordinate system. A tenable concept of mass, resp. energy, must therefore necessarily include in some way the second derivatives of the metric, i.e. the curvature of the space-time. By now, it has been established that useful ideas link a notion of energy to some extended and finite volume, i.e. on a "quasi-local" level,

cf. the extensive review [Szabados, 2004]. This class of energy concepts is consequently referred to as quasi-local energy.

It is not intended to go into this discussion in detail, instead we merely present one such concept for spherically symmetric space-times, that is the notion of *Misner-Sharp energy*, cf. [Misner & Sharp, 1964], which has been worked out in more detail by [Cahill & McVittie, 1970]. It essentially gives an energy content within a rotationally invariant two-sphere S_2 of constant circumferential radius r for a time instant $t = \text{const}$. The circumferential radius is defined for an instant t by a circle of radius r to have a proper circumference of $2\pi r$, which further extends to proper area in a spherical symmetric setting. A general spherically symmetric metric in isotropic form may be written as

$$ds^2 = -A(t,r)dt^2 + B(t,r)\left(dr^2 + r^2 d\Omega^2\right) \tag{2.64}$$

for positive functions A, B and the metric $d\Omega^2$ of a two-sphere with unit radius. The Misner-Sharp energy may then be defined as

$$E \doteq \frac{r}{2G}\left(1 - g^{\mu\nu}(\partial_\mu r)(\partial_\nu r)\right) \tag{2.65}$$

Throughout the first section, we have established that the Riemann tensor $R^\lambda{}_{\sigma\mu\nu}$ features 20 independent components. The Einstein field equations relate 10 of these degrees of freedom to a given energy content of the space-time – consequently another 10 free degrees remain which determine the gravitational effects in the vacuum $R_{\mu\nu} = 0$. Accordingly, one can decompose the Riemann tensor and split it into the different parts, namely on the one hand the trace part consisting of the Ricci tensor $R_{\mu\nu}$ and the Ricci scalar $\mathcal{R}$ (covering the energy content and fixed via the Einstein equations), and on the other hand the traceless part $C^\lambda{}_{\sigma\mu\nu}$ called the *Weyl* tensor. It is defined by

$$\begin{aligned} C_{\mu\nu\rho\sigma} = R_{\mu\nu\rho\sigma} &- \frac{1}{2}\left(g_{\mu\rho}R_{\nu\sigma} + R_{\mu\rho}g_{\nu\sigma} - g_{\nu\rho}R_{\mu\sigma} - R_{\nu\rho}g_{\mu\sigma}\right) + \\ &+ \frac{1}{6}\mathcal{R}\left(g_{\mu\rho}g_{\nu\sigma} - g_{\nu\rho}g_{\mu\sigma}\right) \end{aligned} \tag{2.66}$$

and features the same symmetries as the Riemann tensor by construction, moreover all traces $C^\lambda{}_{\mu\lambda\nu}$ vanish. In the vacuum for a vanishing energy-

momentum tensor $T_{\mu\nu} = 0$, the Weyl tensor is the only remaining part of the Riemann tensor $R^{\lambda}{}_{\sigma\mu\nu} = C^{\lambda}{}_{\sigma\mu\nu}$. Consequently, vacuum physics such as gravitational waves, the stationary exterior gravitational field curvature of a star and the like are contained in the Weyl part of the Riemann tensor.

Accordingly, one can also split the Misner-Sharp energy into its Ricci trace part and its Weyl trace-free part in order to separate the contributions attributed to the energy content of the space-time contained in $T_{\mu\nu}$ from the contributions by vacuum physics,

$$E = E_{\text{Ricci}} + E_{\text{Weyl}} \quad . \tag{2.67}$$

[Carrera & Giulini, 2009a] derive the Ricci contribution for a spherically symmetric perfect fluid (without assuming an equation of state $p = p(\rho)$, e.g. in the case of the McVittie space-time this would lead to drastic constraints). As a result, the Ricci part of the Misner-Sharp energy yields

$$G \cdot E_{\text{Ricci}} = \frac{4\pi}{3} r^3 \rho \quad . \tag{2.68}$$

For instance, the FLRW space-time is filled with the diluting cosmic matter described by the perfect fluid (2.48). The Ricci part of the Misner-Sharp energy directly reflects this energy content in the intuitive terms of energy density times volume.

In contrast, the static Schwarzschild metric in its nature of describing the exterior stationary gravitational field of a body of mass M and, according to Birkhoff's theorem, being the only spherically symmetric solution to the vacuum Einstein equations $R_{\mu\nu} = 0$ therefore provides a nice example for a non-vanishing Weyl part of the Misner-Sharp energy (as its Ricci part gives zero). Its Misner-Sharp energy (2.65) yields

$$E = E_{\text{Weyl}} = \frac{r}{2G}\left(1 - \left(1 - \frac{2m}{r}\right)\right) = \frac{m}{G} = M \quad , \tag{2.69}$$

which essentially states that the energy in a sphere of any radius around the origin (within the defined domain) is attributed to the curvature singularity at the origin itself. This coincides with the interpretation of the Schwarzschild metric as the exterior solution for the gravitational field of a mass-particle M sitting at the origin.

We will come back to this at a later point during the discussions of the Einstein-Straus vacuole in chapter 4 and the McVittie space-time in chapter 5.

2.5.3 Vielbein Formalism

Instead of a coordinate system $\{x^\mu\}$, as introduced in the beginning of the first section, one can also use a local system $\{e^a\}$ called *vielbein* or *tetrad*, which assigns a linearly independent set of vectors to every point. These vectors are related to the coordinates by a pointwise defined invertible matrix $e^a_\mu(x)$. Accordingly, the coordinate basis ∂_μ translates to the tetrad basis $\{e_a\}$ via the pointwise conversion

$$e_a = e_a{}^\mu \frac{\partial}{\partial x^\mu} \quad . \tag{2.70}$$

Tensors can accordingly be translated into the tetrad basis in the fashion of

$$T'_{ab} = e_a{}^\mu e_b{}^\nu T_{\mu\nu} \quad . \tag{2.71}$$

Note that we use Latin indices $a, b, ...$ (and also attach a prime to the Tensor) to indicate that components refer to the tetrad base as opposed to Greek indices $\mu, \nu, ...$ for the coordinate base.

For a given metric $g_{\mu\nu}$, there is always a distinguished class of choices for a tetrad basis $\{e_a\}$ such that the transformed metric gives the Minkowski metric for every point,

$$g_{\mu\nu} = e_\mu{}^a e_\nu{}^b \eta_{ab} \quad . \tag{2.72}$$

This tetrad basis is called an *orthonormal tetrad basis*. It is pointwise determined up to Lorentz transformations $\Lambda_a{}^b(x)\Lambda_c{}^d(x)\eta_{bd} = \eta_{ac}$. For a diagonal metric an orthonormal tetrad basis may assume the particularly simple form

$$e_a = e_a{}^\mu \partial_\mu = \frac{\delta_a{}^\mu}{\sqrt{|g_{\mu\mu}|}} \partial_\mu \quad . \tag{2.73}$$

3

Newtonian Discussion

Let us approach the two central questions posed in the introductory chapter in a first qualitative discussion: we explore an extended Newtonian two-body situation which exhibits an additional force term doing justice to the cosmic expansion. For our purposes of modelling a solar system and focusing on its planetary orbits, it is sufficient to fixate the star and describe its Newtonian gravitational attraction on a test body by a radial force term $F_{\text{grav}} \propto -1/r$ (r denotes the distance to the star). Cosmological expansion is then included by considering a linear oscillator term $F_{\text{exp}} \propto r$. We examine its effect on planetary orbits and will subsequently find a condition on the strength of global expansion which needs to be satisfied in order to encounter stable (circular) orbits at all.

The idea of introducing such a cosmological expansion term $(\ddot{a}/a)\, r$ into the equation of motion goes back to [Pachner, 1964] and earlier. Pachner discusses the dynamics of such a "Next-to-Newtonian" situation and analyses the non-conservation of energy particularly with regard to the high angular momenta of galaxies. Experimental evidence for the latter has been mentioned already by Fritz Zwicky back in 1933 and has been accounted for by the notion of "dark matter", but, in fact, dark matter has still not

consistently been understood up to the present day.

As Pachner stresses himself, "the deviations from the exact validity of the law of conservation of energy are immeasurably small in terrestrial physics, but they probably play an important role in cosmology". However, here we want to examine the qualitative behaviour (the *dynamics*) of two-body orbits under the influence of cosmological expansion. Our approach follows more or less the detailed discussion of the two-body problem in an expanding universe in [Carrera & Giulini, 2006]. [Price & Romano, 2012] also explore this situation in a neatly presented discussion.

Recall that Bertrand's theorem states that the only potentials exhibiting stable and closed solutions – i.e. some sort of orbits – are the harmonic oscillator $V(r) = \frac{1}{2}m\omega^2 r^2$ (m being the oscillator's mass and ω its frequency) and inverse-square forces with potentials $V(r) = -|C|/r$ such as gravitational or electromagnetic attraction. The situation we are discussing here therefore applies to a binary gravitationally bound system just as well as to an electromagnetically bound hydrogen atom.

3.1 A Modified Newtonian Equation of Motion

In the introduction to this thesis, it has been pointed out that galaxies and other objects far away from us exhibit a systematic redshift – the farther away they are located, the stronger the emitted light gets redshifted. The increase appears approximately linear in distance, which is expressed in Hubble's law:

$$\dot{r} = Hr \quad , \tag{3.1}$$

where $H(t) = (\dot{a}/a)(t)$ denotes the Hubble constant along with $a(t)$ being the cosmological scale factor ($H_0 \doteq H(t_0)$ refers to its value today) and r labels the (proper) distance between the emitter and the observer (in this case us). The derivative of the latter, $\dot{r} = \frac{d}{dt}r$, is usually called "recessional" velocity due to Hubble's initial interpretation of the redshift as a Doppler shift. Nowadays, this view has been discarded and the redshift is attributed to the intrinsic expansion of space between the emitter and the observer. Consequently the emitter only appears to be receding from the observer.

However, the terminology has been retained ever since.

It has been established in the chapter on fundamentals that freely falling observers in an expanding universe (described by the FLRW metric) sit at constant comoving coordinates. This suggests that, in a Newtonian picture, inertial frames should in some way include the effect of intrinsic expansion. A test body of mass $m = 1$ following Hubble's law (3.1) would be subject to an expansion force (suppressing the time arguments)

$$F_{\text{exp}} = \ddot{r} = \left(\frac{d}{dt}\,\frac{\dot{a}}{a}\right) r + \frac{\dot{a}}{a}\left(\frac{\dot{a}}{a}\,r\right) = \frac{\ddot{a}}{a}\,r \quad . \tag{3.2}$$

Any additional force $\vec{F}$ (as for instance gravitation or electromagnetic interaction) acting on the test body would now appear as a deviation

$$\ddot{\vec{r}} - \frac{\ddot{a}}{a}\,\vec{r} = \vec{F} \quad . \tag{3.3}$$

This suggestion can be substantiated by means of the geodesic deviation equation within a general relativistic argumentation which is carried out in the next section.

As we want to understand the effect of the expansion term (3.2) on two-body orbits, we include an angular momentum barrier term as well and arrive at the "Next-to-Newtonian" equation of motion

$$\ddot{r} = \frac{L^2}{r^3} - \frac{C}{r^2} + \frac{\ddot{a}}{a}\,r \quad . \tag{3.4}$$

C stands for the magnitude of the interaction in question,

$$C = \begin{cases} GM & \text{for gravitation} \\ \dfrac{qQ}{4\pi\epsilon_0} & \text{for electrostatic attraction} \end{cases} \tag{3.5}$$

(qQ denotes the product of electric charges and ϵ_0 the vacuum permittivity, bear in mind that $m = 1$). We need to add the conservation of the angular momentum L to the radial equation of motion (3.4) in form of the differential equation

$$L = r^2\dot{\varphi} \tag{3.6}$$

(φ being the azimuthal angular coordinate). The motion of the test particle is therefore, w.l.o.g., chosen to be situated within the equatorial plane for a

polar angle of $\vartheta = \pi/2$.

For further analysis of the Next-to-Newtonian equation of motion, we assume that the period of the orbiting test object is negligibly small compared to the cosmological expansion time scale. Consequently, we disregard the time dependence of the expansion force coefficient $\ddot{a}/a \doteq A \stackrel{!}{=} \text{const}$. This is exact for a Λ-dominated universe (with a cosmological constant Λ) featuring a scale factor $a(t) \propto \exp(\sqrt{\Lambda/3}\, t)$ which leads to $A = \Lambda/3 = \text{const}$. For a matter or radiation dominated universe we have a power-law scale factor $a(t) \propto t^n$, i.e. for late times t the derivative of the expansion force coefficient A vanishes asymptotically:

$$\left(\frac{d}{dt}\,\frac{\ddot{a}}{a}\right) / \left(\frac{\ddot{a}}{a}\right) \propto \frac{1}{t} \quad . \tag{3.7}$$

Note that $A = \text{const} < 0$ entails that the expansion force (3.2) simply corresponds to a harmonic oscillator.

We are now enabled to integrate (3.4) and obtain the ordinary expression for the total energy E (the constant of integration) of the system

$$E = \frac{1}{2}\dot{r}^2 + V(r) \tag{3.8}$$

with the potential

$$V(r) = \frac{L^2}{2r^2} - \frac{C}{r} - \frac{A}{2}r^2 \quad , \tag{3.9}$$

3.2 Justification for the $\ddot{a}/a$ Term

According to (3.3), free particles follow the Hubble flow. We identify the previously used set $\{t, r, \vartheta, \varphi\}$ (restricted to a sufficiently small region) to be of Fermi normal (henceforth FN) coordinate type within a general relativistic picture. FN coordinates feature vanishing Christoffel symbols $\Gamma^{\mu}{}_{\nu\lambda}(\gamma) = 0$ along some reference trajectory γ, i.e. there are no Coriolis and centrifugal-like forces along γ. Since in our case we consider a modification of inertial frames, the γ would correspond to the trajectory of a freely falling particle, and the FN coordinates are hence just local coordinates adapted to a certain geodesic γ. Suppose we take a point x_0 on γ: the time coordinate of the metric in FN form (constrained to a sufficiently small region around x_0)

corresponds to the proper time of the freely falling particle, and the spatial metric along γ simply describes the Euclidean metric, $g_{\mu\nu}(\gamma) = \eta_{\mu\nu}$. For more details, the interested reader may refer to [Manasse & Misner, 1963].

Therefore, to motivate the modification (3.3) of the Newtonian inertial frame concept from a general relativistic point of view, we use the geodesic deviation equation as an aid. Adjacent Geodesics $\gamma + \delta x$ close to the reference geodesic γ correspond to other freely falling particles at some distance $\vec{r}$ within our coordinate system in the Newtonian picture. Their behaviour compared to the reference system is described by (2.30), the geodesic deviation equation. The setting for (3.3) consists of freely falling particles within a homogeneously and isotropically expanding universe – hence we naturally consider geodesics (comoving observers) in an FLRW metric. As demonstrated in the following, the geodesic deviation consequently yields the suggested form of modified inertial frames.

Since the reference geodesic γ takes the form $x(\tau) = (\tau, 0, 0, 0)$ (τ being its proper time) in FN coordinates, its velocity simply reads

$$\dot{x}(\tau) = (1, 0, 0, 0) \quad . \tag{3.10}$$

Thus, the geodesic deviation equation (2.30) assumes its FN form

$$\delta\ddot{x}^{\mu} = R^{\mu}{}_{\sigma\rho\lambda}\, \delta^{\sigma}{}_{0}\, \delta^{\rho}{}_{0}\, \delta x^{\lambda} = -R^{\mu}{}_{0\lambda 0}\, \delta x^{\lambda} \quad . \tag{3.11}$$

The Riemann tensor is antisymmetric in its first and last pair of indices which is why $\delta\ddot{x}^0$ necessarily vanishes. The relevant compontents of the Riemann tensor for the FLRW metric in FN form, i.e. in comoving coordinates, are $R^{i}{}_{0j0} = -(\ddot{a}/a)\, \delta^{i}{}_{j}$ (cf. appendix A.1.2). Due to the fact that this expression does not depend on the spatial directions, it is invariant under spatial coordinate transformations. We therefore finally obtain the explicit form of the geodesic deviation equation

$$\delta\ddot{x}^{k}(\tau) - \frac{\ddot{a}}{a}(t)\, \delta x^{k}(\tau) = 0 \quad , \tag{3.12}$$

which is equivalent to statement (3.3) (given $\tau \mathrel{\widehat{=}} t$ as established before).

3.3 Critical Radius and Discussion

By the nature of the terms in the Next-to-Newtonian equation of motion, gravitational attraction decreases with the distance to the central star while the effect of intrinsic expansion of space increases. There is a radius r_{crit} at which gravitation (resp. electromagnetism) succumbs to cosmic expansion. The existence of closed trajectories outside of r_{crit} depends on the signature of the expansion term, which determines whether the universe is subject to accelerated or decelerated expansion. The latter case $A < 0$ implies that cosmic expansion simply acts like a harmonic oscillator and the initial conditions

$$(r, \dot{r}, \varphi, \dot{\varphi})(t_0) \doteq (r_0, v_0, \varphi_0, \omega_0) \tag{3.13}$$

determine the form of the orbit (the angular velocity ω_0 goes into $L = r_0^2\omega_0$ corresponding to the strength of the angular momentum barrier). In contrast, for $A > 0$ we are confronted with an accelerated expansion and particles leaving the reach of attraction across r_{crit} will be dominated by the Hubble flow. r_{crit} itself corresponds to the location where the magnitude of gravitation (or electromagnetic attraction) amounts to cosmic expansion for a particle at rest ($L = 0$):

$$\begin{aligned} & |F_{\text{grav}}| \stackrel{!}{=} |F_{\text{exp}}| \\ \Longrightarrow \quad & \frac{C}{r_{\text{crit}}^2} = |A|\ r_{\text{crit}} \\ \Longrightarrow \quad & r_{\text{crit}} = \sqrt[3]{\frac{C}{|A|}} \quad . \end{aligned} \tag{3.14}$$

This condition is equivalent to the extremum of the potential (3.9) for $L = 0$.

Turning to the initially posed questions, we now want to examine the existence and the behaviour of closed trajectories in more detail. The closed nature of the solution is affected by its determining initial conditions (such as high velocities) and some parameters (such as a high acceleration of the universe or high angular momenta). So let us kill two birds with one stone and combine the initial conditions with the parameters of the potential to include them. Ideally we achieve this by identifying natural scales of the situation and use them to express parameters and initial conditions in di-

mensionless parameters.

Using the relation (1.4), A may be expressed in terms of the deceleration parameter q, which leads to

$$r_{\text{crit}} = \sqrt[3]{\frac{C}{|q|\,H^2}} \quad , \tag{3.15}$$

To get an idea of the magnitude of the cosmic expansion of our Universe, some values for r_{crit} have been compiled in table 3.1:

Object	Critical Radius r_{crit}
Earth	5×10^{16} m $\widehat{=}$ 6 ly
Sun	4×10^{18} m $\widehat{=}$ 400 ly
Hydrogen atom (electromagnetic)	4.6×10^{12} m $\widehat{=}$ 30 AU

Table 3.1: Compilation of some rough estimates for the critical radius assuming a deceleration parameter of $|q_0| = 0.5$ and a Hubble constant amounting to $H_0 = 70$ km s^{-1} Mpc^{-1}.

As one can see, the critical radius assumes quite large values for objects of our Solar System. Especially in the case of the hydrogen atom, cosmic expansion takes over at a radius of 30 AU (Astronomical Units, the mean Earth-Sun distance) which corresponds to the orbit of Neptune. This is almost 23 orders of magnitude larger than the size of the hydrogen atom itself, which is about 50 pm. This suggests that cosmic expansion is completely negligible for electromagnetically bound systems.

A corresponding natural time scale is given by the period T_{Kep} of the Keplerian orbit of a test particle with $L = r_0^2\omega_0$ and initial conditions (3.13) in the standard Newtonian two-body problem, i.e. $A = 0$. At the time $t = t_0$, the energy relation (3.8) yields

$$E = \frac{1}{2}v_0^2 + \frac{r_0^2\omega_0^2}{2} - \frac{C}{r_0} \quad . \tag{3.16}$$

The extremal radii r_{extr} of the trajectory can be found via requiring $\dot{r}_{\text{extr}} \stackrel{!}{=} 0$ so that $E = V(r_{\text{extr}})$.

We encounter the three well-known cases of

(i) *circular motion*
with an energy of $E = -\dfrac{C}{2L^2}$ and a constant radius of
$r_{\text{extr}} \equiv r(t) = \dfrac{L^2}{C} = \text{const}$,

(ii) *open hyperbola*
corresponding to an infalling particle from infinity with an energy $E = 0$, which, after being deflected by the star at a minimal radial distance $r_{\text{extr}} = \dfrac{2L^2}{C}$, leaves the scenery back to infinity ,

and last but not least

(iii) *elliptical motion*
with an energy between $-\dfrac{C^2}{2L^2} < E < 0$ and the two semi-axes amounting to $r_\pm = \dfrac{C}{2\,|E|} \pm \Delta r$, where $\Delta r = \dfrac{1}{2\,|E|}\sqrt{C^2 - 2EL^2}$.

Neglecting the open hyperbolic solution, Kepler's third law provides an estimate for the time scale of closed solutions of the non-expanding $A = 0$ Newtonian equation of motion, namely

$$T_{\text{Kep}} = 2\pi\sqrt{\frac{r_+^3}{C}} \quad . \tag{3.17}$$

W.l.o.g., we may choose t_0 such that $r_0 = r_+$ for elliptic orbits. In the case of circular orbits we obviously have $r_+ \equiv r(t) \equiv r_0$ for any time t.

Going back to the full Next-to-Newtonian equaton of motion, we consider the cosmic expansion as a small perturbation (as already anticipated by the term "next-to"). We make use of the natural space and time scales, r_{crit} and T_{Kep}, to transcribe the initial conditions r_0 and ω_0 as

$$\lambda \doteq \left(\frac{\omega_0}{2\pi/T_{\text{Kep}}}\right)^2 = \left(\frac{1}{2\pi}\cdot\frac{L}{r_0^2}\cdot 2\pi\sqrt{\frac{r_+^3}{C}}\right)^2 = \frac{L^2}{Cr_0} \quad \text{and} \tag{3.18}$$

$$\alpha \doteq \text{sgn}(A)\left(\frac{r_0}{r_{\text{crit}}}\right)^3 = \frac{Ar_0^3}{C} \quad . \tag{3.19}$$

The positive parameter λ embodies the factor by which the angular velocity (in the system including cosmic expansion) varies compared to the unper-

turbed Newtonian angular velocity. $\lambda > 1$ indicates that for a fixed initial velocity v_0 the particle needs a higher angular momentum L to account for the cosmic expansion. Vice versa, $\lambda < 1$ indicates that a lower angular momentum is needed for compensation. This is intuitively linked to the magnitude of the influence of cosmic expansion on the trajectory, which is represented by α. $\alpha < 0$ is equivalent to the harmonic oscillator situation of the decelerated universe with $A < 0$, $\alpha \approx 0$ implies $r_0 \ll r_{\text{crit}}$ (and hence a small influence of cosmic expansion on the orbit bound by the attractive force) and $\alpha = 1$ corresponds to $r_0 = r_{\text{crit}}$ in an accelerated universe. $\alpha > 1$ reflects the complete domination of cosmic expansion, the particle is not captivated by the attracting central body in any way.

We express the radial distance in relation to its initial value, $x(t) \doteq r(t)/r_0$. The Next-to-Newtonian energy conservation (3.8) now reads

$$\frac{1}{2}\,\dot{x}^2 + \left(\frac{2\pi}{T_{\text{Kep}}}\right)^2 \cdot \underbrace{\left(\frac{\lambda}{2x^2} - \frac{1}{x} - \frac{\alpha}{2}\,x^2\right)}_{\text{reduced effective potential } u_{\lambda,\alpha}(x)} = \frac{E}{r_0^2} = \text{const} \tag{3.20}$$

along with the conservation of angular momentum

$$x^2\dot{\varphi} = \frac{L}{r_0^2} = \omega_0 \quad . \tag{3.21}$$

The reduced effective potential $u_{\lambda,\alpha}(x)$ only depends on the two parameters λ and α, whereas the original potential (3.9) features three parameters (namely L, C and A). As we are only interested in the ratio between the attractive force and the cosmic expansion, we pull out the overall strength of the forces as a factor of C represented by the inverse time scale squared. Thus, the remaining parameters λ and α are only relative quantities which can immediately be seen from their explicit expressions.

The transcribed set of initial conditions reads

$$\begin{aligned}(x, \dot{x}, \varphi, \dot{\varphi})(t_0) &= \left(\frac{r(t_0)}{r_0}, \frac{\dot{r}(t_0)}{r_0}, \varphi_0, \omega_0\right) \\ &= \left(1, \frac{v_0}{r_0}, \varphi_0, \omega_0\right) \quad .\end{aligned} \tag{3.22}$$

3.3.1 Circular Orbits

To squeeze some more information out of (3.20), we consider circular orbits corresponding to an extremum of the reduced effective potential,

$$\frac{\partial u_{\lambda,\alpha}}{\partial x} \stackrel{!}{=} 0 \quad \Longrightarrow \quad -\frac{\lambda}{x^3} + \frac{1}{x^2} - \alpha x = 0 \quad . \tag{3.23}$$

Since for circular orbits we have $x(t) = x(t_0) = 1$, this condition reduces to the simple relation

$$1 - \alpha = \lambda \quad . \tag{3.24}$$

This expresses in a compact and neat way the statements made after introducing the two parameters α and λ. For a decelerated universe, $\alpha < 0$, the orbit exhibits super-Newtonian angular momentum $\lambda > 1$ to compensate for the compressing expansion effect – whereas for an accelerated universe, $\alpha > 0$, it has sub-Newtonian angular momentum $\lambda < 1$ ($\alpha \geq 1$ excludes circular orbits).

For the circular orbits to be stable, we require the second derivative of the potential to be positive:

$$\frac{d^2 u_{\lambda,\alpha}}{dx^2}(x = 1) \stackrel{!}{>} 0 \quad \Longrightarrow \quad 3\,(1 - \alpha) - 2 - \alpha > 0 \quad .$$

This restricts the allowed influence of cosmic expansion to

$$\alpha < \frac{1}{4} \quad . \tag{3.25}$$

A plot of the reduced effective potential (3.20) is shown in figure 3.1, the angular momentum has been adapted to circular orbits.

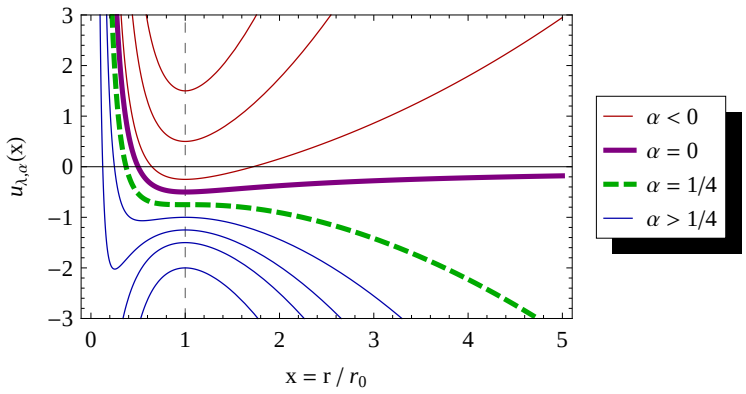

Figure 3.1: A plot of the reduced effective potential $u_{\lambda,\alpha}(x)$ of (3.20), the angular momentum is fixed by the circular orbit condition (3.24). The dashed line at $x = 1$ indicates the circular orbit solution and the purple thick potential corresponds to the non-expanding Newtonian two-body potential.

Re-expressing α via (3.19) in terms of the radius r_{circ} of the circular orbit for the $A > 0$ case, the stability condition of circular orbits (3.25) translates to

$$r_0 < 4^{-1/3}\, r_{\text{crit}} \doteq r_{\text{stable}} \approx 0.63\, r_{\text{crit}} \quad . \tag{3.26}$$

In summary, a universe with decelerated cosmic expansion always exhibits stable circular orbits – in contrast, for a universe with accelerated cosmic expansion, we encounter three different regions:

- $r_0 < r_{\text{stable}}$: stable circular orbits exist,
- $r_{\text{stable}} \leq r_0 \leq r_{\text{crit}}$: circular orbits are unstable, and
- $r_0 > r_{\text{stable}}$: closed trajectories are not possible.

4

The Einstein-Straus Vacuole

An attempt to model a star in an expanding universe within a general relativistic picture has been made by Einstein and Straus in 1945. Their paper [Einstein & Straus, 1945] along with the corresponding correction [Einstein & Straus, 1946] proves that the simple insertion of a star, resp. its surrounding gravitational field, into an expanding homogeneous and flat universe indeed is a solution to the Einstein equations. In 1954, Schücking seized on the idea and presented the corresponding line element as the sought-for solution in [Schücking, 1954]. In the course of his extensive derivation, the radius r_{vac} of the Einstein-Straus "vacuole" emerges in equation (35). It is this matching radius (nowadays sometimes called the "Schücking radius") that will give us a hint at the scale on which the global expansion begins to dominate over the local gravitational field of the single massive object. However, there will be no influence of the exterior expanding space on the orbits around the star *by construction*.

In more detail: in a Schwarzschild space-time (denoted by a subscript S), we retain the inside of a two-sphere of radius $r_{\mathrm{S}} = r_{\mathrm{S,match}}$ around the central star, i.e. the spatial volume $V_{\mathrm{S}} = r_{\mathrm{S,match}} \times S^2$. Next, we excise a two-sphere $V_{\mathrm{F}} = R_{\mathrm{F,match}} \times S^2$ from an FLRW space-time (denoted by a sub-

script F) at a certain circumferential radius $R_{\mathrm{F}} = R_{\mathrm{F,match}}$ and we fit the Schwarzschild patch into it. More precisely, we match the boundary hypersurfaces $\partial V_{\mathrm{S}} \doteq \Sigma_{\mathrm{S}}$ and $\partial V_{\mathrm{F}} \doteq \Sigma_{\mathrm{F}}$ and identify the coordinates on both sides.

As both metrics are isotropic, the coefficients are independent of the angular coordinates and we can immediately identify $\vartheta_{\mathrm{S}} = \vartheta_{\mathrm{F}} \doteq \vartheta$ and $\varphi_{\mathrm{S}} = \varphi_{\mathrm{F}} \doteq \varphi$. It also appears useful to relate the measuring of time in the Schwarzschild metric to the one in the FLRW metric across the matching surface. We are left with the identification of the radial coordinates: the matching radii $r_{\mathrm{S,match}}$ and $R_{\mathrm{F,match}}$ may now in principle depend on a timelike parameter (there is no dependence on angular coordinates due to spherical symmetry).

An effective and yet intuitive strategy is to examine the Painlevé-Gullstrand (henceforth abbreviated PG) form of both the $k = 0$ FLRW and the Schwarzschild metric in spherical coordinates and then immediately read off the matching condition. This approach is neatly presented in more detail in the script on general relativity [Blau, 2012] by Matthias Blau. PG coordinates are adapted to radially freely falling observers, i.e. specific timelike geodesics. "Relating the measurement of time across the matching surface" (as stated above) therefore refers to the identification of the PG transformed Schwarzschild time coordinate $\widetilde{t}_{\mathrm{S}}$ with the comoving FLRW time coordinate t_{F}. We will elaborate on this further down.

Note that the energy-momentum tensor is essentially zero on the inside of the vacuole (up to the central mass), whereas on the outside it describes the diluting cosmic matter fluid of the FLRW space-time. The transition is necessarily first-order, which (due to the Einstein equations) consequently shows up as a discontinuity in the second derivatives of the metric, namely the Riemann tensor. Therefore, we can only require the metric itself (equivalent to the first fundamental form w.r.t. $\Sigma_{\mathrm{S,F}}$) as well as its first derivatives (i.e. the second fundamental form w.r.t. $\Sigma_{\mathrm{S,F}}$), respectively, to be continuous across the vacuole surface.

4.1 Painlevé-Gullstrand Transformation

In order to obtain the Schwarzschild line element and the FLRW line element in PG coordinate form, we will consider the transformations

$$t_{\mathrm{S}} \longrightarrow \widetilde{t}_{\mathrm{S}} \doteq t_{\mathrm{S}} + \Theta(r_{\mathrm{S}}) \quad \text{and} \tag{4.1}$$

$$r_{\mathrm{F}} \longrightarrow R_{\mathrm{F}} \doteq a(t_{\mathrm{F}})\, r_{\mathrm{F}} \tag{4.2}$$

for some yet to be determined function $\Theta = \Theta(r_{\mathrm{S}})$ and the scale parameter $a(t_{\mathrm{F}})$.

4.1.1 Schwarzschild Metric in PG Form

The transformation (4.1) conserves the stationary form of the Schwarzschild line element – however, we give up the static feature by creating off-diagonal time and radial elements. This becomes evident when computing the differential of the new time coordinate $\widetilde{t}_{\mathrm{S}}$:

$$d\widetilde{t}_{\mathrm{S}} = dt_{\mathrm{S}} + \frac{d\Theta}{dr_{\mathrm{S}}}\, dr_{\mathrm{S}} \quad . \tag{4.3}$$

The squared line element accordingly yields

$$\begin{aligned} ds_{\mathrm{S}}^2 &= -f(r_{\mathrm{S}})\, dt_{\mathrm{S}}^2 + f(r_{\mathrm{S}})^{-1} dr_{\mathrm{S}}^2 + r_{\mathrm{S}}^2\, d\Omega^2 \\ &= -f(r_{\mathrm{S}}) \left[d\widetilde{t}_{\mathrm{S}}{}^2 - 2\frac{d\Theta}{dr_{\mathrm{S}}}\, d\widetilde{t}_{\mathrm{S}}\, dr_{\mathrm{S}} + \left(\frac{d\Theta}{dr_{\mathrm{S}}}\right)^2 dr_{\mathrm{S}}^2 \right] + \\ &\quad + f(r_{\mathrm{S}})^{-1} dr_{\mathrm{S}}^2 + r_{\mathrm{S}}^2\, d\Omega^2 \\ &= -f(r_{\mathrm{S}})\, d\widetilde{t}_{\mathrm{S}}{}^2 + 2C(r_{\mathrm{S}})\, d\widetilde{t}_{\mathrm{S}}\, dr_{\mathrm{S}} + \\ &\quad + f(r_{\mathrm{S}})^{-1} \left(1 - C(r_{\mathrm{S}})^2\right) dr_{\mathrm{S}}^2 + r_{\mathrm{S}}^2\, d\Omega^2 \end{aligned} \tag{4.4}$$

with the (up to now arbitrary) function

$$C(r_{\mathrm{S}}) \doteq \frac{d\Theta}{dr_{\mathrm{S}}}\, f(r_{\mathrm{S}}) \equiv \frac{d\Theta}{dr_{\mathrm{S}}} \left(1 - \frac{2m}{r_{\mathrm{S}}}\right) \quad . \tag{4.5}$$

Now, we require the radial diagonal element $g_{r_{\mathrm{S}} r_{\mathrm{S}}} \stackrel{!}{=} 1$ (so that for slices of constant time instants $\widetilde{t}_{\mathrm{S}} = \text{const}$ the induced metric describes Euclidean

space), which directly implies

$$\left(1-\frac{2m}{r_{\mathrm{S}}}\right)^{-1}\left(1-C(r_{\mathrm{S}})^2\right)=1 \quad\Longrightarrow\quad C(r_{\mathrm{S}})=\pm\sqrt{\frac{2m}{r_{\mathrm{S}}}} \quad . \tag{4.6}$$

Here, we shall choose the negative sign corresponding to outbound (instead of radially inbound) freely falling observers. The idea is to continue the trajectories of outgoing observers across the vacuole boundary into the expanding FLRW space-time. Consequently, we are interested in the region $r_{\mathrm{S}} \gg 2m$ far outside of the Schwarzschild radius, i.e. $f(r_{\mathrm{S}}) > 0$, hence the line element reads

$$ds_{\mathrm{S}}^2 = -d\widetilde{t}_{\mathrm{S}}{}^2 + \left(dr_{\mathrm{S}} - \sqrt{\frac{2m}{r_{\mathrm{S}}}}\, d\widetilde{t}_{\mathrm{S}}\right)^2 + r_{\mathrm{S}}^2\, d\Omega^2 \quad . \tag{4.7}$$

This is the Painlevé-Gullstrand coordinate form of the Schwarzschild line element (modulo signs) with $\widetilde{t}_{\mathrm{S}}$ being equivalent to the proper time of (outbound) freely falling observers, cf. section 2.3. For any fixed time instant $\widetilde{t}_{\mathrm{S}} = \text{const}$, the spatial part represents flat Euclidean space.

4.1.2 FLRW Metric in PG Form

In order to obtain a PG form of the flat $k = 0$ FLRW metric (2.45), we will promote the proper radius (4.2) (coinciding with the proper circumferential radius) as the new radial coordinate. Its differential reads

$$dR_{\mathrm{F}} = a(t_{\mathrm{F}})dr_{\mathrm{F}} + \dot{a}(t_{\mathrm{F}})\, r_{\mathrm{F}}\, dt_{\mathrm{F}} \quad , \tag{4.8}$$

where the dot denotes differentiation w.r.t. t_{F}. Conversely,

$$dr_{\mathrm{F}} = \frac{dR_{\mathrm{F}}}{a(t_{\mathrm{F}})} - H(t_{\mathrm{F}})\, r_{\mathrm{F}}\, dt_{\mathrm{F}} = \frac{dR_{\mathrm{F}} - H(t_{\mathrm{F}})\, R_{\mathrm{F}}\, dt_{\mathrm{F}}}{a(t_{\mathrm{F}})} \tag{4.9}$$

having introduced the Hubble constant $H \doteq \dot{a}/a$. The line element thus becomes

$$\begin{aligned} ds_{\mathrm{F}}^2 &= -dt_{\mathrm{F}}^2 + a(t_{\mathrm{F}})^2 \left(dr_{\mathrm{F}}^2 + r_{\mathrm{F}}^2 \, d\Omega^2 \right) \\ &= -dt_{\mathrm{F}}^2 + \frac{a(t_{\mathrm{F}})^2}{a(t_{\mathrm{F}})^2} \Big[dR_{\mathrm{F}}^2 - 2H(t_{\mathrm{F}}) \, R_{\mathrm{F}} \, dR_{\mathrm{F}} \, dt_{\mathrm{F}} + \\ &\qquad + H(t_{\mathrm{F}})^2 \, R_{\mathrm{F}}^2 \, dt_{\mathrm{F}}^2 \Big] + R_{\mathrm{F}}^2 \, d\Omega^2 \\ &= -dt_{\mathrm{F}}^2 + \left(dR_{\mathrm{F}} - H(t_{\mathrm{F}}) \, R_{\mathrm{F}} \, dt_{\mathrm{F}} \right)^2 + R_{\mathrm{F}}^2 \, d\Omega^2 \quad , \end{aligned} \tag{4.10}$$

and we arrive at the Painlevé-Gullstrand form of the FLRW metric. Again, note the relation $t_{\mathrm{F}} \leftrightarrow \tau$. Freely falling observers (timelike radial geodesics $R_{\mathrm{F}}(\tau)$ parametrised by their proper time τ) follow the Hubble relation

$$\frac{dR_{\mathrm{F}}(\tau)}{d\tau} = \frac{da(\tau)}{d\tau} \, r_{\mathrm{F}} = H(\tau) \, R_{\mathrm{F}} \quad , \tag{4.11}$$

as they stay at fixed values of the comoving coordinate r_{F}. Inserting this in the above line element naturally recovers $d\tau^2 = dt_{\mathrm{F}}^2$, i.e. proper time runs with coordinate time t_{F}.

4.2 Merging the Metrics

Gathering both metrics in PG form, we have

$$ds_{\mathrm{S}}^2 = -d\widetilde{t}_{\mathrm{S}}{}^2 + \left(dr_{\mathrm{S}} - \sqrt{\frac{2m}{r_{\mathrm{S}}}} \, d\widetilde{t}_{\mathrm{S}} \right)^2 + r_{\mathrm{S}}^2 \, d\Omega^2 \tag{4.7}$$

$$ds_{\mathrm{F}}^2 = -dt_{\mathrm{F}}^2 + \left(dR_{\mathrm{F}} - H(t_{\mathrm{F}}) \, R_{\mathrm{F}} \, dt_{\mathrm{F}} \right)^2 + R_{\mathrm{F}}^2 \, d\Omega^2 \quad . \tag{4.10}$$

As anticipated above, we want to extend time measuring across the junction hypersurface. Since both line elements in the above form exhibit time coordinates equivalent to the proper time of freely falling observers, it is natural to identify both time coordinates $\widetilde{t}_{\mathrm{S}} \stackrel{!}{=} t_{\mathrm{F}} \doteq t$. Note that this requires the case of a *pressureless dust-filled* FLRW space-time: it is only here that timelike geodesics evolve as $R(\tau) \propto \tau^{2/3}$ which coincides with the behaviour of radially moving observers in the Schwarzschild metric. Besides the time identification, the above notation already suggests the (trivial) identification

of the angular coordinates so that we are left with the radial coordinates r_{S} and R_{F}.

We now constrain the Schwarzschild line element to the region $r_{\mathrm{S}} < r_{\mathrm{S,match}}$ and the FLRW line element to $R_{\mathrm{F}} > R_{\mathrm{F,match}}$. Glueing together the two regions therefore determines the vacuole surface

$$r_{\mathrm{S,match}} = R_{\mathrm{F,match}} \doteq r_{\mathrm{vac}} \quad . \tag{4.12}$$

A generalised radial coordinate r would correspond to r_{S} for $r < r_{\mathrm{vac}}$ and to R_{F} for $r > r_{\mathrm{vac}}$. We will make use of this shorthand notation throughout the next section.

The two metrics should blend at the surface of the vacuole, i.e. the induced metrics on Σ_{S} and Σ_{F} are required to match:

$$\begin{aligned} ds^2_{\Sigma_{\mathrm{S}}} = ds^2_{\mathrm{S}}\Big|_{r_{\mathrm{S}}=r_{\mathrm{vac}}} &= -(1-\frac{2m}{r_{\mathrm{vac}}})\,dt^2 + r^2_{\mathrm{vac}}\,d\Omega^2 \\ &\stackrel{!}{=} -(1-H(t)^2\,r^2_{\mathrm{vac}})\,dt^2 + r^2_{\mathrm{vac}}\,d\Omega^2 \\ &= ds^2_{\mathrm{F}}\Big|_{R_{\mathrm{F}}=r_{\mathrm{vac}}} = ds^2_{\Sigma_{\mathrm{F}}} \quad . \end{aligned} \tag{4.13}$$

This yields a condition on r_{vac}, namely

$$\frac{2m}{r_{\mathrm{vac}}} \stackrel{!}{=} H(t)^2\,r^2_{\mathrm{vac}} \quad \Longrightarrow \quad r^3_{\mathrm{vac}} = \frac{2m}{H^2} \quad . \tag{4.14}$$

The qualitative statement of this final relation is evident: increasing the central mass will enlarge the vacuole radius whereas intensifying the rate of global expansion diminishes it. The determination of the vacuole radius implements a rather intuitive condition, namely that the mass of the central star should exactly amount to the excised mass from the cosmic matter fluid. This will be further discussed in the physical interpretation section at the end of this chapter by means of a concept of quasi-local mass (viz. the Misner-Sharp energy).

To compare our final result (4.14) to Schücking's expression (35) in [Schücking, 1954], one needs to make use of the first Friedmann equation (2.57a) (considering vanishing curvature $k = 0$ and cosmological constant $\Lambda = 0$, i.e. the critical density (2.58))

$$H^2 = \frac{8\pi G}{3}\,\rho \quad , \tag{4.15}$$

which leads to

$$r_{\text{vac}} = \sqrt[3]{\frac{6m}{8\pi G\rho}} \quad . \tag{4.16}$$

(For comparative purposes, note that Schücking uses $\kappa \doteq 8\pi G$.)

4.3 Extrinsic Curvature on the Vacuole Surface

In the previous section we have established the continuous transition of the intrinsic geometrical properties, namely that both metrics merge across the vacuole surface Σ_{vac}. For this transition to be smooth, we expect the first derivatives of the metrics to merge as well, i.e. the second fundamental forms on both sides should coincide on the hypersurface. This results in the energy-momentum tensor (related via the Einstein equations to the second derivatives of the metric, namely the Riemann tensor) to merely feature a finite discrete jump at the radius r_{vac}. As anticipated above, on the inner side of the vacuole there is vacuum $T_{\mu\nu} = 0$, whereas on the outside we have the homogeneously distributed cosmic matter fluid.

The derivatives tangent to Σ_{vac} trivially coincide because the two metrics are completely equivalent at the fixed radius r_{vac} due to (4.14), as shown above. Hence, we only need to check for the normal directions on Σ_{vac}. Since we consider a four-dimensional space-time and a three-dimensional hypersurface, we are left with one linearly independent vector being normal to Σ_{vac}, which we call N. We further know that N must be spacelike since the hypersurface has a basis of one timelike and two spacelike vectors. Now we can use the extrinsic curvature tensor defined in chapter 2 to compare the two sides of Σ_{vac}. The procedure comprises computing $K_{\mu\nu}$ for both the Schwarzschild and the FLRW line element, subsequently we check whether both expressions coincide.

First things first: we begin to construct the normal vector N^μ on the vacuole surface. The tangent vectors spanning Σ_{vac} are on the one hand

(i) the two spacelike (and orthogonal to one another) vectors on S^2,

and on the other hand

(ii) the timelike geodesics whose trajectories are described by the velocity field u^μ.

The orthogonality to (i) leads to the conclusion that the spatial part of N must be purely radial, i.e. the angular components $N^\vartheta = N^\varphi = 0$ with $N^\mu N_\mu = 1$. Recall that our PG coordinates are adapted to freely falling outbound observers, i.e. the velocity field u matches the geodesics $u = \partial/\partial\widetilde{t}_{\text{S}}$. It therefore has components $u^\mu = (1, 0, 0, 0)$, resp.

$$u_\mu = g_{\mu\nu}u^\nu = g_{\mu\nu}(-\partial^\nu \widetilde{t}_{\text{S}}) = -\partial_\mu \widetilde{t}_{\text{S}} = (-1, 0, 0, 0) \tag{4.17}$$

in PG coordinates for the Schwarzschild case. The same trivially applies to the FLRW case (the expression for N on the vacuole surface cannot depend on the Schwarzschild or FLRW line element, they both coincide for r_{vac} anyway). Thus, the normal vector is also orthogonal to the timelike tangent vector field (ii), $N^\mu u_\mu = 0$, so that we obtain

$$N^\mu = (0, 1, 0, 0) \quad , \quad \text{resp.} \quad N = \frac{\partial}{\partial r} \quad . \tag{4.18}$$

Since the radial entries of both metrics amount to 1 in the PG coordinate system, a vector field extension of N^μ will have the same radial components within the whole vicinity of Σ_{vac}.

We now introduce the first fundamental form of Σ_{vac}, resp. the induced metric $h_{\mu\nu} \doteq g_{\mu\nu} - N_\mu N_\nu$, where the extended covector field N_μ has a radial component of 1 and a non-vanishing time component

$$N_t = \begin{cases} \sqrt{\dfrac{2m}{r}} & , r \leq r_{\text{vac}} \\ H(t)\, r & , r \geq r_{\text{vac}} \end{cases} \quad . \tag{4.19}$$

The induced metric provides us with projectors $h_\mu{}^\nu = \delta_\mu{}^\nu - N_\mu N^\nu$, which project tensor fields reduced to the hypersurface onto Σ_{vac} itself.

This we use to finally determine a nice expression for the symmetric extrinsic curvature tensor (2.63)

$$\begin{aligned} K_{\mu\nu} &= h_\mu{}^\rho h_\nu{}^\sigma \nabla_\rho N_\sigma \\ &= h_\mu{}^\rho h_{\nu\sigma} \underbrace{\nabla_\rho N^\sigma}_{\cancel{\partial_\rho N^\sigma} + \Gamma^\sigma{}_{\rho\lambda} N^\lambda} \\ &= h_\mu{}^\rho h_{\nu\sigma} \Gamma^\sigma{}_{\rho\lambda} N^\lambda \quad . \end{aligned} \tag{4.20}$$

Having the explicit form of the second fundamental form (4.20), we are now enabled to check whether the extrinsic curvature on Σ_{vac} is of the same value regardless whether we are coming from the outer FLRW or inner Schwarzschild region.

(i) entries involving one *radial* index: the extrinsic curvature tensor of Σ_{vac} lives on the tangent submanifold and is therefore orthogonal to the normal vector by construction. Accordingly, fixing one index to be radial by considering the inner product of K with N gives

$$K_{\mu\nu} N^\nu = h_\mu{}^\rho \left(\nabla_\rho N^\sigma\right) \underbrace{h_{\sigma\nu} N^\nu}_{=0} = 0 \quad . \tag{4.21}$$

We are left to check the coincidence of the angular and time components of $K^{\text{S,F}}_{\mu\nu}$.

(ii) pure *angular* part: let $a, b \in \{\vartheta, \varphi\}$.
The only non-vanishing component of N^μ is the radial one, as a consequence the surface projector fully reproduces the angular part, $h_a{}^\mu = \delta_a{}^\mu$. This entails

$$K_{ab} = \Gamma_{bar} N^r = \frac{1}{2} \left(\partial_r g_{ba} + \partial_a \cancel{g_{br}} - \partial_b \cancel{g_{ar}} \right) \quad . \tag{4.22}$$

The angular parts of both metrics are the same, hence

$$K^{\text{S}}_{ab} = \frac{1}{2} \partial_{r_{\text{S}}} g^{\text{S}}_{ab} = \frac{1}{2} \partial_{R_{\text{F}}} g^{\text{F}}_{ab} = K^{\text{F}}_{ab} \quad . \tag{4.23}$$

(iii) pure *time* component: the scalar product of the extrinsic curvature tensor with the (timelike) geodesic flow vector field u^μ reveals the amount of curvature in pure time direction,

$$\begin{aligned} K_{\mu\nu}u^\mu u^\nu &= h^\rho{}_\mu u^\mu h^\sigma{}_\nu u^\nu \nabla_\rho N_\sigma = u^\rho u^\sigma \nabla_\rho N_\sigma \\ &= u^\rho \nabla_\rho (\underbrace{u^\sigma N_\sigma}_{=0}) - u^\rho (\underbrace{\nabla_\rho u^\sigma}_{=0}) N_\rho \quad . \end{aligned} \tag{4.24}$$

The two terms vanish because N is orthogonal to u and geodesics obey $\nabla_\mu u_\nu = 0$ ("freely moving" test particles) per definition.
Therefore, there is no extrinsic time curvature on the hypersurface

$$K_{tt}^{\mathrm{S,F}} = 0 \quad . \tag{4.25}$$

This result is intuitive because we match the two metrics along timelike geodesics u^μ, their time progression should be undistorted.

And last but not least the off-diagonal entries concerning the

(iv) mixed *time and angular* part: as before, we contract the extrinsic curvature tensor by one u and restrict the other index to the angular entries,

$$\begin{aligned} K_{a\nu}u^\nu &= \underbrace{h_a{}^\rho}_{=\delta_a{}^\rho} h_{\nu\sigma}\Gamma^\sigma{}_{\rho r}u^\nu \\ &= (g_{\nu\sigma}u^\nu - \underbrace{N_\nu u^\nu}_{=0} N_\sigma)\Gamma^\sigma{}_{ar} \\ &= u^\nu \frac{1}{2}\,(\underbrace{\partial_a g_{\nu r}}_{=0} + \partial_r g_{\nu a} - \partial_\nu \cancel{g_{ar}}) \quad . \end{aligned}$$

The remaining term yields zero since u^ν exhibits no angular part and corresponding to the non-vanishing components of u^ν, we come across $g_{ta} = g_{ra} = 0$ (the metric does not feature any off-diagonal angular entries). Consequently, Σ_{vac} features no extrinsic curvature in the mixed time and angular directions. That way we obtain

$$K_{at}^{\mathrm{S,F}} = 0 \quad . \tag{4.26}$$

Summarising, the only non-vanishing components of the extrinsic curvature tensor are the diagonal angular entries and these coincide for the Schwarzschild side as well as the FLRW side of the vacuole surface.

We have established that the first and the second fundamental forms on Σ_{vac} are continuous across the hypersurface. This should not be too surprising as we have glued together the two space-time regions using geodesics so that the metrics merge in a second-order transition (at least, in principle). Recall the discussion in the introduction to this chapter concerning the discontinuous behaviour of the Riemann tensor: it necessarily exhibits a discrete jump since the Einstein equations directly relate the curvature of the space-time to the energy-momentum tensor, which features the aforementioned discrete step from vacuum to diluting (pressureless) cosmic matter fluid on the vacuole surface. If the transition of the metrics was of first order, the Riemann tensor and the energy-momentum tensor would rather exhibit something rare like an infinitely high peak at r_{vac}.

4.4 Physical Interpretation

We have reconstructed a model for the embedding of the exterior gravitational field of a star or, in general, a massive object into an expanding FLRW space-time. The radius r_{vac} of this Einstein-Straus vacuole gives a hint at the scale, from which on global expansion dominates local attraction of the central massive body. Our Sun may be modelled by the Schwarzschild solution, so let us apply the Einstein-Straus concept to learn about its predictions for the Solar System. Table 4.1 contains a compilation of values of the Schücking radius for comparative purposes.

The huge values for the smaller-sized objects strike the eye: e.g. r_{vac} for the Sun is about two orders of magnitude larger than the distance to the next star within our galaxy. In principle one could simply insert more non-overlapping vacuoles into the FLRW space-time – the model is often referred to as the "Swiss cheese" model – but this would then consequently not be applicable to our Solar System and its neighbouring stars. Accordingly, the Einstein-Straus vacuole is no appropriate model at the scale of stars within a galaxy since the vacuoles of the stars would overlap (the average distance

Object	Mass	Schücking Radius r_{vac}
Earth	$M_\oplus \approx 6 \times 10^{24}$ kg	6 ly
Sun	$M_\odot \approx 2 \times 10^{30}$ kg	400 ly
Local Group	$10^{12}\, M_\odot \approx 10^{42}$ kg	4×10^6 ly

Table 4.1: Compilation of some rough estimates for the Schücking radius assuming the critical density $\rho = \rho_{\text{critical}} = 3H^2/(8\pi G)$ for a dust-filled FLRW space-time and a Hubble constant of $H_0 = 70$ km s^{-1} Mpc^{-1}.

between stars in the Milky Way is of the same order of magnitude as in the special case of our Sun).

However, things change at the scale of whole galaxies, e.g. at the structural level of the Local Group. Its centre of mass is located between its two most massive objects, viz. the Andromeda galaxy and our Milky Way. The former has recently been measured to lie at a distance of about 2.5 million light years, cf. [Ribas *et al.* , 2005]. The vacuole of the Local Group only just evades overlapping the next vacuoles of our neighbouring galaxy groups, as for instance the one of M81 Group. The mass of the M81 Group amounts to slightly less than the Local Group's mass, i.e. the Schücking radius of M81 is of the same magnitude, and its centre of mass is located a little more than 11 million light years away from us, cf. [Karachentsev, 2005]. This little comparison shows that the Swiss cheese model could in principle be applied on scales of galaxy groups, i.e. 10 million light years and upwards. Consequently, objects at these distances are predicted to recede from each other. Actually, the experimental results of the last decades confirm that most objects indeed recede from the Milky Way from this order of magnitude on, as expounded in the introductory chapter.

As a side note, the Swiss cheese model has also been used to study domain walls and voids (cf. [Nolan, 1998]).

Note also that the Einstein-Straus vacuole can easily be extended to include a cosmological constant $\Lambda \neq 0$, which would promote the Schwarzschild region to a Schwarzschild-de-Sitter space-time and add some $\rho_\Lambda = \Lambda/(8\pi G)$ to the perfect fluid density. The derived expression (4.14) for the Schücking radius nevertheless remains unaffected.

Another beautiful and intuitive way to arrive at the expression for the Schücking radius is to understand the vacuole excision and matching in the following way (cf. [Carrera & Giulini, 2009a]): one cuts out a sphere of the FLRW metric and fits in the vacuole taking into account that the central mass object has to correspond exactly to the removed cosmic matter inside of the sphere. Within the Newtonian framework we are well aware of the fact that the gravitational attraction outside of a spherically symmetric object is independent of its radial distribution. This argument applies in the same way to a general relativistic picture, thus justifying the above statement of replacing the uniformly distributed perfect fluid within the sphere by a point-like object of the same mass and surrounding vacuum. This is guaranteed by Birkhoff's theorem (cf. chapter 2). The dynamics outside of the vacuole are not affected by this replacement. We remark that the vacuole surface expands with the FLRW space-time as it is fixed at a certain comoving radius.

The notion of Misner-Sharp energy comes in handy at this point. The energy content of the Schwarzschild space-time simply corresponds to the mass parameter $G \cdot E = m$, whereas the mass content of a sphere of circumferential radius R in the FLRW space-time indeed gives $G \cdot E = \frac{4}{3}\pi R_{\mathrm{F}}^3 \rho$ (corresponding to the volume of a sphere with constant mass content times the mass density). Demanding these two to be equal and considering the critical energy density $\rho = \rho_{\mathrm{crit}} = 3H^2/(8\pi G)$ of a flat and dust-filled FLRW space-time (see (2.58)), one directly retrieves expression (4.14). Bringing a non-vanishing cosmological constant into play emerges in the same way in both expressions for the Misner-Sharp energy, which is why the expression for the Schücking radius does not change in an explicit way:

$$G \cdot E_{\mathrm{F}} = \frac{4}{3}\pi R_{\mathrm{F}}^3(\rho + \rho_\Lambda) \quad \text{and} \quad G \cdot E_{\mathrm{S}} = m + \frac{4}{3}\pi r_{\mathrm{S}}^3 \rho_\Lambda \quad , \tag{4.27}$$

the ρ_Λ contributions are equal for $r_{\mathrm{S,match}} = R_{\mathrm{F,match}} = r_{\mathrm{vac}}$. However, Λ will implicitly enter the Schücking radius expression via H.

This mass matching viewpoint immediately indicates a conceptually critical feature of the Einstein-Straus vacuole: slight perturbations of the matching radius would result in an either too "light-weight" or too "heavy" vacuole compared to the mass of the removed cosmic matter. As the derived vac-

uole radius corresponds to an equilibrium where the gravitational attraction exactly cancels the expansion effect, the prevailing one of the two would completely determine the evolution of the vacuole in case they were out of balance. This has been analysed in great detail in [Krasiński, 1997] throughout the third chapter. The bottom line is that the Einstein-Straus vacuole constitutes an unstable situation corresponding in metaphorical way to a pencil balanced on its very tip.

5

On McVittie Space-times

In the first third of the last century, among others, George C. McVittie studied the description of an observer in the vicinity of a mass-particle like the Sun, which itself is situated within a cosmic background. In his setting, he sought for an interpolation between the Schwarzschild space-time, which describes the exterior gravitational field of a spherically symmetric massive body, and the FLRW space-time, which models global isotropic homogeneous expansion far away from the object. In 1933, McVittie published a paper [McVittie, 1933], in which he presents and analyses a space-time describing a transition between these two. In contrast to the concept of the Einstein-Straus vacuole to be developed about ten years later (cf. chapter 4), the orbits in the McVittie space-time may in principle indeed be affected by the global expansion of space.

McVittie's "mass-particle in an expanding universe" was subject to many subsequent studies: it triggered controversial discussions about the physical interpretation of the central object and the different horizons. In the late 1990s, Brien C. Nolan thoroughly examined the McVittie space-time in a series of three papers [Nolan, 1998], [Nolan, 1999a] and [Nolan, 1999b]. His work provides a quite firm base for the recently rekindled debate on that

topic. Take, for example, the Pioneer anomaly, which gave rise to (in that case unjustified) doubts about the neglect of cosmic expansion on the scale of the Solar System (cf. [Carrera & Giulini, 2009a]). A few issues in Nolan's work concerning the interpretation of the central object have recently been rectified in [Kaloper *et al.* , 2010] and refined by [Lake & Abdelqader, 2011].

Throughout the following discussion, we restrict ourselves to an asymptotically spatially flat geometry, i.e. $k = 0$. [Kaloper *et al.* , 2010] reinforces this restriction by considering that for $k = \pm 1$, the curvature radius $a(t)$ is much larger than the gravitational radius (resp. the spatial dimension) of the mass-particle for most astrophysical applications. Thus, the spatial curvature of the FLRW geometry should not significantly influence the behaviour of the metric close to the mass-particle. Now, McVittie's idea is based upon the Schwarzschild metric for a black hole of mass M in its isotropic form (2.37) while allowing for a time dependence of $M \to M(t)$ as well as introducing the scale parameter $a(t)$ to the spatial part. Denoting $m(t) \doteq GM(t)$, one obtains

$$ds^2_{\mathrm{MV}} = -\left(\frac{1-\frac{m(t)}{2r}}{1+\frac{m(t)}{2r}}\right)^2 dt^2 + \left(1+\frac{m(t)}{2r}\right)^4 a(t)^2 \left(dr^2 + r^2 d\Omega^2\right) \quad . \quad (5.1)$$

The two non-negative functions $a(t)$ and $m(t)$ are yet to be determined. We refer to this distinguished case (featuring $k = 0$ asymptotic curvature) of the general McVittie class when using the designation "the McVittie metric". In analogy to the Schwarzschild case in section 2.3, we restrict the metric to the region $r > m(t)/2$. In the limit $r \to \infty$, (5.1) asymptotically fades to the FLRW metric. The case $r \leq m(t)/2$ has been analysed in [Nolan, 1999b].

Per construction, the McVittie metric reduces to the Schwarzschild metric when fixing $a(t) = \text{const}$ and to the ordinary FLRW metric in the limit $m \to 0$. For reasons of convenience, we rewrite the McVittie metric (featuring coordinates $\{x^\mu = t, r, \vartheta, \varphi\}$) in terms of the accordingly adapted orthonormal tetrad basis $\{e_a = e_a{}^\mu \partial_\mu\}_{a=0\ldots3}$, the coefficients of which are

$$e_a{}^\mu = \|\partial_a\|^{-1} \, \delta_a{}^\mu = \frac{\delta_a{}^\mu}{\sqrt{|g_{\mu\mu}|}} \quad (5.2)$$

due to the diagonal form of (5.1) (cf. chapter 2.5.3). We observe that e_0

and e_1 are orthogonal to the two-spheres of constant radius r and that e_2 and e_3 are tangent to them.

For the energy content of the McVittie space-time, we assume a perfect fluid flowing along the vector field u^μ:

$$T^{\mu\nu} = (\rho + p)\, u^\mu u^\nu + p\, g^{\mu\nu} \quad , \tag{5.3}$$

where ρ marks the cosmic matter density and p the isotropic pressure. A cosmological constant of the form $\Lambda/(8\pi G)$ (in addition to the energy-momentum tensor $T_{\mu\nu}$) is in principle allowed. We do not assume any equation of state $p = p(\rho)$. The reason for this will fall into place soon. Concerning the energy content we assume the fluid to follow the timelike integral lines of e_0:

$$u^\mu = {e_0}^\mu \quad . \tag{5.4}$$

Hence, the energy-momentum tensor in the said tetrad base (indicated by a prime) reads

$$\begin{aligned} T'^{ab} &= {e^a}_\mu {e^b}_\nu\, (\rho + p)\, {e_0}^\mu {e_0}^\nu + p\, {e^a}_\mu {e^b}_\nu\, g^{\mu\nu} \\ \Longrightarrow \quad & T'^{00} = \rho \quad \text{and} \quad T'^{ij} = p\, \delta^{ij} \quad . \end{aligned} \tag{5.5}$$

5.1 Einstein Equations

We start from (5.1) and (5.5) and apply Einstein's equation. First of all, the Einstein tensor in the tetrad base (5.2) reads

$$\begin{cases} G'_{00} = 3F(t,r)^2 \\ G'_{01} = G'_{10} = \dfrac{2}{R(t,r)^2} \left(\dfrac{1 + \frac{m(t)}{2r}}{1 - \frac{m(t)}{2r}} \right)^2 \dfrac{\partial}{\partial t}(a(t)m(t)) \\ G'_{02} = G'_{03} = G'_{20} = G'_{30} = 0 \\ G'_{ij} = -\left(3F(t,r)^2 + 2 \left(\dfrac{1 + \frac{m(t)}{2r}}{1 - \frac{m(t)}{2r}} \right) \dfrac{\partial F}{\partial t}(t,r) \right) \delta_{ij} \end{cases} \tag{5.6}$$

where we define the functions

$$\begin{aligned} F(t,r) &\doteq \frac{\dot{a}(t)}{a(t)} + \frac{1}{r - \frac{m(t)}{2}} \frac{\frac{\partial}{\partial t}\big(a(t)m(t)\big)}{a(t)} \qquad \text{and} \\ R(t,r) &\doteq \left(1 + \frac{m(t)}{2r}\right)^2 a(t)\, r \end{aligned} \tag{5.7}$$

(dots represent derivatives w.r.t. t).

Let us take things slowly and dwell on the Einstein tensor in order to discern its structure. First of all, its spatial part is isotropic $G'_{ij} \propto \delta_{ij}$ which immediately implies that, whatever the energy content of the space-time, it must necessarily exhibit spatial isotropy as well. The function R resembles a more complex version of the FLRW proper circumferential distance, more information on R can be found in section 5.3. Note that F can be written as a divergence, $F = \nabla_\mu e_0{}^\mu/3$ (cf. appendix B.1), i.e. F describes the expansion of the vector field e_0, which is the velocity of the perfect fluid. Another quantity strikes the eye: $a(t) \cdot m(t)$ amounts to the Weyl part of the Misner-Sharp energy. This statement will be explained and substantiated in the next section.

Now we demand Einstein's equations

$$G_{\mu\nu} = 8\pi G\, T_{\mu\nu} \tag{5.8}$$

to hold. This gives us several conditions in analogy to the Friedmann equations (2.57). We go through them one by one:

$$G'_{01} \stackrel{!}{=} 0 \quad \Longrightarrow \quad \frac{\partial}{\partial t}\big(a(t)m(t)\big) = 0 \quad \Longrightarrow \quad m(t) = \frac{m_0}{a(t)} \tag{5.9}$$

with a constant m_0. We will suppress arguments from here on. (5.9) entails $F = \dot{a}/a \doteq H$ which is the usual Hubble parameter that we know from the FLRW space-time. Consequently, the above-mentioned interpretation of F is justified: as expounded in the introductory chapter, other galaxies recede with apparent velocities $v \approx H_0 D$ (with D being the proper distance), i.e. the cosmic matter dilutes with H. Observe that, hereby, the Einstein equations explicitly relate the originally independent functions $m(t)$ and $a(t)$.

Furthermore we have

$$G'_{00} \stackrel{!}{=} 8\pi G\, T'_{00} \quad \Longrightarrow \quad 3\left(\frac{\dot{a}}{a}\right)^2 = 8\pi G\,\rho \quad , \tag{5.10}$$

i.e. $\rho = \rho(t)$ as one would expect for spatially homogeneously distributed cosmic matter.

Last but not least, the spatial part of the Einstein equations yields

$$\begin{gathered} G'_{ij} \stackrel{!}{=} 8\pi G\, T'_{ij} \\ \Longrightarrow \quad -3\left(\frac{\dot{a}}{a}\right)^2 - 2\left(\frac{1+\frac{m(t)}{2r}}{1-\frac{m(t)}{2r}}\right)\frac{\partial}{\partial t}\left(\frac{\dot{a}}{a}\right) = 8\pi G\, p \quad , \end{gathered} \tag{5.11}$$

i.e. $p = p(t, r)$. This explains why we could not simply impose an equation of state beforehand: the pressure p also depends on the radius r as opposed to the cosmic matter density ρ.

5.2 Physical Interpretation

There are two simple ways to enforce an equation of state for the McVittie space-time, namely requiring either (i) $p = 0$ or (ii) $p = -\rho$:

(i) $p = 0$ entails

$$\left(\frac{\dot{a}}{a}\right)^2 = 0 \quad \text{and} \quad \left(\frac{1+\frac{m(t)}{2r}}{1-\frac{m(t)}{2r}}\right)\frac{\partial}{\partial t}\left(\frac{\dot{a}}{a}\right) = 0 \quad , \tag{5.12}$$

separately (if $m_0 > 0$). Therefore we have $H = 0$, which implies $a(t) = \text{const}$. W.l.o.g. we set $a(t) = 1$ and simply recover the Schwarzschild metric.

(ii) $p = -\rho$ leads to

$$\begin{aligned} 8\pi G(\rho + p) &= 3\cancel{\left(\frac{\dot{a}}{a}\right)^2} - 3\cancel{\left(\frac{\dot{a}}{a}\right)^2} - 2\left(\frac{1+\frac{m(t)}{2r}}{1-\frac{m(t)}{2r}}\right)\frac{\partial}{\partial t}\left(\frac{\dot{a}}{a}\right) \\ &\stackrel{!}{=} 0 \quad , \end{aligned} \tag{5.13}$$

i.e. $\dot{H} = 0$ and therefore $H = \text{const}$. W.l.o.g. we set $H(t) = \sqrt{\Lambda/3}$ which implies $a(t) \propto \exp(\sqrt{\Lambda/3}\, t)$ having a cosmological constant Λ.

Wee see that this entails

$$\frac{\partial p}{\partial r} = \frac{1}{8\pi G}\frac{\partial}{\partial r}\left[-3\left(\frac{\dot{a}}{a}\right)^2 - 2\left(\frac{1+\frac{m(t)}{2r}}{1-\frac{m(t)}{2r}}\right)\underbrace{\frac{\partial}{\partial t}\left(\frac{\dot{a}}{a}\right)}_{=0}\right]$$

$$\Longrightarrow \quad \frac{\partial p}{\partial r} \propto \dot{H} = 0 \quad , \tag{5.14}$$

as well as

$$\frac{\partial p}{\partial t} \propto \left\{\dot{H}, \ddot{H}\right\} = 0 \quad . \tag{5.15}$$

Taken together, these two ensure $dp = 0$ and thus $d\rho = 0$.

In summary, setting $p = -\rho$ induces the presence of a cosmological constant Λ (we have $-8\pi G\, p = 8\pi G\, \rho = \Lambda$) and the Einstein equations $G'_{ab} + \Lambda\eta_{ab} = 0$ indicate that Λ is indeed all there is besides the mass-particle. Therefore, the underlying assumption of $p = -\rho$ necessarily leads to a simple Schwarzschild-de-Sitter space-time.

We conclude that for a genuine McVittie space-time, no equation of state $p = p(\rho)$ can be assumed beforehand, instead both ρ and p are determined by Einstein's equations.

The asymptotic scale factor $a(t)$ may be freely chosen and determines $m(t)$ via (5.9) for a fixed m_0. [Nolan, 1998] used the concept of the Hawking mass (which is equivalent to the Misner-Sharp energy in a spherically symmetric space-time) to analyse the meaning of m_0. Here, [Carrera & Giulini, 2009a] provides a detailed and neatly arranged discussion. According to our discussion in 2.5.2, the Ricci and Weyl part of the Misner-Sharp energy read

$$G \cdot E_{\text{Ricci}} = \frac{4}{3}\pi R^3 \rho \quad \text{and} \quad G \cdot E_{\text{Weyl}} = a(t)\, m(t) = m_0 \quad . \tag{5.16}$$

E_{Weyl} vanishes if and only if the Weyl tensor does so (cf. appendix D of [Carrera & Giulini, 2009a] for a rigorous derivation). As discussed in section 2.5.2, the Ricci part of the Riemann tensor $R^{\mu}{}_{\sigma\mu\nu}$ is orthogonal to the Weyl part w.r.t. the metric $g_{\mu\nu}$. Recall that the Weyl tensor is trace-free and essentially encodes the vacuum part of the gravitational information contained in the Riemann tensor. In our case, this is the source of the gravitational potential – namely the curvature singularity at $r = 0$, i.e. our mass-particle. Consequently, the mass of the central object may be identi-

fied with E_{Weyl}. Its constancy expresses the fact that the central object does not accrete mass from its surroundings, realised by the substantial increase of the pressure $p(t, r)$ towards the mass-particle right up to the divergence in the limit $r \to r_{\text{div}}(t) \doteq m(t)/2$. Interestingly, in his original paper from 1933, G. C. McVittie argued the other way round by first assuming the central mass-particle to not accrete mass and imposing a corresponding condition and thus, afterwards, arriving at (5.9).

That r_{div} indeed constitutes a true singularity can be directly inferred from the Ricci scalar

$$R = \eta^{ab} G'_{ab} = -12F^2 - 6\left(\frac{1 + \frac{m(t)}{2r}}{1 - \frac{m(t)}{2r}}\right)\frac{\partial F}{\partial t} \quad . \tag{5.17}$$

Expression (5.17) does not yet make use of the Einstein equations, based upon which F reduces to H. One immediately observes that the Ricci scalar diverges at $r \to m(t)/2$ if the space-time is not equivalent to either an FLRW, Schwarzschild or Schwarzschild-de-Sitter space-time.

As anticipated in the introduction to this chapter, the horizons and singularities of the McVittie space-time (in the special case of containing a positive cosmological constant Λ) have been studied in some detail in [Kaloper *et al.* , 2010] and [Lake & Abdelqader, 2011]. They both agree that for $\lim_{t\to\infty} H(t) \doteq H_\infty > 0$, the McVittie metric describes a regular black hole embedded in a flat FLRW space-time which is what we aimed for. Due to the asymptotic exponential expansion of the FLRW metric, the singularity r_{div} is hidden inside a trapped region behind an event horizon. Moreover, they show that, regardless of the specific form of H, the singularity sits at finite affine distance for null geodesics. That means that light rays can in some sense meaningfully reach $r_{\text{div}}(t) = m(t)/2$. However, they disagree on the interpretation of the central mass-particle and its horizon given $H_\infty = 0$, i.e. in the case that the asymptotic FLRW space-time consists of dust and/or radiation.

As a last point, some numerical values for the Solar System are presented in table 5.1.

Quantity	Numerical Value
$\dot{H}_0 = -(1+q_0)H_0^2$	8×10^{-17} km s^{-2} Mpc^{-1}
$\frac{m(t)}{2r} = \frac{2M_\oplus G}{c^2 R} \doteq \Delta_\oplus$	6×10^{-14}
$\frac{1+\frac{m(t)}{2r}}{1-\frac{m(t)}{2r}} = \frac{1+\Delta_\oplus}{1-\Delta_\oplus}$	$1 + 1.2 \times 10^{-13}$
McVittie pressure at distances around planetary orbits $p \approx -\frac{3c^2H_0^2}{8\pi G}$	-8×10^{-10} Pa

Table 5.1: Numerical values for the Solar System, based upon a Hubble constant of $H_0 = 70$ km s^{-1} Mpc^{-1} and a deceleration parameter of $q_0 = -0.5$.

5.3 Transformation to Circumferential Radius

In order to analyse non-expanding circular orbits, we will transform the coordinates of the McVittie metric (5.1) (given (5.9) with $m(t) = m_0/a(t)$) using a new set of coordinates (t, R, ϑ, ϕ), where

$$R(t,r) \doteq \left(1 + \frac{m_0}{2a(t)r}\right)^2 a(t)\, r \tag{5.18}$$

is the already anticipated circumferential radius (in some sources it is called "areal radius" for spherical symmetric metrics). It is defined for an instant t by a circle of radius R (centred at the origin) to have a proper circumference of $2\pi R$. Note that, for the general McVittie metric class, R does not coincide with proper radius – this is only the case for a flat asymptotic curvature $k = 0$. The circumferential radius (5.18) can easily be deduced from the spherically symmetric angular part (let r_0, t_0 be some fixed constant values):

$$\begin{aligned} \int \sqrt{ds^2}\Big|_{r=r_0,\, t=t_0,\, \vartheta=\frac{\pi}{2}} &= \left(1 + \frac{m_0}{2a(t_0)r_0}\right)^2 a(t_0)\, r_0 \underbrace{\int d\varphi}_{=2\pi} \\ &\stackrel{!}{=} 2\pi R \quad . \end{aligned} \tag{5.19}$$

As the original metric (5.1) is restricted to the region $r > m_0/(2a)$, where the boundary corresponds to $R = 2m_0$, we will restrict the coordinate transformation itself to $R > 2m_0$ as well. Thus, the coordinate transformation

constitutes a diffeomorphism.

Intuitively, a circular trajectory at a fixed R describes the path of a "local" observer orbiting around the central mass-particle. This statement will be investigated throughout the next sections.

We define the following set of functions

$$\begin{aligned} \mu(R) &\doteq \frac{m_0}{R} \qquad \text{and} \\ h(t,R) &\doteq H(t)R \quad , \end{aligned} \tag{5.20}$$

where $H(t) = \frac{\dot{a}(t)}{a(t)}$ stands for the usual Hubble parameter. Arguments of functions will be suppressed from here on.

Now the time part of the McVittie metric may be written as

$$\begin{aligned} \left(\frac{1-\frac{m_0}{2ar}}{1+\frac{m_0}{2ar}}\right)^2 &= \frac{ar+m_0-2m_0+\frac{m_0^2}{4ar}}{(1+\frac{m_0}{2ar})^2 ar} = \frac{(1+\frac{m_0}{2ar})^2 ar - 2m_0}{(1+\frac{m_0}{2ar})^2 ar} \\ &= 1 - \frac{2m_0}{(1+\frac{m_0}{2ar})^2 ar} = 1 - \frac{2m_0}{R} \\ &= 1 - 2\mu \quad . \end{aligned} \tag{5.21}$$

Note that this entails

$$1 - \frac{m_0}{2ar} > 0 \quad \Longrightarrow \quad 1 - 2\mu > 0 \quad . \tag{5.22}$$

For the coordinate transformation, we need the derivatives of $R(t,r)$:

$$\begin{aligned} \frac{\partial R}{\partial t} &= 2\left(1+\frac{m_0}{2ar}\right) ar \left(\frac{\partial}{\partial t}\frac{m_0}{2ar}\right) + \left(1+\frac{m_0}{2ar}\right)^2 Har \\ &= -2\left(1+\frac{m_0}{2ar}\right)\frac{m_0}{2ar} Har + \left(1+\frac{m_0}{2ar}\right)\left(1+\frac{m_0}{2ar}\right) Har \\ &= \left(1+\frac{m_0}{2ar} - 2\frac{m_0}{2ar}\right)\left(1+\frac{m_0}{2ar}\right) Har \\ &= \left(1-\frac{m_0}{2ar}\right)\left(1+\frac{m_0}{2ar}\right) Har \\ &= \sqrt{1-2\mu}\, h \quad , \end{aligned} \tag{5.23}$$

as well as

$$\begin{aligned}\frac{\partial R}{\partial r} &= 2\left(1+\frac{m_0}{2ar}\right)ar\left(\frac{\partial}{\partial r}\frac{m_0}{2ar}\right)+\left(1+\frac{m_0}{2ar}\right)^2 a \\ &= -2\left(1+\frac{m_0}{2ar}\right)\frac{m_0}{2ar}a+\left(1+\frac{m_0}{2ar}\right)\left(1+\frac{m_0}{2ar}\right)a \\ &= \left(1+\frac{m_0}{2ar}-2\frac{m_0}{2ar}\right)\left(1+\frac{m_0}{2ar}\right)a \\ &= \left(1-\frac{m_0}{2ar}\right)\left(1+\frac{m_0}{2ar}\right)a \\ &= \sqrt{1-2\mu}\,\frac{R}{r} \quad . \end{aligned} \tag{5.24}$$

In each case, the square root of (5.21) has been used in the last step. Summarising the two yields the differential

$$dR = \frac{\partial R}{\partial t}dt+\frac{\partial R}{\partial r}dr = \sqrt{1-2\mu}\left(\frac{R}{r}\,dr+h\,dt\right) \quad ,$$

which gets rearranged to

$$\frac{R\,dr}{r} = \frac{dR}{\sqrt{1-2\mu}}-h\,dt \quad . \tag{5.25}$$

Putting everything together, we rewrite the McVittie metric (5.1) as

$$\begin{aligned} ds^2_{\mathrm{MV}} &\overset{(5.21)}{=} -(1-2\mu)\,dt^2+\frac{R^2dr^2}{r^2}+R^2d\Omega^2 \\ &\overset{(5.25)}{=} -(1-2\mu)\,dt^2+\left(\frac{dR}{\sqrt{1-2\mu}}-h\,dt\right)^2+R^2d\Omega^2 \end{aligned}$$

and finally arrive at the now non-diagonal form of the metric, expressed in terms of the circumferential radius R:

$$\begin{aligned} ds^2_{\mathrm{MV}} = &-\left(1-2\mu(R)-h(t,R)^2\right)dt^2+ \\ &-\frac{2h(t,R)}{\sqrt{1-2\mu(R)}}\,dt\,dR+\frac{dR^2}{1-2\mu(R)}+R^2d\Omega^2 \quad . \end{aligned} \tag{5.26}$$

5.4 Geodesics in the McVittie Space-time

As we are interested in local dynamics, we will investigate the geodesic equation for the McVittie metric in the following section. Here, the circumferential radius R comes in handy – hence, we use (5.26) as a starting point.

A timelike geodesic $x = x(\tau)$ that is parametrised w.r.t. its proper time τ satisfies equation (2.21). In the following, we will derive a set of equations determining the trajectory of a test particle (such as a planet, spacecraft or the like) by means of the Euler-Lagrange method presented in section 2.2. We assume the test particle to have unit rest mass, which is supposed to be negligibly small compared to the central mass M.

Since the McVittie metric is spherically symmetric, we may fix a spatial plane in which the trajectory will be situated. W.l.o.g., $\vartheta = \pi/2$ is a reasonable choice of coordinate system such that $\sin(\vartheta) = 1$ and $\dot{\vartheta} = 0$, i.e. the motion takes place in the equatorial plane. Now we obtain four Euler-Lagrange equations for the Lagrangian

$$\begin{aligned}\mathcal{L} = &- \left(1 - 2\mu(R) - h(t,R)^2\right) \dot{t}^2 + \\ &- \frac{2h(t,R)}{\sqrt{1-2\mu(R)}} \dot{R}\,\dot{t} + \frac{1}{1-2\mu(R)}\dot{R}^2 + R^2\dot{\varphi}^2 \quad .\end{aligned} \tag{5.27}$$

The equation for $\vartheta(\tau)$ is trivial due to our choice of coordinate system. The spherical symmetry of the metric implies conservation of angular momentum, which is expressed in the equation for $\varphi(\tau)$:

$$\frac{\partial \mathcal{L}}{\partial \varphi} \overset{!}{=} \frac{d}{d\tau}\frac{\partial \mathcal{L}}{\partial \dot{\varphi}} \qquad \overset{\frac{\partial}{\partial\varphi}\mathcal{L}=0}{\Longrightarrow} \qquad L \doteq R^2\dot{\varphi} = \text{const} \quad . \tag{5.28}$$

L labels the angular momentum (per unit rest mass). The parametrisation invariance of the Lagrangian, $\frac{d}{d\tau}\mathcal{L} = 0$, can be expressed in terms of the normalisation condition:

$$\begin{aligned}-1 = &- \left(1 - 2\mu(R) - h(t,R)^2\right) \dot{t}^2 + \\ &- \frac{2h(t,R)}{\sqrt{1-2\mu(R)}} \dot{R}\,\dot{t} + \frac{1}{1-2\mu(R)}\dot{R}^2 + \frac{L^2}{R^2}\end{aligned} \tag{5.29}$$

(which is thus an integral of the Euler-Lagrange equation for $t(\tau)$). We note

that this implies $1 - 2\mu(R) - h(t,R)^2 > 0$.

The two remaining Euler-Lagrange equations for $t(\tau)$ and $r(\tau)$ provide a system of coupled second-order ordinary differential equations. Its derivation and the ensuing elimination of $\ddot{t}$ terms leading to a radial equation of motion are carried out in appendix B.2.

The resulting set of equations – comprising angular momentum conservation (5.28), the normalisation condition (5.29) and the radial equation (B.8) – completely determines the timelike trajectory of an (equatorially moving) observer in the McVittie space-time:

$$\begin{cases} L = R^2\dot{\varphi} = \text{const} \\ -1 = -\left(1 - 2\mu(R) - h(t,R)^2\right)\dot{t}^2 + \\ \qquad - \dfrac{2h(t,R)}{\sqrt{1-2\mu(R)}}\,\dot{R}\,\dot{t} + \dfrac{1}{1-2\mu(R)}\dot{R}^2 + \dfrac{L^2}{R^2} \\ 0 = \ddot{R} - \left(1 - 2\mu - h^2\right)\dfrac{L^2}{R^3} + \dfrac{\mu}{R}(1-2\mu)\,\dot{t}^2 + \\ \qquad - R\left(\dfrac{\partial H}{\partial t}\sqrt{1-2\mu} + \dfrac{h^2}{R^2}\left(1 - \mu - h^2\right)\right)\dot{t}^2 + \\ \qquad - \dfrac{\mu - h^2}{1-2\mu}\,\dfrac{\dot{R}^2}{R} + \dfrac{2\left(\mu - h^2\right)}{\sqrt{1-2\mu}}\,\dfrac{h}{R}\,\dot{R}\,\dot{t} \quad . \end{cases} \tag{5.30}$$

Up to here, no approximations have been made, all equations are exact. As the McVittie metric interpolates between the Schwarzschild and the FLRW metric, (5.30) indeed reduces to the Schwarzschild geodesics in the case of $a(t) = \text{const}$ and to the FLRW geodesics in the case of $m_0 = 0 \Rightarrow \mu = 0$ (as well as $L = 0$ for freely falling observers).

Comparing to the Next-to-Newtonian equation of motion (3.4) (where $t = \tau$ and hence $\dot{t} \equiv 1$, as well as $m_0 = GM = C$),

$$0 = \ddot{R} - \frac{L^2}{R^3} + \frac{\mu}{R} - \frac{\ddot{a}}{a}\,R \quad ,$$

we observe many higher-order "corrections" in (5.30).

5.4.1 Reduction to Next-to-Newtonian Case

The Next-to-Newtonian case can be recovered by applying some approximations. We focus on Keplerian orbits, i.e. we are interested in the region far away from the Schwarzschild radius R_S (cf. (1.5)), which is still not overly dominated by the expansion effect from the vicinity of the Hubble radius R_H (cf. (1.6)) on outwards:

$$R_S \ll R \ll R_H \quad . \tag{5.31}$$

Hence, we are in a slow-motion regime, orbiting test objects have velocities $v \ll 1$ (in units where $c \doteq 1$).

Our Solar System, for instance, satisfies (5.31): the Sun has a Schwarzschild radius of $R_S \approx 3\,\mathrm{km} \approx 1.97 \times 10^{-8}\,\mathrm{AU}$, the planets orbit between approximately 0.4 AU (Mercury) and 30 AU (Neptune) and the current Hubble radius of our Universe amounts to $R_H \approx 9.9 \times 10^9\,\mathrm{ly} \approx 6.26 \times 10^{14}\,\mathrm{AU}$.

Besides that, the region (5.31) corresponds to a weak-field regime, i.e. the strong gravitational effects which rely on a general relativistic description can be neglected.

Furthermore, the typical time scale T of a test object, e.g. the period of an orbiting planet $T \propto R/v$, should be very small in comparison to the age of the universe, which has an upper bound of H_0^{-1}. In addition, $H(t)$ should not change considerably over the time scale T.

These requirements can be expressed in two dimensionless parameters

$$\varepsilon_1 \doteq \frac{v}{c} = v \quad \text{and} \quad \varepsilon_2 \doteq \mathrm{HT} \quad , \tag{5.32}$$

where ε_1 encodes the weak-field and slow-motion requirement and ε_2 represents the ratio of the test object's time scale to the age of the universe. They are both assumed to be constant within this approximation.

In the Newtonian picture for Keplerian orbits, the centripetal force amounts to the gravitational force so that

$$F_{cent} \stackrel{!}{=} F_{grav} \quad \Longrightarrow \quad \frac{v^2}{R} = \frac{GM}{R^2}$$
$$\Longrightarrow \quad \varepsilon_1 \approx \left(\frac{m_0}{R}\right)^{\frac{1}{2}} = \sqrt{\mu} \quad . \tag{5.33}$$

Furthermore, we see that

$$\varepsilon_1 \varepsilon_2 = v\, H\, T \approx v\, H\, \frac{R}{v} = h \quad . \tag{5.34}$$

From the first equation in set (5.30), we can derive the order of the angular momentum barrier term:

$$L = R^2 \dot{\varphi} \approx \frac{R^2}{T} \quad \Longrightarrow \quad \frac{L}{R} \approx \varepsilon_1 \quad . \tag{5.35}$$

The following results are derived in detail in appendix B.3. Expressing the second equation in set (5.30) in terms of the expansion parameters and neglecting quartic terms, we find

$$\dot{t}^2 = 1 + \dot{R}^2 + \underbrace{\frac{L^2}{R^2} + 2\mu + 4\mu \dot{R}^2}_{\mathcal{O}(\varepsilon_1^2)} + \mathcal{O}\left(\varepsilon_1^4, \varepsilon_1^2 \varepsilon_2^2, \varepsilon_2^4\right) \quad . \tag{B.9}$$

(B.9) reduces to $\tau = t$ (Newtonian absolute time) considering negligible radial velocities $\dot{R} \ll 1$. We keep the $\dot{R}^2$ terms for now though.

Since we assumed $\varepsilon_2 = HT$ to be constant, i.e. $R\, \partial_t H = \varepsilon_1 \partial_t \varepsilon_2 \stackrel{!}{=} 0$ vanishes, we can deduce the order of the acceleration term:

$$0 = \frac{dH}{dt} R = \frac{\partial_t^2 a}{a} R - \frac{h^2}{R} \quad \Longrightarrow \quad \frac{\partial_t^2 a}{a}\, R = \frac{\varepsilon_1^2 \varepsilon_2^2}{R} \quad . \tag{5.36}$$

Finally, we are all set to have a look at the radial equation, which (as computed in appendix B.3) reduces to

$$\begin{aligned} 0 = \ddot{R} - \frac{L^2}{R^3} + \frac{\mu}{R} + \frac{3\mu L^2}{R^3} - \frac{\partial_t^2 a}{a}\, R + \\ + h^2\, \frac{\dot{R}^2}{R} + 2\mu h\, \frac{\dot{R}}{R} + \mathcal{O}\left(\varepsilon_1^6, ..., \varepsilon_2^6\right) \quad . \end{aligned} \tag{B.11}$$

Restoring the expressions for μ and h, we thus arrive at

$$\begin{aligned} 0 = \ddot{R} - \underbrace{\frac{L^2}{R^3}}_{\mathcal{O}(\varepsilon_1^2)} + \underbrace{\frac{m_0}{R^2}}_{\mathcal{O}(\varepsilon_1^2)} + \underbrace{\frac{3m_0L^2}{R^4}}_{\mathcal{O}(\varepsilon_1^4)} + \quad &\Big\} \text{ pure Schwarzschild terms} \\ - \underbrace{\frac{\ddot{a}}{a}R}_{\mathcal{O}(\varepsilon_1^2\varepsilon_2^2)} + \underbrace{H^2\dot{R}^2R}_{\mathcal{O}(\varepsilon_1^2\varepsilon_2^2)} + \quad &\Big\} \text{ pure FLRW terms} \\ + \underbrace{2m_0H\dot{R}}_{\mathcal{O}(\varepsilon_1^3\varepsilon_2)} + \quad &\Big\} \text{ McVittie specific terms} \\ + \mathcal{O}\left(\varepsilon_1^6, ..., \varepsilon_2^6\right) \quad . \end{aligned} \tag{5.37}$$

Truncating the expansion at this point is valid when ε_1 and ε_2 are roughly of the same order of magnitude. Observe that, for Keplerian orbits, the radial velocity $\dot{R}$ usually amounts to the dimension of ε_1, i.e. the last two terms can also be neglected for $\varepsilon_1 \approx \varepsilon_2$. The term $3m_0L^2/R^4$ effectuates a relativistic correction – refer to section 2.3 for the geodesics discussion in which its integral $-m_0L^2/R^3$ is derived. We conclude that for a qualitative analysis of the effect of cosmic expansion, the Next-to-Newtonian picture with (3.4) is indeed backed up by the McVittie space-time as a general relativistic case.

Last but not least, note that most of the terms in (5.37) can immediately be attributed to either the Schwarzschild or the FLRW metric solely, as indicated on the right side. Their effects can well be understood within the respective isolated space-time itself. However, with higher orders, we also obtain mixed terms in the McVittie space-time – e.g. $2m_0H\dot{R}$, which disappears in both limits $H \to 0$ (Schwarzschild) and $m \to 0$ (FLRW).

The Solar System

The above approximation is all well and good, but let us have a look at our Solar System to gain some insight into the legitimacy of our assumptions. The numerical values of ε_1 and ε_2 for the Earth (including all previously omitted factors of 2π and c) amount to

$$\varepsilon_1 = \frac{2\pi R}{cT} = 10^{-4} \quad \text{and} \quad \varepsilon_2 = H_0T = 7 \times 10^{-11} \approx 10^{-10} \quad , \tag{5.38}$$

i.e. they are *not* of the same order of magnitude. In order to estimate the radial velocity $\dot{R}$ we divide the doubled difference between perihelion and aphelion by one year, the period of the Earth, and obtain

$$\dot{R} \approx 0.067 \, \frac{\mathrm{AU}}{\mathrm{year}} \quad \Longrightarrow \quad \frac{\dot{R}}{c} = 10^{-6} \quad . \tag{5.39}$$

The mean radial velocities of other objects of the Solar System (such as the dwarf planet Eris or Mercury) are of the same order.

In summary, we have $\varepsilon_2 \approx \varepsilon_1^{2.5}$ and $\dot{R}/c \approx \varepsilon_1^{1.5}$. We can hence determine the most important terms for the Solar System within the reduction of the McVittie geodesics to Keplerian orbits. One important observation here: the mixed term $2m_0 H\dot{R}$ is of the *same* order as the cosmological expansion term $R\,\ddot{a}/a$ and can therefore in principle not be neglected.

In order to understand the effect of the mixed term, which has the form of some sort of friction, let us have a look at the phase space of solutions. We break up the radial second-order ordinary differential equation (5.37) into a coupled system of first-order ordinary differential equations

$$\begin{aligned} \dot{R} &= S \\ \dot{S} &= -\frac{\ddot{a}}{a} R - \frac{m_0}{R^2} + \frac{L^2}{R^3} - 2m_0 H \frac{S}{R} \quad . \end{aligned} \tag{5.40}$$

Here, we neglect the less important term $H^2\dot{R}^2 R \mathrel{\widehat{=}} \mathcal{O}(\varepsilon_1^{8.5})$ (compared to the order of magnitude of $R\,\ddot{a}/a \mathrel{\widehat{=}} \mathcal{O}(\varepsilon_1^7) \mathrel{\widehat{=}} 2m_0 H\dot{R}$) and also leave aside the relativistic correction $3m_0 L^2/R^4$. Now, figures 5.1 and 5.2 show the phase space of solutions, the first including the friction term and the second disregarding it for comparative purposes. For the plots, we consider a Schwarzschild-de-Sitter space-time with positive $\ddot{a}/a = \text{const}$. Hence, the acceleration term acts practically like a harmonic oscillator. The term m_0/R^2 represents the attractive gravitational potential and L^2/R^3 the angular momentum barrier keeping the test-particle on a fixed orbit in the friction-free case. All parameters except for L are given by the space-time. The angular momentum itself is determined by the particles initial radius $R(0)$ and angular velocity $\dot{\varphi}(0)$ by $L = R(0)^2\dot{\varphi}(0) = \text{const}$, cf. (5.28).

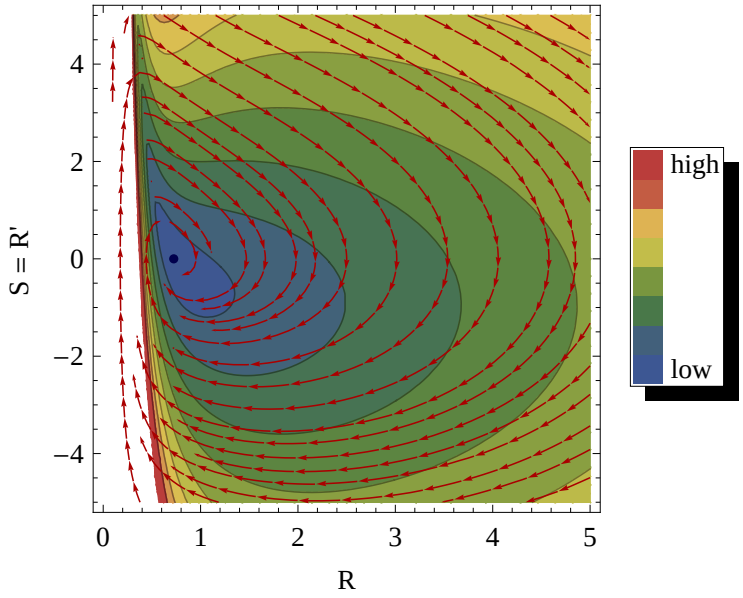

Figure 5.1: Phase space $\{R, R'\}$ including the "friction" term. The red stream lines indicate the solutions of (5.40) and the background contours display the magnitude of the vector field. The blue spot marks the stationary circular orbit solution. All parameters have been set to 1.

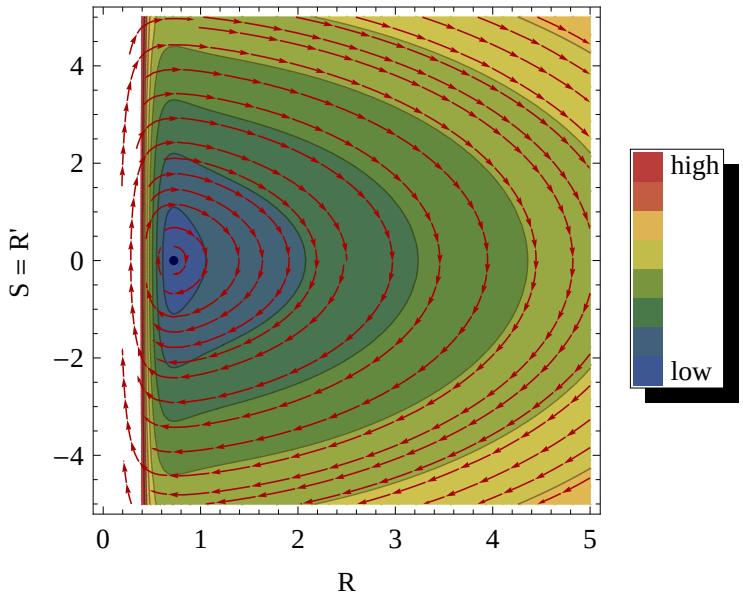

Figure 5.2: Phase space $\{R, R'\}$ without the "friction" term. The red stream lines now indicate the solutions of (5.40) disregarding the term $2m_0 H\dot{R}$.

In both cases, the blue point marks the circular orbit solution. In the friction-free case, the solutions consist of closed trajectories describing (possibly eccentric) orbits around the central mass. The harmonic oscillator behaviour induced by the constant acceleration term $\ddot{a}/a > 0$ guarantees for stability and ensures that the trajectories are closed. Adding the $2m_0 H\dot{R}$ term indeed results in what one would intuitively describe as a sort of friction: a series of test particles with the same angular momentum L are thrown into the space-time with varying initial radius $R(0) > 0$ and radial velocity $\dot{R}(0)$, and they all converge to the circular orbit solution, which hence constitutes a universal fix point.

In the case of $\ddot{a}/a \to 0$, the harmonic oscillator part vanishes (and so does the friction term, since then also $H \to 0$) and nothing guarantees for the (asymptotic) stability of the solutions for a given L and arbitrary $\{R, \dot{R}\}(0)$. This is merely the reduced Schwarzschild case featuring a boundary orbit behind which the trajectories reduce to open hyperbolae. The solution phase space is shown in figure 5.3.

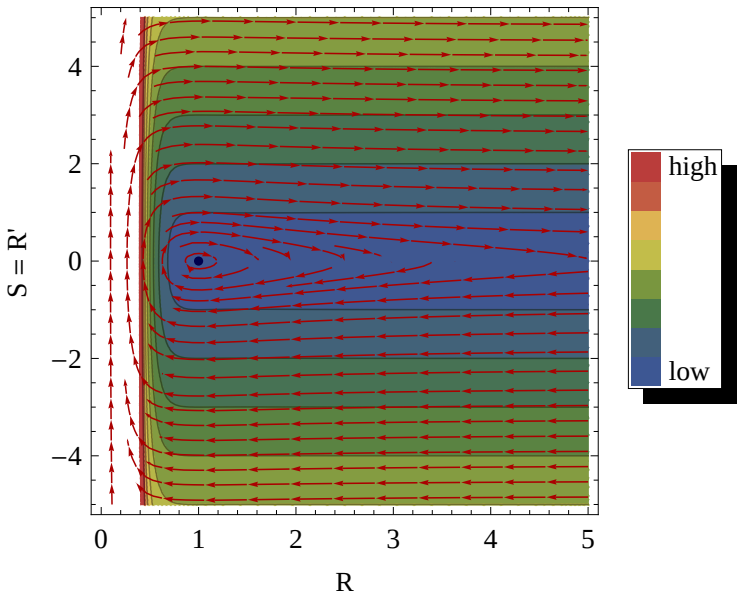

Figure 5.3: Phase space $\{R, R'\}$ for the ODE (5.40) considering $\ddot{a}/a \to 0$, i.e. the red stream lines show the Schwarzschild geodesics.

5.5 Non-expanding Circular Orbits

In the previous section we have derived exact equations for the geodesics in the McVittie space-time. As a special case, we now examine non-expanding circular orbits, i.e. geodesics that have a constant radial distance to the central mass:

$$R(\tau) \stackrel{!}{=} \text{const}$$

Defining $l \doteq L/R$, the radial geodesic equation (5.30) implies

$$\begin{aligned} 0 = &- \left(1 - 2\mu - h^2\right) \frac{l^2}{R} + \frac{\mu}{R}(1 - 2\mu)\, \dot{t}^2 + \\ &- R \left(\frac{\partial H}{\partial t} \sqrt{1 - 2\mu} + \frac{h^2}{R^2} \left(1 - \mu - h^2\right) \right) \dot{t}^2 \quad . \end{aligned} \tag{5.41}$$

The normalisation condition (5.29) yields

$$\dot{t}^2 = \frac{1 + l^2}{1 - 2\mu - h^2} \quad . \tag{5.42}$$

It is important to see that for $R(\tau) = \text{const}$, equation (5.29) excludes $1 - 2\mu - h^2 = 0$ because the real-valued momentum cannot satisfy $1 + l^2 = 0$ (and we have $\dot{t} > 0$ in the considered space-time).

Inserting (5.42) into (5.41) leads to

$$R \frac{\partial h}{\partial t} = \frac{\left(1 - 2\mu - h^2\right) \left(\mu \left(1 + 3l^2\right) - l^2 - h^2\right)}{\left(1 + l^2\right) \sqrt{1 - 2\mu}} \quad . \tag{5.43}$$

This is a first-order ordinary differential equation for the Hubble parameter. The right-hand side is a second-order polynomial of $h(t, R = \text{const})^2$, which is in principle solvable. However, the solution of the ODE comprising the inverse function of a superposition of arc tangents is not very enlightening.

Non-expanding circular orbits in the McVittie space-time, which are described by their radius R and momentum l, must therefore comply with condition (5.43). In the same way as in the previous subsection, observe that to leading order in μ, h^2 and l^2, (5.43) reduces to

$$R \frac{\partial h}{\partial t} = \mu - l^2 - h^2 \quad , \tag{5.44}$$

which exactly reproduces condition (3.24) for Next-to-Newtonian circular

orbits

$$R\,\frac{\partial h}{\partial t} + h^2 \equiv \frac{\ddot{a}}{a}\,R \stackrel{!}{=} \mu - l^2$$
$$\implies \quad 1 - \underbrace{\frac{\ddot{a}}{a}\,\frac{R^3}{m_0}}_{\alpha} = \underbrace{\frac{L^2}{m_0 R}}_{\lambda} \quad . \tag{3.24}$$

In the case of no acceleration, i.e. $a(t)$ depends at most linearly on t, we recover the Newtonian condition for a circular orbiting test particle in an inertial frame. Hence, as presented in section 3.3.1, for an accelerated universe ($R\,\ddot{a}/a \doteq \kappa^2 > 0$), we need sub-Newtonian angular momentum $l^2 = \mu - \kappa^2$ for the particle to stay in its non-expanding orbit. For a decelerated universe ($R\,\ddot{a}/a \doteq \nu^2 < 0$), on the other hand, we need super-Newtonian angular momentum $l^2 = \mu + \nu^2$ to achieve the same.

Let us go back to the full and exact condition (5.43) and check for stationary solutions $h(t) \stackrel{!}{=} h_0 = \text{const}$. This corresponds to a Schwarzschild-de-Sitter space-time with $a(t) \propto \exp(Ht)$. (5.43) then yields

$$\mu = \frac{l^2 + h_0^2}{1 + 3l^2} \quad \implies \quad l^2 = \frac{\mu - h_0^2}{1 - 3\mu} \quad . \tag{5.45}$$

We observe that the momentum l diverges if R approaches $3m_0$, no stable circular orbits are to be found within the region $R \leq 3m_0$ of a Schwarzschild-de-Sitter type space-time.

On the other hand, we can determine the largest stable "orbit" by examining $l \to 0$. In this case, the angular velocity $\omega = \dot{\varphi} \to 0$, i.e. the particle does not move at all. This corresponds to the critical point r_{crit} of the Next-to-Newtonian discussion, at which cosmic expansion and gravitational attraction are at balance. For $l \to 0$, condition (5.45) reads

$$\mu = h_0^2 \quad \implies \quad \frac{GM}{R} = H_0^2 R^2 \quad \implies \quad R^3 = \frac{GM}{H_0^2} \quad . \tag{5.46}$$

Thus, we indeed exactly recover the critical point (3.15) for a deceleration parameter of

$$q_0 = -\frac{\ddot{a}}{a} H_0^{-2} = -H_0^2 H_0^{-2} = -1 \quad . \tag{5.47}$$

Our actual Universe is about to become dark energy dominated and thus asymptotically of de-Sitter type. Even in this violently expanding situation, the McVittie model confirms that local orbits remain stable, since the radii of our planet orbits are much smaller than the critical radius of the Sun. This, in fact, is a stroke of luck as opposed to the fate of the large-scale structures, which will be exponentially drawn apart (although this will most probably not be of our personal concern anymore).

6 Conclusion

6.1 Summary

Throughout the course of this master thesis, we have explored different models that link the phenomenon of global expansion within the Universe to local physics such as gravitational attraction or the situation in electromagnetically bound systems, viz.

1. a Next-to-Newtonian situation, in which the inertial frame structure has been modified to resemble comoving observers in an expanding Friedmann-Lemaître space-time,
2. the Einstein-Straus vacuole, which consists of a sphere comprising a pure Schwarzschild space-time region around a massive object that is integrated and fitted into an FLRW space-time, and
3. the asymptotically flat McVittie space-time describing a mass-particle whose gravitational field merges into an expanding FLRW cosmos.

These models have been analysed with respect to the two questions posed in the introductory motivation chapter – the first asking whether we can retrieve the scale at which global expansion prevails over local attraction,

and the second asking to what extent the local dynamics are influenced by the expanding cosmos. In the following, we restate some of the central outcomes.

Within the Newtonian approach, we derived an expression for the critical radius at which the attractive force on the test particle is in equilibrium with the force attributed to the cosmic expansion,

$$r_{\mathrm{crit}} = \sqrt[3]{\frac{C}{|q|\,H^2}} \quad . \tag{3.15}$$

In this context, we found that electromagnetically bound systems exhibit incredibly large critical radii at which cosmic expansion would have a noteworthy influence. In realistic applications, the influence of cosmic expansion can therefore be completely neglected.

The restriction to circular orbits revealed that, in a decelerated universe, orbiting test particles have to raise a higher angular momentum compared to the non-expanding Newtonian two-body situation. Likewise, they need less angular momentum in the case of an accelerated universe. Moreover, stable circular orbits (with radius r_0) are only to be found within the region

$$r_0 < r_{\mathrm{stable}} \approx 0.63\, r_{\mathrm{crit}} \quad . \tag{3.26}$$

The following chapter treated the Einstein-Straus vacuole. Since its interior features a pure Schwarzschild geometry, closed geodesics (i.e. the orbits around the central mass within the vacuole) remain unaffected by the surrounding expanding cosmos *by construction*. However, the size of the vacuole indicates the scale at which cosmic expansion supersedes gravitational attraction by the massive object. The expression for the Schücking radius,

$$r_{\mathrm{vac}} = \sqrt[3]{\frac{2MG}{H^2}} \quad , \tag{4.14}$$

actually assumes similar values like the critical radius (3.15) of the Next-to-Newtonian situation for astrophysical objects in our Universe considering $q \approx -0.5$. The Einstein-Straus vacuole can easily be extended to include a cosmological constant Λ, as outlined in the concluding section of chapter 4 – however, the expression for the vacuole radius remains unaffected by this.

Finally, we studied the McVittie metric and determined the form of its timelike geodesics. Within a controlled approximation, we could retrieve the Next-to-Newtonian equation of motion which supports the analysis we have made in chapter 3 from a general relativistic point of view. In the course of this approximation, we had a closer look at the first few low-order terms. Besides some well-understood terms of either Schwarzschild or FLRW origin, we also encountered mixed terms that vanish in the resp. reduction of the McVittie metric to the Schwarzschild or FLRW metric. Subsequently, the effect of an occurring mixed term of a friction-type form has been studied in some more detail.

As a last point in the McVittie chapter, we discussed circular orbits. The emerging condition (5.43) has been shown to reduce to its counterpart of the Newtonian situation, (3.24), within the same approximation scheme as before. Hence, non-expanding circular orbits in the flat McVittie space-time feature the same basic behaviour as stated above when summarising the Next-to-Newtonian chapter. The section finishes with a remarkable result that occurs with the reduction of the general McVittie to a Schwarzschild-de-Sitter space-time: the *exact* general relativistic expression for the largest possible radius of non-expanding circular orbits (considering a constant expansion rate $H = \text{const}$), (5.46), coincides with the Next-to-Newtonian critical radius (3.15) (with a corresponding deceleration parameter of $q = -1$).

Therefore, we find the presented Newtonian picture to be backed up and justified by the regarded aspects of the general relativistic model depicting the gravitational field of a massive body merged into an expanding FLRW cosmos.

Altogether, the experimentally attested onset of the effects of cosmic expansion from the magnitude of 10 Mly on, that has been set out in the motivation chapter, has been reconstructed and confirmed by all three discussed theoretical models.

6.2 Perspective

In the different chapters, we have commented on various problems of the considered general relativistic models. The Einstein-Straus vacuole constitutes an unstable equilibrium since the vacuole size is adjusted according to the exact cancellation of the gravitational attraction and the expansion effect at its boundary. As [Krasiński, 1997] derives in full length, this poses a very fragile situation. We argued that slight perturbations of the vacuole size would result in an either too "light-weight" or too "heavy" vacuole w.r.t. the excised mass of the diluting cosmic matter (in terms of the Misner-Sharp energy measuring quasi-local mass) which results in an infinite expansion or collapse of the vacuole, respectively (cf. [Carrera & Giulini, 2009a]).

In contrast to the conceptual problems of the Einstein-Straus vacuole, the McVittie space-time exhibits other unacceptable characteristics. In this context, we commented on the diverging pressure and the consequent prevention of the central mass from accreting more matter from its surroundings. The McVittie Einstein tensor (5.6) always exhibits a true singularity for $r \to m(t)/2$ as long as the McVittie space-time does not reduce to either a pure FLRW ($m(t) \to 0$), Schwarzschild ($a = \text{const}$) or Schwarzschild-de-Sitter ($H = \text{const}$) geometry.

One could in general consider different enhancements of the regarded models. Among these we already mentioned the Swiss cheese model as an extension of the Einstein-Straus vacuole which consists of inserting several non-overlapping spheres filled with Schwarzschild geometries into the FLRW background. Another possibility is to generalise the FLRW background to a still spherically symmetric yet inhomogeneous Lemaître-Tolman-Bondi (LTB) background, which has been studied in [Bonnor, 2000].

Extending the McVittie metric and retrieving a genuinely new metric is not easy. A good review and analysis of the various approaches has been published by [Carrera & Giulini, 2009b]. There it is shown that any models trying to release the stringent no-matter-accretion condition (5.9) (in order to get rid of the diverging pressure) do not lead to new physical solutions – they rather reduce to Schwarzschild-de-Sitter space-times.

We mentioned in the motivation that according to D. Giulini, there are no further well-understood metrics besides the above-mentioned ones that describe massive bodies embedded in an FLRW cosmos. This situation is not least attributable to the difficulty to actually characterise the meaning of "body" and "embed". On top of that, we have restricted ourselves to the simple embedding of one single massive object into the expanding cosmos – in view of the different structural levels of our neighbourhood in the Universe, this appears to be a radical oversimplification. To do justice to the layers we presented in the introductory chapter, one should ultimately search for a model describing and including the hierarchy of mutually embedded systems when zooming out from the Earth, viz. the Solar System, the Galaxy, the Local Group, the Cluster, the Supercluster, and last but not least the homogeneous and isotropic cosmological solution. Especially the latter transition from Superclusters as local inhomogeneities to uniformly distributed cosmic matter attracts attention of recent research. However, to the present day one has only very little knowledge of how to analytically approach this hierarchical embedding problem [Carrera & Giulini, 2009a]. Furthermore, it has been shown that it is not possible to embed a non-spherically-symmetric body into an FLRW cosmos – although one would rather expect the characteristics of such an embedded object (whose influence asymptotically vanishes at some scale) to have no impact on global features of the space-time. This is addressed for example by the above-mentioned LTB models.

Who would have thought – many interesting questions remain open and more realistic solutions to Einstein's field equations (satisfying the demands to describe the embedding of local structures in our Universe) are to be sought...

R

References

Barnes, Luke A.; Francis, Matthew J.; James, J. Berian & Lewis, Geraint F. 2006. Joining the Hubble flow: Implications for Expanding Space. *Monthly Notices of the Royal Astronomical Society*, **373**(1), 382–390.

Blau, Matthias. 2012. Lecture Notes on General Relativity. `http://www.blau.itp.unibe.ch/Lecturenotes.html`.

Bonnor, Wiliam B. 2000. A Generalization of the Einstein-Straus Vacuole. *Classical and Quantum Gravity*, **16**, 2739–2748.

Cahill, Michael E. & McVittie, George C. 1970. Spherical Symmetry and Mass-energy in General Relativity I. General Theory. *Journal of Mathematical Physics*, **11**, 1382–1391.

Carrera, Matteo & Giulini, Domenico. 2006. On the Influence of the Global Cosmological Expansion on the Local Dynamics in the Solar System. *arXiv*, gr–qc/0602.098v2.

Carrera, Matteo & Giulini, Domenico. 2009a. Influence of Global Cosmological Expansion on Local Dynamics and Kinematics. *arXiv*, gr–qc/0810.2712v2.

Carrera, Matteo & Giulini, Domenico. 2009b. On the Generalization of McVittie's Model for an Inhomogeneity in a Cosmological Spacetime. *arXiv*, gr–qc/0908.3101v1.

Einstein, Albert & Straus, Ernst G. 1945. The Influence of the Expansion of Space on the Gravitation Fields Surrounding the Invidual Stars. *Reviews of Modern Physics*, **17**(2-3), 120–124.

Einstein, Albert & Straus, Ernst G. 1946. Corrections and Additional Remarks to our Paper: The Influence of the Expansion of Space on the Gravitation Fields Surrounding the Invidual Stars. *Reviews of Modern Physics*, **18**(1), 148–149.

Francis, Matthew J.; Barnes, Luke A.; James, J. Berian & Lewis, Geraint F. 2007. Expanding Space: The Root of all Evil? *Publications of the Astronomical Society of Australia*, **24**(2), 95–102.

Freedman, Wendy L., *et al.* . 2001. Final Results from the Hubble Space Telescope Key Project to Measure the Hubble Constant. *The Astrophysical Journal*, **553**(1), 47–72.

Gamow, George. 1970. *My World Line: an Informal Autobiography.* Viking Press.

Gillessen, S.; Eisenhauer, F.; Trippe, S.; Alexander, T.; Genzel, R.; Martins, F. & Ott, T. 2009. Monitoring Stellar Orbits Around the Massive Black Hole in the Galactic Center. *The Astrophysical Journal*, **692**(2), 1075–1109.

Kaloper, Nemanja; Kleban, Matthew & Martin, Damien. 2010. McVittie's Legacy: Black Holes in an Expanding Universe. *arXiv*, hep–th/1003.4777v3.

Karachentsev, Igor. D. 2005. The Local Group and Other Neighboring Galaxy Groups. *Astronomical Journal*, **129**(1), 178.

Krasiński, Andrzej. 1997. *Inhomogeneous Cosmological Models.* Cambridge University Press.

Kumar, Suresh. 2012. Constraints on Hubble Constant and Deceleration Parameter in Power-law Cosmology from the Observational $H(z)$ and SNe Ia Data. *arXiv*, gr–qc/1109.6924v2.

Lake, Kayll & Abdelqader, Majd. 2011. More on McVittie's Legacy: A Schwarzschild - de Sitter Black and White Hole Embedded in an Asymptotically ΛCDM Cosmology. *arXiv*, gr–qc/1106.3666v2.

Lemaître, Georges. 1927. Un univers homogène de masse constante et de rayon croissant rendant compte de la vitesse radiale des nébuleuses extra-galactiques. *Annales de la Société Scientifique de Bruxelles*, **A47**, 49–56.

Manasse, F. K. & Misner, C. W. 1963. Fermi Normal Coordinates and Some Basic Concepts in Differential Geometry. *Journal of Mathematical Physics*, **4**, 735–745.

McVittie, George C. 1933. The Mass-particle in an Expanding Universe. *Monthly Notices of the Royal Astronomical Society*, **93**(5), 325–339.

Misner, Charles W. & Sharp, David H. 1964. Relativistic Equations for Adiabatic, Spherically Symmetric Gravitational Collapse. *Physical Review*, **136**(Oct.), 571–576.

Misner, Charles W.; Thorne, Kip S. & Wheeler, John Archibald. 1973. *Gravitation.* San Francisco: William H. Freeman and Co.

Nolan, Brien C. 1998. A Point Mass in an Isotropic Universe. Existence, Uniqueness and Basic Properties. *Physical Review*, **D58**, 064006.

Nolan, Brien C. 1999a. A Point Mass in an Isotropic Universe: II. Global Properties. *Classical and Quantum Gravity*, **16**, 1227–1254.

Nolan, Brien C. 1999b. A Point Mass in an Isotropic Universe: III. The Region $R \leq 2m$. *Classical and Quantum Gravity*, **16**, 3183–3191.

Pachner, Jaroslav. 1964. Nonconservation of Energy during Cosmic Evolution. *Physical Review Letters*, **12**(4), 117–118.

Perlmutter, S., *et al.* . 1999. Measurements of Ω and Λ from 42 High-Redshift Supernovae. *The Astrophysical Journal*, **517**(2), 565–586.

Price, Richard H. & Romano, Joseph D. 2012. In an Expanding Universe, What Doesn't Expand? *arXiv*, gr–qc/0508052v2.

Ribas, Ignasi; Jordi, Carme; Vilardell, Francesc; Fitzpatrick, Edward L.; Hilditch, Ron W., *et al.* . 2005. First Determination of the Distance and Fundamental Properties of an Eclipsing Binary in the Andromeda Galaxy. *Astrophysical Journal*, **635**, L37–L40.

Riess, Adam G.; Schmidt, Brian P., *et al.* . 1998. Observational Evidence from Supernovae for an Accelerating Universe and a Cosmological Constant. *The Astronomical Journal*, **116**(3), 1009–1038.

Riess, Adam G., *et al.* . 2011. A 3% Solution: Determination of the Hubble Constant with the Hubble Space Telescope and Wide Field Camera 3. *The Astrophysical Journal*, **730**(2), 119–136.

Robertson, Howard P. 1935. Kinematics and World-Structure. *Astrophysical Journal*, **82**, 284–301.

Schücking, Engelbert L. 1954. Das Schwarzschildsche Linienelement und die Expansion des Weltalls. *Zeitschrift für Physik*, **137**, 595–603.

Stachel, John, *et al.* (eds). 1987–2012. *The Collected Papers of Albert Einstein, Vols. 1-13.* Princeton University Press.

Szabados, László B. 2004. Quasi-Local Energy-Momentum and Angular Momentum in GR: A Review Article. *Living Reviews in Relativity*, **7**(4).

Wald, Robert M. 1984. *General Relativity.* The University of Chigaco Press.

Walker, Arthur G. 1935. On Riemannian Spaces with Spherical Symmetry about a Line, and the Conditions for Isotropy in General Relativity. *The Quarterly Journal of Mathematics: Oxford Journals*, **6**(1), 81–93.

Xu, Lix-In; Zhang, Cheng-Wu; Chang, Bao-Rong & Liu, Hong-Ya. 2007. Reconstruction of Deceleration Parameters from Recent Cosmic Observations. *arXiv*, astro–ph/0701519v2.

Sources of Images

Figure 1.3: http://map.gsfc.nasa.gov/media/060915/

Figure 1.4: http://commons.wikimedia.org/wiki/File:Earth%27s_Location_in_the_Universe_%28JPEG%29.jpg

Figure 2.1: http://en.wikipedia.org/wiki/File:Friedmann_universes.svg

A

Fundamental Space-times

A.1 Geometric Properties

A.1.1 Schwarzschild Metric

The Schwarzschild metric in its standard form (featuring "Schwarzschild coordinates") reads

$$ds^2 = -f(r)dt^2 + f(r)^{-1}dr^2 + r^2 d\Omega^2 \quad . \tag{2.31}$$

with $f(r) \doteq 1 - 2m/r$.

The non-vanishing Christoffel symbols of the second kind amount to

$$\begin{aligned}
\Gamma^t{}_{tr} &= \frac{m}{r(r-2m)} & & \\
\Gamma^r{}_{tt} &= \frac{m(r-2m)}{r^3} & \Gamma^r{}_{rr} &= -\frac{m}{r(r-2m)} \\
\Gamma^r{}_{\vartheta\vartheta} &= -(r-2m) & \Gamma^r{}_{\varphi\varphi} &= -(r-2m)\sin^2(\vartheta) \\
\Gamma^\vartheta{}_{r\vartheta} &= \frac{1}{r} & \Gamma^\vartheta{}_{\varphi\varphi} &= -\sin(\vartheta)\cos(\vartheta) \\
\Gamma^\varphi{}_{r\varphi} &= \frac{1}{r} & \Gamma^\varphi{}_{\vartheta\varphi} &= \cot(\vartheta) \quad .
\end{aligned} \tag{A.1}$$

The non-vanishing components of the Riemann tensor yield

$$\begin{aligned} R_{trtr} &= -\frac{2m}{r^3} & R_{t\vartheta t\vartheta} &= \frac{m(r-2m)}{r^2} \\ R_{t\varphi t\varphi} &= \frac{m(r-2m)\sin^2(\vartheta)}{r^2} & R_{r\vartheta r\vartheta} &= -\frac{m}{r-2m} \\ R_{r\varphi r\varphi} &= -\frac{m\sin^2(\vartheta)}{(r-2m)} & R_{\vartheta\varphi\vartheta\varphi} &= 2mr\sin^2(\vartheta) \quad . \end{aligned} \tag{A.2}$$

The Schwarzschild metric constitutes the unique solution to the vacuum Einstein equations (Birkhoff's theorem), its Ricci tensor

$$R_{\mu\nu} = 0 \tag{A.3}$$

and, correspondingly, the Ricci scalar vanishes as well,

$$\mathcal{R} = 0 \quad . \tag{A.4}$$

A.1.2 Friedmann-Lemaître-Robertson-Walker Metric

The Friedmann-Lemaître-Robertson-Walker metric in comoving spherical coordinates reads

$$ds^2 = -dt^2 + a(t)^2\left(\frac{dr^2}{1-kr^2} + r^2\, d\Omega^2\right) \quad . \tag{2.46}$$

$k = -1, 0, +1$ corresponds to the three maximally symmetric space geometries, namely the hyperbolic space H^3, flat Euclidean space $\mathbb{R}^3$ or the three-sphere S^3, respectively. Encapsulating all three, we replace the spatial part by the generic expression $a(t)^2\tilde{g}_{ij}dx^i dx^j$ where the tilde (and the latin indices i, j, k) denotes that $\tilde{g}_{ij}$ is a three-dimensional object referring to the bare, non-scaled spatial components.

Now, the non-vanishing Christoffel symbols of the second kind amount to

$$\begin{aligned} \Gamma^t{}_{ij} &= a(t)\,\dot{a}(t)\,\tilde{g}_{ij} \\ \Gamma^i{}_{tj} &= \frac{\dot{a}(t)}{a(t)}\,\delta^i{}_j \\ \Gamma^i{}_{jk} &= \tilde{\Gamma}^i{}_{jk} \quad . \end{aligned} \tag{A.5}$$

The relevant components of the Riemann tensor yield

$$\begin{aligned} R^{t}{}_{itj} &= a(t)\,\ddot{a}(t)\,\tilde{g}_{ij} \\ R^{i}{}_{tjt} &= -\frac{\ddot{a}(t)}{a(t)}\,\delta^{i}{}_{j} \\ R^{k}{}_{ikj} &= 2k\tilde{g}_{ij} + 2\dot{a}(t)^2\tilde{g}_{ij} \quad . \end{aligned} \tag{A.6}$$

The non-vanishing components of the Ricci tensor yield

$$\begin{aligned} R_{tt} &= -3\,\frac{\ddot{a}(t)}{a(t)} \\ R_{ij} &= \Big(a(t)\ddot{a}(t) + 2\dot{a}(t)^2 + 2k\Big)\,\tilde{g}_{ij} \quad . \end{aligned} \tag{A.7}$$

Finally, the Ricci scalar gives

$$\mathcal{R} = \frac{6}{a(t)^2}\,\Big(a(t)\ddot{a}(t) + \dot{a}^2 + k\Big) \quad . \tag{A.8}$$

B

McVittie Detailed Computations

B.1 Divergence of the Velocity Field e_0

Let us define the functions

$$A \doteq 1 + \frac{m(t)}{2r} \quad \text{and} \quad B \doteq 1 - \frac{m(t)}{2r} \tag{B.1}$$

and denote derivatives w.r.t. t by a dot $\dot{A}$. Dumping arguments, the velocity vector field of the perfect fluid reads

$$e_0 = \left(\frac{A}{B}\right) dt \quad . \tag{B.2}$$

Denoting by g the determinant of the metric $g_{\mu\nu}$, we compute

$$\begin{aligned}
\frac{1}{3}\nabla_\mu\, {e_0}^\mu &= \frac{1}{3}\,\frac{1}{\sqrt{g}}\,\partial_\mu(\sqrt{g}\,{e_0}^\mu) = \frac{1}{3}\,\frac{1}{\sqrt{g}}\,\frac{\partial}{\partial t}\left[\sqrt{g}\,\left(\frac{A}{B}\right)\right] \\
&= \frac{1}{3}\,\frac{\frac{\partial}{\partial t}\left(A^6a^3\right)}{BA^5a^3} = \frac{6A^5\dot{A}a^3+3A^6a^2\dot{a}}{3BA^5a^3} = \frac{1}{3}\,\frac{6\frac{\dot{m}}{2r}+3A\dot{a}}{Ba} \\
&= \frac{a\dot{m}+\dot{a}m}{Bra} + \frac{\dot{a}}{Ba} - \frac{\dot{a}m}{2Bra} = \frac{1-\frac{m}{2r}}{B}\,\frac{\dot{a}}{a} + \frac{1}{Br}\,\frac{\frac{\partial}{\partial t}(am)}{a} \\
&= \frac{\dot{a}}{a} + \frac{1}{Br}\,\frac{\frac{\partial}{\partial t}(am)}{a} \quad ,
\end{aligned}$$

which establishes

$$F = \frac{1}{3}\nabla_\mu\, {e_0}^\mu \quad . \tag{B.3}$$

B.2 Geodesics

Throughout this section, we derive the radial equation of motion for the McVittie geodesics of section 5.4 via the Lagrangian method. Point of departure is the Lagrangian (5.27). Since

$$\frac{\partial}{\partial R}\mu(R) = -\frac{\mu}{R} \quad , \quad \frac{\partial}{\partial R}h(t,R) = \frac{h}{R} \quad \text{and} \quad \frac{\partial}{\partial R}\frac{L^2}{R^2} = \frac{\partial}{\partial R}R^2\dot{\varphi}^2 = 2\frac{L^2}{R^3} \quad ,$$

we get for $R(\tau)$:

$$\begin{aligned}
&\frac{\partial\mathcal{L}}{\partial R} \stackrel{!}{=} \frac{d}{d\tau}\,\frac{\partial\mathcal{L}}{\partial\dot{R}} \\
\Longrightarrow \quad &\left(-2\frac{\mu}{R}+2\frac{h^2}{R}\right)\dot{t}^2 - 2\frac{\frac{h}{R}\sqrt{1-2\mu}-h\,\frac{1}{2\sqrt{1-2\mu}}(-2)\frac{-\mu}{R}}{1-2\mu}\,\dot{R}\dot{t} + \\
&+\frac{-1}{(1-2\mu)^2}(-2)\frac{-\mu}{R}\,\dot{R}^2 + 2\frac{L^2}{R^3} \\
&= \frac{d}{d\tau}\left(-2\frac{h}{\sqrt{1-2\mu}}\,\dot{t} + 2\frac{1}{1-2\mu}\,\dot{R}\right) \\
&= -2\frac{\dot{h}\sqrt{1-2\mu}-h\frac{1}{2\sqrt{1-2\mu}}(-2)\dot{\mu}}{1-2\mu}\,\dot{t} - 2\frac{h}{\sqrt{1-2\mu}}\,\ddot{t} + \\
&+2\frac{-2\dot{\mu}}{-(1-2\mu)^2}\,\dot{R} + 2\frac{1}{1-2\mu}\,\ddot{R} \quad .
\end{aligned} \tag{B.4}$$

The derivatives w.r.t. τ read

$$\dot{h}(t,R) = \frac{\partial H}{\partial t} R\,\dot{t} + \frac{h}{R}\dot{R} \quad \text{and} \quad \dot{\mu}(R) = -\frac{\mu}{R}\dot{R} \quad .$$

Inserting these into (B.4) and multiplying by $-\frac{1-2\mu-h^2}{2}$ yields

$$\begin{aligned}
0 = \frac{1}{R} \underbrace{\left(1-2\mu-h^2\right)\left(\mu-h^2\right)}_{=\mu(1-2\mu)-h^2(1-\mu-h^2)} \dot{t}^2 + \\
+ \cancel{\frac{1-2\mu-h^2}{1-2\mu}\left(\frac{h}{R}\sqrt{1-2\mu} - \frac{h}{R}\frac{\mu}{\sqrt{1-2\mu}}\right)\dot{R}\,\dot{t}} + \\
+ \cancel{\frac{1-2\mu-h^2}{1-2\mu}}\mu\frac{\dot{R}^2}{R} - \left(1-2\mu-h^2\right)\frac{L^2}{R^3} + \\
- \frac{1-2\mu-h^2}{1-2\mu}\left(\frac{\partial H}{\partial t}\sqrt{1-2\mu}\,R\,\dot{t} + \right. \\
\left. + \cancel{\frac{h}{R}\sqrt{1-2\mu}\,\dot{R} - \frac{h}{R}\frac{\mu}{\sqrt{1-2\mu}}\dot{R}}\right)\dot{t} + \\
- \frac{1-2\mu-h^2}{\sqrt{1-2\mu}}\,h\,\ddot{t} - \cancel{2}\frac{1-2\mu-h^2}{1-2\mu}\mu\frac{\dot{R}^2}{R} + \frac{1-2\mu-h^2}{1-2\mu}\,\ddot{R} \quad .
\end{aligned}$$

Hence, the Euler-Lagrange equation for $R(\tau)$ reads

$$\begin{aligned}
0 = \frac{\mu}{R}(1-2\mu)\,\dot{t}^2 - \frac{h^2}{R}\left(1-\mu-h^2\right)\dot{t}^2 + \\
- (1-2\mu-h^2)\frac{L^2}{R^3} - \frac{1-2\mu-h^2}{1-2\mu}\,\frac{\partial H}{\partial t}R\,\dot{t}^2 + \\
- \frac{1-2\mu-h^2}{\sqrt{1-2\mu}}\,h\,\ddot{t} - \frac{1-2\mu-h^2}{(1-2\mu)^2}\frac{\dot{R}^2}{R} + \frac{1-2\mu-h^2}{1-2\mu}\,\ddot{R} \quad .
\end{aligned} \tag{B.5}$$

It contains both $\ddot{R}$ and $\ddot{t}$ terms, which are also present in the equation for $t(\tau)$. Hence, we can use the latter to eliminate the $\ddot{t}$ part.

$$\frac{\partial \mathcal{L}}{\partial t} \stackrel{!}{=} \frac{d}{d\tau}\frac{\partial \mathcal{L}}{\partial \dot{t}}$$

$$
\begin{aligned}
\Longrightarrow \quad & \frac{\partial h}{\partial t}\left(2h\,\dot{t}^2 - \frac{2}{\sqrt{1-2\mu}}\,\dot{R}\,\dot{t}\right) = \frac{d}{d\tau}\left(-2\left(1-2\mu-h^2\right)\,\dot{t} - \frac{2h}{\sqrt{1-2\mu}}\,\dot{R}\right) \\
\Longrightarrow \quad & 0 = \frac{\partial H}{\partial t} R \left(\cancel{-h\,\dot{t}^2} + \cancel{\frac{1}{\sqrt{1-2\mu}}\,\dot{R}\,\dot{t}}\right) - \left(1-2\mu-h^2\right)\,\ddot{t} - \frac{2\mu}{R}\,\dot{R}\,\dot{t} + \\
& \quad + 2h\Big(\cancel{1}^{\frac{1}{2}}\frac{\partial H}{\partial t} R\,\dot{t} + \frac{h}{R}\,\dot{R}\Big)\dot{t} - \frac{h}{\sqrt{1-2\mu}}\,\ddot{R} + \\
& \quad - \dot{R}\,\frac{\sqrt{1-2\mu}\left(\cancel{\frac{\partial H}{\partial t} R\dot{t}} + \frac{h}{R}\dot{R}\right) - h\frac{1}{2\sqrt{1-2\mu}}(-2)\frac{-\mu}{R}\dot{R}}{1-2\mu} \\
& = -\left(1-2\mu-h^2\right)\,\ddot{t} + \frac{\partial H}{\partial t} R\,h\,\dot{t}^2 + \frac{2}{R}\left(h^2-\mu\right)\,\dot{R}\,\dot{t} + \\
& \quad + \frac{3\mu-1}{(1-2\mu)^{3/2}}\,h\,\frac{\dot{R}^2}{R} - \frac{h}{\sqrt{1-2\mu}}\,\ddot{R} \quad .
\end{aligned}
\tag{B.6}
$$

Multiplying (B.6) by $-\frac{h}{\sqrt{1-2\mu}}$, we arrive at an expression for $\ddot{t}$:

$$
\begin{aligned}
-\frac{1-2\mu-h^2}{\sqrt{1-2\mu}}\,h\,\ddot{t} = & -\frac{h^2}{\sqrt{1-2\mu}}\,\frac{\partial H}{\partial t} R\,\dot{t}^2 + 2\frac{h}{R}\,\frac{\mu-h^2}{\sqrt{1-2\mu}}\,\dot{R}\,\dot{t} + \\
& + \frac{1-3\mu}{(1-2\mu)^2}\,h^2\,\frac{\dot{R}^2}{R} + \frac{h^2}{1-2\mu}\,\ddot{R} \quad .
\end{aligned}
\tag{B.7}
$$

This is the Euler-Lagrange equation for $t(\tau)$. As mentioned in section 5.4, its integral is the normalisation condition (5.29). Inserting (B.7) into the radial Euler-Lagrange equation (B.5) yields

$$
\begin{aligned}
0 = & \cancel{\frac{1-2\mu-h^2+h^2}{1-2\mu}}^{1}\,\ddot{R} - \left(1-2\mu-h^2\right)\frac{L^2}{R^3} + \\
& + \frac{\mu}{R}(1-2\mu)\,\dot{t}^2 - \frac{h^2}{R}\left(1-\mu-h^2\right) - \frac{1-2\mu-\cancel{h^2}}{\sqrt{1-2\mu}}\,\frac{\partial H}{\partial t} R\,\dot{t}^2 + \\
& - \cancel{\frac{h^2}{\sqrt{1-2\mu}}\,\frac{\partial H}{\partial t} R\,\dot{t}^2} + 2\frac{\mu-h^2}{\sqrt{1-2\mu}}\,\frac{h}{R}\,\dot{R}\,\dot{t} + \\
& + \underbrace{\frac{h^2(1-3\mu)-\mu\left(1-2\mu-h^2\right)}{(1-2\mu)^2}}_{\frac{\cancel{(1-2\mu)}\left(h^2-\mu\right)}{\cancel{(1-2\mu)^2}}}\,\frac{\dot{R}^2}{R} \quad ,
\end{aligned}
$$

and we finally arrive at the radial equation of motion:

$$\begin{aligned} 0 = \ddot{R} &- \left(1 - 2\mu - h^2\right) \frac{L^2}{R^3} + \frac{\mu}{R}(1-2\mu)\,\dot{t}^2 + \\ &- R\left(\frac{\partial H}{\partial t}\sqrt{1-2\mu} + \frac{h^2}{R^2}\left(1-\mu-h^2\right)\right)\dot{t}^2 + \\ &- \frac{\mu - h^2}{1-2\mu}\,\frac{\dot{R}^2}{R} + \frac{2\left(\mu - h^2\right)}{\sqrt{1-2\mu}}\,\frac{h}{R}\,\dot{R}\,\dot{t} \quad . \end{aligned} \tag{B.8}$$

B.3 Reduction to Next-to-Newtonian Case

Expressing the normalisation condition (5.29) (the second equation in set (5.30)) in terms of the expansion parameters ε_1 and ε_2 yields

$$\begin{aligned} &\dot{t}^2 + \frac{2\varepsilon_1^2\varepsilon_2^2}{\sqrt{1-2\varepsilon_1^2}\,\left(1-2\varepsilon_1^2-\varepsilon_1^2\varepsilon_2^2\right)}\,\dot{t}\,\dot{R} + \\ &- \frac{1}{\left(1-2\varepsilon_1^2\right)\left(1-2\varepsilon_1^2-\varepsilon_1^2\varepsilon_2^2\right)}\,\dot{R}^2 - \frac{1+\varepsilon_1^2}{1-2\varepsilon_1^2-\varepsilon_1^2\varepsilon_2^2} = 0 \quad . \end{aligned}$$

Neglecting quartic terms and translating back to μ and h, we find

$$\dot{t}^2 = 1 + \dot{R}^2 + \underbrace{\frac{L^2}{R^2} + 2\mu + 4\mu\dot{R}^2}_{\mathcal{O}\left(\varepsilon_1^2\right)} + \mathcal{O}\left(\varepsilon_1^4, \varepsilon_1^2\varepsilon_2^2, \varepsilon_2^4\right) \quad . \tag{B.9}$$

Let us now examine the radial equation which is the third in set (5.30):

$$\begin{aligned} 0 = \ddot{R} &- \frac{L^2}{R^3} + \frac{2\mu L^2}{R^3} + \frac{\mu}{R}\,\dot{t}^2 - 2\frac{\mu^2}{R}\,\dot{t}^2 + \\ &- R\left(\frac{\partial_t^2 a}{a} - \frac{h^2}{R^2}\right)\left(1 + \mathcal{O}\left(\varepsilon_1^2\right)\right) + \\ &- \frac{h^2}{R}\,\dot{t}^2 - \left(\mu - h^2\right)\left(1 + 2\mu + \mathcal{O}\left(\varepsilon_1^4\right)\right)\frac{\dot{R}^2}{R} + \\ &+ 2\mu h\,\frac{\dot{R}}{R}\,\dot{t} + \mathcal{O}\left(\varepsilon_1^6, ..., \varepsilon_2^6\right) \quad . \end{aligned} \tag{B.10}$$

Recall that in (5.36) we established $R\,(\partial_t^2 a)/a = \varepsilon_1^2\varepsilon_2^2/R$ since we had $\varepsilon_2 = HT = \text{const}$. Inserting (B.9) into (B.10) yields

$$\begin{aligned} 0 = \ddot{R} &- \frac{L^2}{R^3} + \frac{2\mu L^2}{R^3} + \frac{\mu}{R} + \cancel{\mu\frac{\dot{R}^2}{R}} + \frac{\mu L^2}{R^3} + \\ &+ \cancel{2\frac{\mu^2}{R}} + \cancel{4\mu^2\frac{\dot{R}^2}{R}} - \cancel{2\frac{\mu^2}{R}} - \cancel{2\mu^2\frac{\dot{R}^2}{R}} + \\ &- R\left(\frac{\partial_t^2 a}{a} - \cancel{\frac{h^2}{R^2}} + \cancel{\frac{h^2}{R^2}}\right) - \cancel{\mu\frac{\dot{R}^2}{R}} + \\ &- \cancel{2\mu^2\frac{\dot{R}^2}{R}} + h^2\,\frac{\dot{R}^2}{R} + 2\mu h\,\frac{\dot{R}}{R} + \mathcal{O}\left(\varepsilon_1^6, ..., \varepsilon_2^6\right) \quad , \end{aligned}$$

which simplifies to

$$\begin{aligned} 0 = \ddot{R} &- \frac{L^2}{R^3} + \frac{\mu}{R} + \frac{3\mu L^2}{R^3} - R\,\frac{\partial_t^2 a}{a} + \\ &+ h^2\,\frac{\dot{R}^2}{R} + 2\mu h\,\frac{\dot{R}}{R} + \mathcal{O}\left(\varepsilon_1^6, ..., \varepsilon_2^6\right) \quad . \end{aligned} \tag{B.11}$$

Erklärung

(gemäss Art. 28 Abs. 2 RSL 05)

Name/Vorname:	Oeftiger, Adrian
Matrikelnummer:	07 120 710
Studiengang:	Theoretische Physik
Studienziel:	Master of Science
Titel der Arbeit:	On the Effect of Global Cosmological Expansion on Local Dynamics
Leiter der Arbeit:	Prof. Dr. Matthias Blau

Ich erkläre hiermit, dass ich diese Arbeit selbständig verfasst und keine anderen als die angegebenen Quellen benutzt habe. Alle Stellen, die wörtlich oder sinngemäss aus Quellen entnommen wurden, habe ich als solche gekennzeichnet. Mir ist bekannt, dass andernfalls der Senar gemäss Artikel 36 Absatz 1 Buchstabe o des Gesetzes vom 5. September 1996 über die Universität zum Entzug des auf Grund dieser Arbeit verliehenen Titels berechtigt ist.

Ort und Datum Unterschrift